



## City Research Online

### City, University of London Institutional Repository

---

**Citation:** Gaudron, J.O. (2015). Design and characterisation of long period grating (LPG) - based optical fibre sensors for acoustic wave detection. (Unpublished Doctoral thesis, City University London)

This is the accepted version of the paper.

This version of the publication may differ from the final published version.

---

**Permanent repository link:** <https://openaccess.city.ac.uk/id/eprint/8340/>

**Link to published version:**

**Copyright:** City Research Online aims to make research outputs of City, University of London available to a wider audience. Copyright and Moral Rights remain with the author(s) and/or copyright holders. URLs from City Research Online may be freely distributed and linked to.

**Reuse:** Copies of full items can be used for personal research or study, educational, or not-for-profit purposes without prior permission or charge. Provided that the authors, title and full bibliographic details are credited, a hyperlink and/or URL is given for the original metadata page and the content is not changed in any way.

---

---

---

City Research Online:

<http://openaccess.city.ac.uk/>

[publications@city.ac.uk](mailto:publications@city.ac.uk)

---

# Design and characterisation of long period grating (LPG) - based optical fibre sensors for acoustic wave detection

By  
Jacques-Olivier Gaudron

Thesis submitted for the degree of  
Doctor of Philosophy

City University London  
Measurement and Instrumentation Centre  
School of Mathematics, Computer Science &  
Engineering  
Northampton Square, London EC1V 0HB

February 2015

# Abstract

Fibre optic sensors have demonstrated a broad range of commercial potential due to their intrinsic characteristics such as low loss, very small size, light weight and immunity to electromagnetic interference. Representing one type of optical fibre sensors, long period gratings (LPGs) have shown a high sensitivity to a number of parameters, including temperature, strain, refractive index and bending, therefore they have been explored widely for a range of potential sensing applications.

This thesis is focused on the design, implementation and evaluation of LPGs for acoustic wave detection. In doing so, the LPG-based sensor has been evaluated and optimized under low frequency conditions (up to 3 kHz) both in air and underwater, with varying acoustic pressure values. This complements the research widely reported for the detection of ultrasounds.

The LPG-based sensor, fixed between two pillars with one pillar being movable, is found to be sensitive over a specific frequency range with a minimum detectable sound pressure to be 63dB (ref 1 $\mu$ Pa) in water and 66.8dB (ref 20 $\mu$ Pa) in air. The sensor has demonstrated a linear response to the variation of the amplitude of the acoustic pressure applied. The sensor performance, by varying the acoustic frequencies, acoustic pressure amplitude and the bending curvature, fits well with the theoretical model derived from the bending effect of the LPG.

Both the in-air and underwater tests of the LPG-based sensor have confirmed the potential of using optical fibre sensors for acoustic signal detection and for working in harsh working conditions, where conventional acoustic sensors have shown some limitations.

# Table of contents

List of figures.....	VI
List of tables.....	IX
Acknowledgements.....	X
Copyright Declaration.....	XI
<b>1. Chapter 1</b> .....	<b>12</b>
1.1. Background and Introduction.....	12
1.2. Aims and objectives of the work.....	13
1.3. Structure of the thesis.....	14
<b>2. Chapter 2</b> .....	<b>16</b>
2.1. Introduction.....	16
2.2. Optical fibres, modes & gratings.....	17
2.2.1. Optical fibre modes.....	17
2.2.2. Fibre Bragg gratings.....	19
2.3. Principles of Long Period gratings.....	21
2.4. Fabrication of Long Period Gratings:.....	25
2.4.1. Physical deformation of the fibre.....	25
a. Mechanical pressing of the fibre:.....	25
b. Deformation of the core or cladding of the fibre:.....	26
2.4.2. Refractive index modulation.....	27
a. Irradiation using CO <sub>2</sub> Laser.....	27
b. Electric arc discharge.....	27
c. Femto second pulse radiation.....	28
d. Ion implantation.....	28
e. UV-radiation.....	28
2.5. Use of Long Period Gratings as sensors.....	32

2.5.1.	Temperature sensitivity.....	32
2.5.2.	Refractive index sensitivity.....	34
2.5.3.	Strain sensitivity.....	35
2.5.4.	Bending sensitivity.....	36
2.5.5.	Sensitivity to other parameters.....	38
2.6.	Summary .....	39
<b>3.</b>	<b>Chapter 3</b> .....	<b>40</b>
3.1.	Introduction .....	40
3.2.	Classification of optical fibre techniques for sound detection .....	42
3.2.1.	Types of modulation: .....	42
3.2.2.	Definitions.....	43
3.2.3.	Acoustic detection setups.....	43
3.3.	Intensity Modulation .....	44
3.3.1.	Radiated wave.....	44
3.3.2.	Evanescent wave based.....	48
3.3.3.	Lock-in demodulation.....	49
3.4.	Phase modulation and demodulation .....	50
3.4.1.	Optical fibre interferometers.....	51
3.4.2.	Optical Fibre Bragg Grating sensors.....	54
3.5.	Polarisation modulation.....	56
3.6.	Distributed acoustic sensors .....	58
3.6.1.	Bragg Reflector based sensors .....	58
3.6.2.	Distributed sensing using Optical Time Domain Reflectometry (OTDR) 58	
3.7.	Summary of reported fibre optic based acoustic sensors .....	59
3.8.	Summary .....	60
<b>4.</b>	<b>Chapter 4</b> .....	<b>61</b>
4.1.	Introduction .....	61
4.2.	Operational Principle.....	63

---

4.2.1.	Long Period grating as a sensing element.....	63
4.2.2.	Modified string theory .....	64
4.2.3.	Sound pressure .....	68
4.3.	Measurement system .....	69
4.3.1.	The light source.....	71
4.3.2.	Choice of the light source .....	72
a.	S-LED at 1550nm and 1580nm .....	72
b.	S-LED source with FBG.....	74
c.	Tunable Laser Source .....	76
d.	C-band light source .....	78
e.	C-band light source with FBG .....	80
4.3.3.	Discussions .....	82
4.4.	The detection system.....	83
4.4.1.	Photodiode selection: .....	84
4.4.2.	Transimpedance amplifier .....	85
4.4.3.	Noise considerations: .....	86
4.4.4.	Processing of the signal: .....	88
4.4.5.	LabVIEW based control software.....	88
4.4.6.	The sound generation.....	91
4.4.7.	Choice of the loudspeaker.....	93
4.5.	Summary .....	94
<b>5.</b>	<b>Chapter 5</b> .....	<b>95</b>
5.1.	Introduction .....	95
5.2.	Detection of sound in air .....	96
5.2.1.	Grating connected to the membrane of a loudspeaker.....	96
5.2.2.	Grating between 2 pillars .....	97
5.2.3.	Frequency response.....	98
5.2.4.	Amplitude response .....	99

---

5.2.5.	Curvature.....	100
5.2.6.	Standard deviation (consistency of the results) .....	102
5.3.	Detection of sound in water .....	105
5.3.1.	Frequency response.....	105
5.3.2.	Amplitude response .....	106
5.3.3.	Distance variation .....	106
5.3.4.	Water level effect.....	107
5.4.	The sensor system architecture .....	108
5.4.1.	Mechanical setups.....	108
5.4.2.	Setups for measurement of sound in air.....	108
5.4.3.	Setups for measurement of sound in water .....	109
5.5.	Summary .....	111
<b>6.</b>	<b>Chapter 6</b> .....	<b>112</b>
6.1.	Conclusions .....	112
6.2.	Future work .....	114
6.3.	List of publications.....	115

# List of figures

Figure 2.1: EM wave propagating along the z axis .....	17
Figure 2.2: Distribution of cladding modes in an optical fibre [5]. $\beta_{01}$ and $\beta_{11}$ correspond to the lowest propagation constants of the propagating lowest order modes. ....	18
Figure 2.3: Principle of a Fibre Bragg grating .....	19
Figure 2.4: Typical in-fibre long period grating .....	21
Figure 2.5: Mode coupling in a Long Period Grating (Hou et al. [14]).....	22
Figure 2.6: Phase matching considerations for long period gratings [5]. ....	22
Figure 2.7: Optical transmission spectrum of a typical LPG with attenuation bandwidth of 10s of nm when it is illuminated by light from a broadband light source. ....	24
Figure 2.8: Side view of a mechanically induced LPG [16]. ....	25
Figure 2.9: Two-step process for the deformation of the fibre core [19]. ....	26
Figure 2.10: LPG Fabrication setup using the point-by-point technique.....	29
Figure 2.11: Typical masks used at City University London for long period grating fabrication. ....	30
Figure 2.12: Fabrication setup of a LPG using an amplitude mask.....	31
Figure 2.13: Transmission spectrum of a LPG depending on the amount of immersion of the LPG. [37] .....	35
Figure 2.14: Setup for the measurement of the bending effect on a LPG [46].....	37
Figure 3.1: Operating principles of acoustic detection systems .....	44
Figure 3.2: Principle of the moving grating based sensor. ....	45
Figure 3.3: Cantilever based setup.....	45
Figure 3.4: Macrobend on an optical fibre.....	46
Figure 3.5: Schematic structure of the microphone based on a moving diaphragm. Song et al. 2007 [65].....	47
Figure 3.6: Spectrum of three different types of light scattering.....	48
Figure 3.7: Fibre micro bend acoustic sensor. From Fields and Cole 1980 [69].....	49
Figure 3.8: Phase Sensitive detector .....	50

Figure 3.9: (a) Mach–Zehnder; (b) Fabry–Perot; (c) Michelson; (d) Sagnac. From Wild et al. [82] .....	52
Figure 3.10: FBG detection system using a narrow line-width laser diode .....	55
Figure 3.11: FBG detection scheme using a SLED source .....	56
Figure 3.12: Setup for the detection of acoustic waves using the polarisation change. ....	57
Figure 4.1: Setup of the curvature and bend measurement. (a) schematic diagram of the LPG sensor setup; (b) the magnified fibre with a LPG in the middle [120] .....	63
Figure 4.2: Setup of a LPG-based acoustic sensor. ....	65
Figure 4.3: LPG transmission spectra when LPG bending curvature changes .....	66
Figure 4.4: Setup of a LPG-based acoustic detector .....	70
Figure 4.5: Spectrum of a 1550nm source .....	72
Figure 4.6: Spectrum of a 1580nm S-LED light source .....	73
Figure 4.7: Principle of operation of a circulator, upper Port 1 to Port 2 lower, port 2 to Port 3 .....	74
Figure 4.8: Diagram of the FBG – broad band source .....	75
Figure 4.9: Reflection spectrum of an FBG used with the broad-band 1550nm S-LED. ....	76
Figure 4.10: Spectrum of a tuneable laser at 1548nm .....	77
Figure 4.11: Transmission spectrum of a C-band light source. ....	78
Figure 4.12: Spectrum of the C-band source measured every minute (Top), Amplitude of the signal at 1550nm measured every minute (Bottom) .....	79
Figure 4.13: Setup of the C-Band source followed by a FBG .....	80
Figure 4.14: Spectrum of the C-band source after an FBG measured every minute (Top), Amplitude of the signal at 1547.7nm every minute (Bottom) .....	81
Figure 4.15: Detector response curve for different materials .....	84
Figure 4.16: Photodiode amplifier used in photovoltaic mode (a); and photoconductive mode (b). ....	85
Figure 4.17: Frequency response of the amplifier used after the photodiode .....	88
Figure 4.18: Flow chart of the LabVIEW based control software .....	90
Figure 4.19: Frequency response of the power amplifier .....	91
Figure 4.20: Power vs. acoustic pressure .....	92
Figure 5.1: Mechanical setup of the LPG connected to the membrane of a speaker ...	96
Figure 5.2: Frequency response of the LPG and FBG-based sensors .....	97

---

Figure 5.3: LPG-based sensor system with the LPG being fixed between two pillars. .....	98
Figure 5.4: Frequency response of the LPG sensor fixed between two pillars when it is exposed to various acoustic pressures. ....	99
Figure 5.5: Frequency response of the LPG when the bending curvature changes ...	102
Figure 5.6: Standard deviation depending on the radius of curvature. ....	103
Figure 5.7: Standard deviation as a function of the frequency of sound wave when its amplitude varies (the bending curvature of the LPG is 0.4mm).....	104
Figure 5.8: Amount of signal detected in relation to the acoustic pressure variation	106
Figure 5.9: Response of the LPG as a function of the distance from the acoustic source. ....	107
Figure 5.10: Response of the LPG at as a function of the depth of the water level...	108
Figure 5.11: Fibre positioned between 2 pillars.....	109
Figure 5.12: Mechanical setup of the underwater system.....	110

# List of tables

Table 4.1: Power emitted by the loudspeaker.....	92
Table 5.1: Comparison between the theoretical and experimental values of the frequencies detected.....	101

# Acknowledgements

Foremost I would like to express my sincere gratitude to my supervisors, Professor Tong Sun and Professor Ken Grattan for their support, patience and guidance throughout my PhD work.

I would like to thank all my colleagues from the optical fibre sensing group and especially Dr. Frederic Surre, for his time and numerous advices. Also I am very grateful to Jim Hooker for his technical assistance throughout my PhD work.

And finally I would like to express appreciation to my family and friends for their love and encouragement throughout this period.

# Copyright Declaration

The author hereby grants powers of discretion to City University London, Librarian to allow the thesis to be copied in whole or in part without further reference to the author. This permission covers only single copies made for study purposes, subject to normal conditions of acknowledgements.

# Chapter 1

## Background and Introduction

### 1.1. Background and Introduction

Acoustic waves are used in a wide range of sensing fields including physical sensing, chemical sensing and bio sensing. The implementation of acoustic based sensing solutions requires specific knowledge of materials, acoustic wave properties, device design and the sensing mechanisms involved for a wide range of applications such as the detection of seismic waves for oil and gas reservoir monitoring, crack detection in civil structures using ultrasounds, perimeter monitoring, leak detection on pipelines.

Most systems used for acoustic detection use a capacitive or inductive effect such as electret microphones as used for low frequency acoustic sound detection, geophones for the detection of seismic waves (acoustic and infrasound waves) and ultrasonic transducers.

In order to satisfy the demand for more reliable acoustic sensing and the need for sound measurements to be made in very harsh environments such as deep underwater, at high or

low temperatures, near electromagnetic or radioactive sources optical based techniques for acoustic sensing have been subject to extensive research and interest in recent years.

Indeed, given such harsh conditions, optical fibre sensors have shown a clear advantage over their electrical counterparts, e.g. conventional microphones, due to their immunity to electromagnetic interference and resistance to corrosive and radiative conditions. In contrast, the use of conventional microphones would be ineffective to detect sounds from motors, turbines or medical application devices, such as magnetic resonance imaging. Optical techniques are now used to replace existing sensing elements in the oil and gas industry as they are proving to be more reliable, lower cost and due to their low cost can be used for periodic measurements simply by connecting to the fibre.

## 1.2. Aims and objectives of the work

In view of the discussions above, this thesis aims to develop, assess and optimise different types of optical fibre acoustic sensors developed using Long Period Gratings (LPG). This aims to overcome the limitations arising from the conventional techniques, but to address the challenges arising from harsh working conditions.

The major aims and objectives of the work are summarized as follows:

- To carry out a detailed literature review of the development of optical fibre sensors based on long period gratings and use the outcome as a research background.
- To design and evaluate different experimental setups in order to systematically characterize the LPG-based sensor performance in response to the variation of acoustic pressure, orientation and frequency.
- To achieve a better understanding of the coupling of acoustic waves with optical fibre sensors, thus to optimize the sensor design.
- To assess the performance of the optimized sensor created using similar techniques used for more conventional sound detection systems and setups.

The design of the acoustic sensor is primarily focused on the following aspects:

- 1) A thorough comparison of the different grating based sensors.
- 2) The acoustic sensitivity of the sensor

- 3) The frequency response of the sensor
- 4) The consistency of the results obtained
- 5) Use of an effective approach to generate consistent and accurately controlled sound pressure.
- 6) To test the sensor in different environments.

### 1.3. Structure of the thesis

In light of the above, this thesis aims to cover the major aspects of sensor development using LPGs. This is based on a comprehensive review of the development and optimization of various type of sensors reported for acoustic detection.

In order to achieve the aims and objectives highlighted above, this thesis is structured in 6 chapters and the content of each is summarised below.

Chapter 1 is an introduction, highlighting the importance of acoustic detection and the wide use of acoustic sensors for various industrial applications before summarizing the aims and objectives of this thesis. This Chapter ends by indicating the structure of the thesis.

Chapter 2 discusses the operational principles of optical fibres, Fibre Bragg Gratings (FBGs) and Long Period Gratings (LPGs). The primary focus of this Chapter is on the fabrication and sensing characteristics of LPGs. Different sensing characteristics of LPGs are presented and discussed together with their applications reported from the research literature.

Chapter 3 presents different optical techniques reported for sound detection, with a particular focus on optical fibre based sensing techniques. Both the advantages and disadvantages of these sensing techniques are discussed in detail in this Chapter based on the cross-comparisons made.

Chapter 4 reports on the implementation of acoustic sensors based on LPGs and the effect of the setup on the performance. Systematic analysis of the sensor data obtained and evaluation of the experimental setup have been undertaken by varying light sources, angles of curvature, sound pressure levels, with an aim to understand better the underpinning principles and thus to optimize the sensor design to achieve an optimum outcome.

Chapter 5 reports on the studies carried out and results obtained from the LPG-based acoustic sensor systems. The results are compared and discussions are made, in relation to both the understanding of the sensor systems and the limitations of the sensors created and evaluated.

Chapter 6 concludes the thesis summarising the achievements made throughout the development of different sensors for acoustic pressure detection. The scope for future development is also presented at the end of the chapter.

# **Chapter 2**

## **Theory and characteristics of long period gratings**

### **2.1. Introduction**

This Chapter includes detailed discussions on the basic operational principle of fibre Bragg gratings (FBGs) and long period gratings (LPGs), highlighting the similarities and differences between FBGs and LPGs when they are used respectively for sensing applications. Their respective fabrication techniques are also discussed in detail in the chapter. The last section of this Chapter is to review the wide spectrum of applications reported using LPG-based sensors.

## 2.2. Optical fibres, modes & gratings

### 2.2.1. Optical fibre modes

An optical fibre guides light waves in a distinct set of electromagnetic waves called modes [1]. Although an optical fibre has an infinite number of modes [2], which satisfy Maxwell's equations and the boundary conditions, only a discrete number of guided modes can travel in an optical fibre each having a propagation constant ( $\beta$ ). In addition radiation modes travel along the fibre; these result from the optical power coupled out of the fibre core and trapped by the cladding's finite radius. These trapped modes are called cladding modes. The energy transfer from the guided modes towards the cladding modes is the underpinning mechanism of long period gratings. Each mode possesses a discrete propagation constant  $\beta$ . This is a function of the wavelength of the light source and the intrinsic parameters of the fibre. It can be determined by using Maxwell's equations and the boundary conditions at the core-cladding interface [3].

The transmission of light in optical fibres can be understood using the wave-model, in which the light is considered as an electromagnetic wave. Such a wave is propagating as time-varying electric and magnetic fields. As illustrated in Figure 2.1, these fields are perpendicular to each other and also to the direction of propagation.

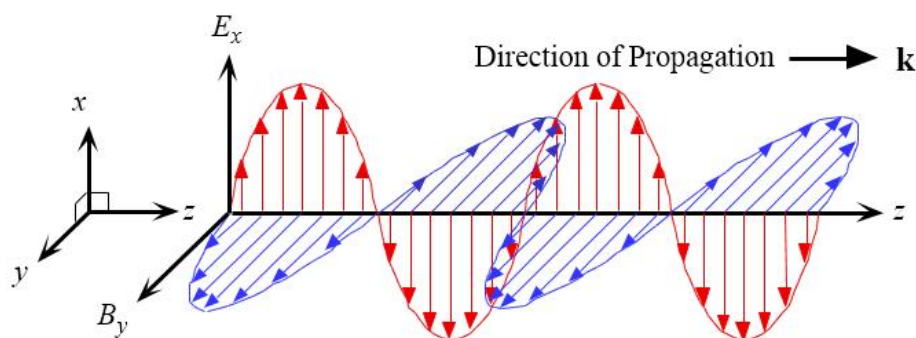


Figure 2.1: EM wave propagating along the z axis

The electric and magnetic fields for a linearly polarised Electromagnetic wave are given by the following formula respectively [4]:

$$\vec{E} = e_x E_{0x} \cos(\omega t - kz) \quad (2.1)$$

$$\vec{E} = e_y E_{0y} \cos(\omega t - kz) \quad (2.2)$$

With:

$\omega = 2\pi f$ : Angular frequency (rad/m)

$k$ : Wavenumber or wave propagation constant (1/m)

$\lambda = \left(\frac{2\pi}{k}\right)$ : Wavelength (m)

As discussed earlier, in an optical fibre, more than one mode can travel thus more than one wave is travelling at a time. The modal analysis of electromagnetic waves in long period gratings would involve fairly complex analytical and numerical analysis thus in this work, the primary research has been focused on the experimental evaluation rather than EM-based modelling.

Bathia et al. [3] proposed the following equation to relate the wavelength to the propagation constant:

$$\beta = \frac{\omega n}{c} = \frac{2\pi}{\lambda} n_{eff} \quad (2.3)$$

Where  $\omega$  is the angular frequency,  $c$  the speed of light in vacuum and  $n_{eff}$  the effective refractive index of the fibre core.

Thus the values of the guided modes propagation constant are required to satisfy the condition below:

$$n_{cl}k < |\beta_{co}| < n_{co}k \quad (2.4)$$

Where  $k$  represents the free space propagation constant at wavelength  $\lambda$ . And with  $n_{cl}$  and  $n_{co}$  the refractive indices of the cladding and the core of the fibre respectively.

Figure 2.2 shows the propagation constants of the forward and reverse propagating guided modes as a function of the wavelength.

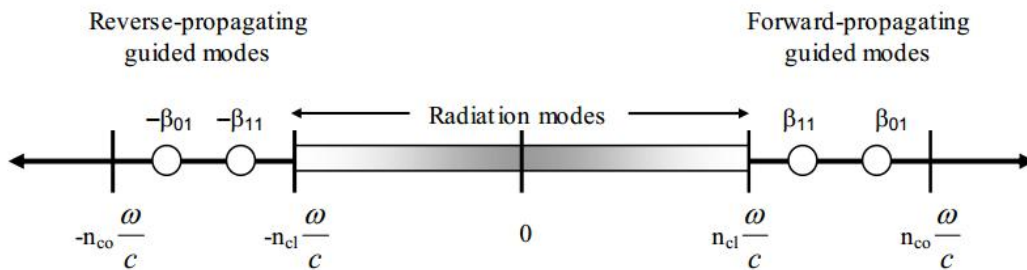


Figure 2.2: Distribution of cladding modes in an optical fibre [5].  $\beta_{01}$  and  $\beta_{11}$  correspond to the lowest propagation constants of the propagating lowest order modes.

Cladding modes however can propagate in either forward or backward direction. Each of these modes possesses a discrete propagation constant. This propagation constant is given by:

$$n_{env}k < |\beta_{cl}| < n_{cl}k \quad (2.5)$$

With  $n_{env}$  is the refractive index of the medium surrounding the cladding. And  $n_{cl}$  the refractive index of the cladding mode.  $k$  is the free space propagation constant given at a wavelength ( $\lambda$ ) [6].

### 2.2.2. Fibre Bragg gratings

A FBG is a piece of an optical fibre, with its core refractive index being periodically modulated. This change in the refractive index creates a change in the propagation properties of the light in the fibre, thus causing a reflection of the light at a particular wavelength, which is called Bragg wavelength ( $\lambda_B$ ). The Bragg wavelength is given by the following formula:

$$\lambda_B = 2n_{eff}\Lambda \quad (2.6)$$

With  $n_{eff}$  is the effective refractive index of the fibre core and  $\Lambda$  is the grating period.

Figure 2.3 shows a typical spectrum of the light reflected by a FBG.

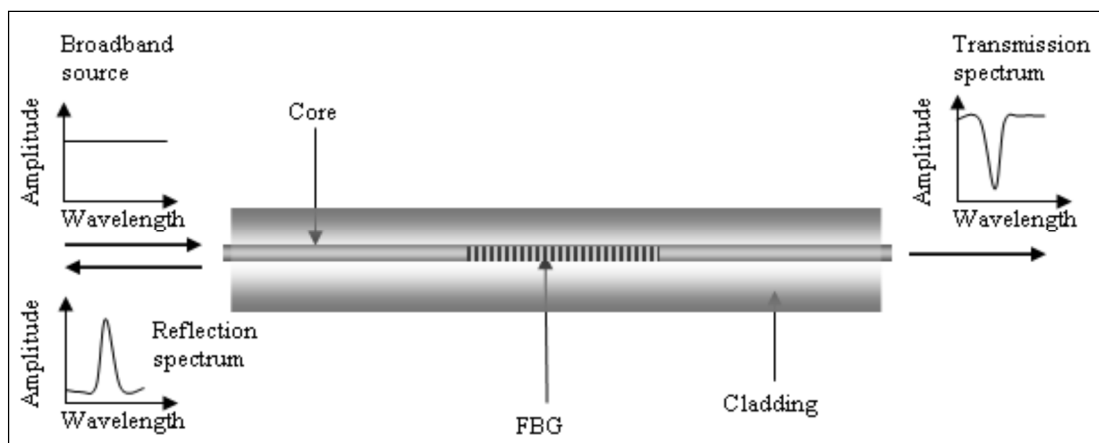


Figure 2.3: Principle of a Fibre Bragg grating

FBGs were first proposed by Hill et al. [7] in 1978. They have demonstrated that creating a modulation of the index of refraction along the fibre core can allow a power coupling from the forward-propagating fundamental guided mode to its backward-propagating counterpart. This is based on the phase-matching between forward and backward-propagating guided modes in an optical fibre.

If a FBG is illuminated by light from a broadband light source, a particular wavelength is reflected, which is called the Bragg wavelength. This is at this particular wavelength that the phase matching between the forward and backwards propagated modes occurs.

FBGs are a key component both in optical communications and in optical sensing. Their attractive features, such as wavelength-encoded sensing principle, ease of multiplexing, coupled with their small size, light weight and immunity to EM interference, have led to their wide applications in structural health monitoring, for example, for the measurement of strain [7], [8], temperature [9] or sound pressure [10] and in telecommunications sector, for example, as a multiplexer [11] and/or demultiplexer.

## 2.3. Principles of Long Period gratings

In terms of fabrication, the major difference between the Long Period Grating (LPG) and FBG is their periods. An LPG is manufactured with a period ( $\Lambda$ ) in the order of hundreds of micrometres, whereas fibre Bragg gratings, usually have periods of less than one micrometre [12].

Another difference between a FBG and a LPG is that the LPG couples light from forward-propagating core mode to co-propagating cladding modes whereas the FBG couples light from forward-propagating core mode to counter-propagating core mode as discussed earlier.

There are different techniques used to fabricate long period gratings, for example by inducing a deformation on the cladding of the fibre or by modifying the refractive index of the fibre core [13]. A common technique for the fabrication of LPGs is to use a photosensitive single mode fibre and to illuminate the core material with ultraviolet (UV) light at regular intervals using an amplitude mask.

The typical period of a LPG varies between  $100\mu\text{m}$  and  $1\text{mm}$ . The fact that in LPGs light is coupled from the forward propagating mode to co-propagating cladding modes and this leads to the appearance of several attenuation bands in the transmission spectra as can be seen in Figure 2.4.

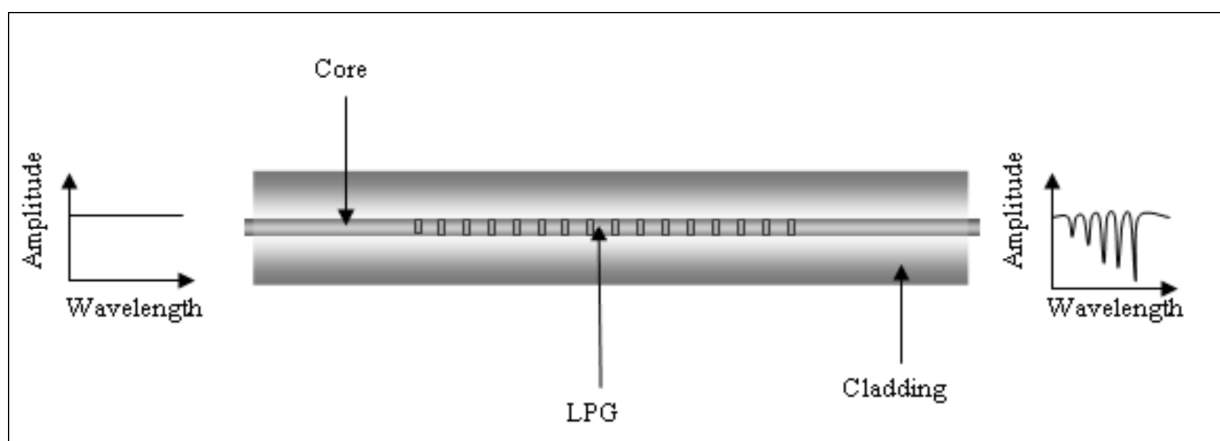


Figure 2.4: Typical in-fibre long period grating

Due to these coupling phenomena, the output spectrum of a LPG has several attenuation bands whereas the FBG has a single attenuation band.

Long Period gratings were first proposed by Vensarkar et al. [12] in 1996 as band-rejection filters. The periodical structure of the grating causes the light to be coupled from the fundamental guided mode to forward propagating cladding modes where the light is lost due to absorption and scattering as shown in Figure 2.5.

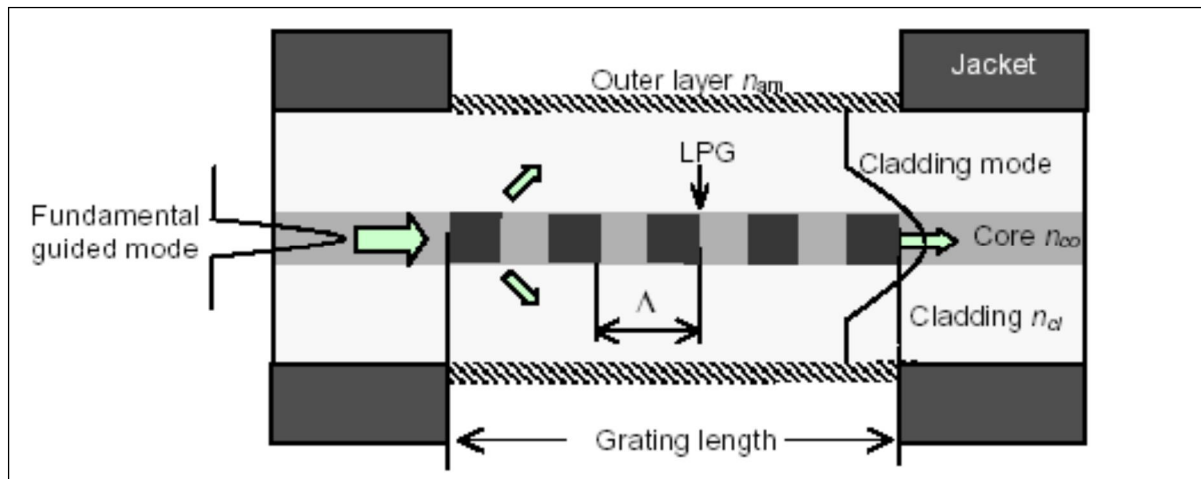


Figure 2.5: Mode coupling in a Long Period Grating (Hou et al. [14])

Resonance loss bands appear in the LPG transmission spectrum due to mode coupling. Since the coupling from the guided mode to cladding modes is wavelength dependent, a spectrally selective loss can thus be obtained [15].

It is important to note that since LPGs couple co-propagating modes, the attenuation bands can only be observed in transmission spectra and the resonance wavelength of the loss band can be obtained from the phase-matching conditions.

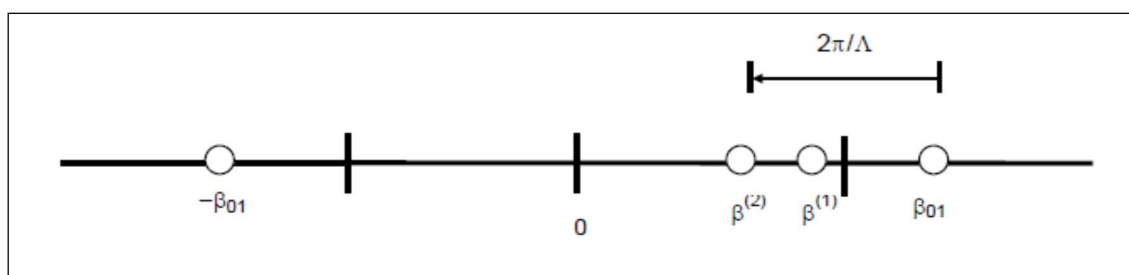


Figure 2.6: Phase matching considerations for long period gratings [5].

From Figure 2.6 it can be seen that the phase matching condition between the guided mode  $LP_{01}$  whose propagation constant is  $\beta_{01}$  and the forward propagating cladding mode  $LP^{(2)}$  whose propagation constant is  $\beta^{(2)}$

The phase matching condition between the guided mode and any forward propagating cladding modes can be given by [15]:

$$\beta_{core} - \beta_{cladding}^{(i)} = \frac{2\pi}{\Lambda} \quad (2.7)$$

With  $\Lambda$  the grating periodicity,  $\beta_{core}$  the propagation constant in the core of the fibre and  $\beta_{cladding}^{(i)}$  the propagation constant in the  $i^{th}$  cladding mode.

Based on equation (2.1), the propagation constant of the core mode can be expressed as:

$$\beta_{core} = \frac{2\pi}{\lambda} n_{eff,core} \quad (2.8)$$

And the propagation constant for the  $i^{th}$  cladding mode can be expressed as:

$$\beta_{cladding}^{(i)} = \frac{2\pi}{\lambda} n_{eff,cladding}^{(i)} \quad (2.9)$$

By combining equations (2.7)-(2.9), the relationship between the resonance wavelengths  $\lambda_i$  and the grating periodicity can thus be established as follows:

$$\lambda_i = (n_{eff,core} - n_{eff,cladding}^i) \Lambda \quad (i = 1, 2 \dots) \quad (2.10)$$

Where  $n_{eff,core}$  and  $n_{eff,cladding}^i$  are respectively the effective refractive indices of the core mode and the  $i^{th}$  cladding mode and  $L$  represents the grating period.

The two key elements in relation to these attenuation bands are the bandwidth and the amount of attenuation. The bandwidth of the attenuation is generally of a few 10's of nm.

Figure 2.7 shows a typical transmission spectrum of a LPG with Length ( $L$ ) being 6mm and period ( $\Lambda$ ) 450 $\mu$ m. The source used to illuminate this LPG was the Ocean Optics LS-1.

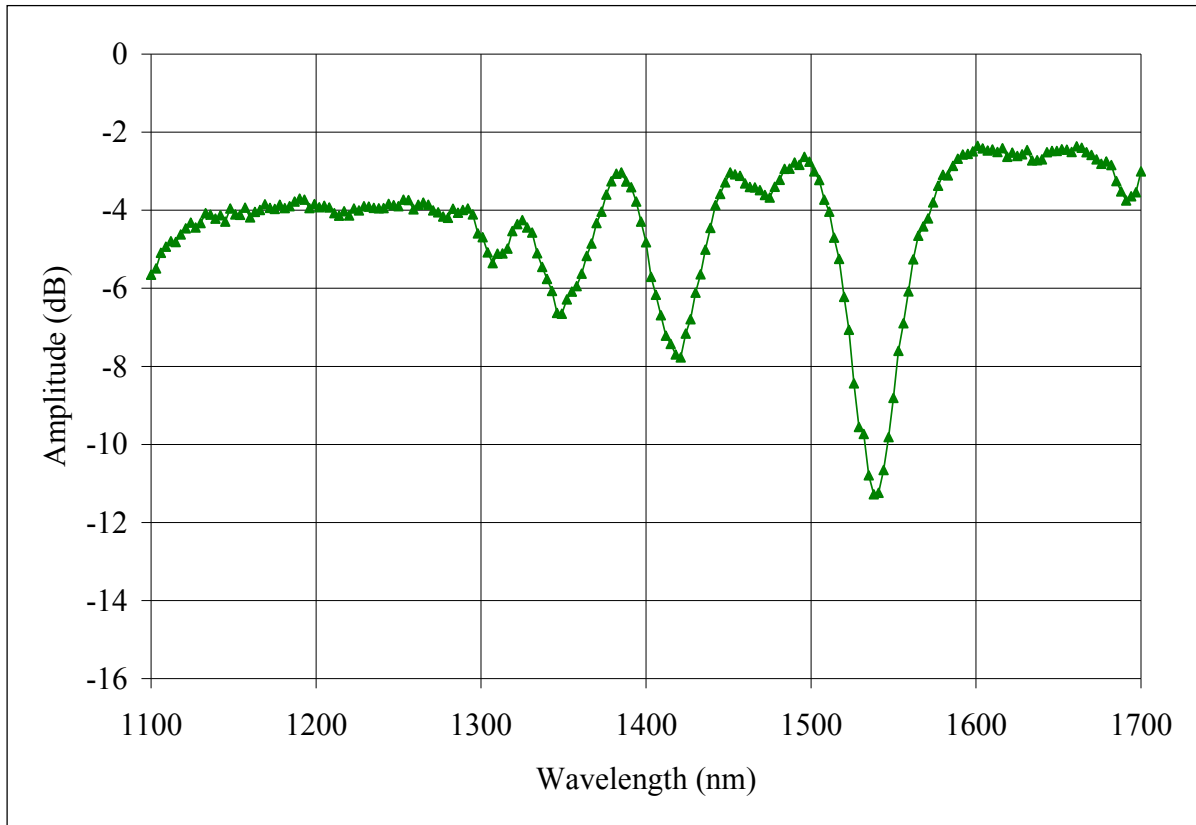


**Figure 2.7:** Optical transmission spectrum of a typical LPG with attenuation bandwidth of 10s of nm when it is illuminated by light from a broadband light source.

## 2.4. Fabrication of Long Period Gratings:

In order to create a LPG it is necessary to modulate the fibre in such a way that facilitates the coupling of light from the guided mode to the co-propagating cladding modes.

This section summarizes different techniques used for LPG fabrication and this includes the use of physical deformation techniques, such as creating a deformation in the core [16] or cladding [17] of the fibre, and the modulation of the fibre core refractive index, such as exposing the fibre to a CO<sub>2</sub> laser irradiation [18], to an electric discharge, using a femto-second laser, Ion implementation or UV irradiation.

### 2.4.1. Physical deformation of the fibre

#### a. Mechanical pressing of the fibre:

A periodic index modulation of the fibre can be induced by placing it between a flat plate and a periodically grooved plate. Figure 2.8 shows the setup of such a system used for the creation of a mechanically induced LPG.

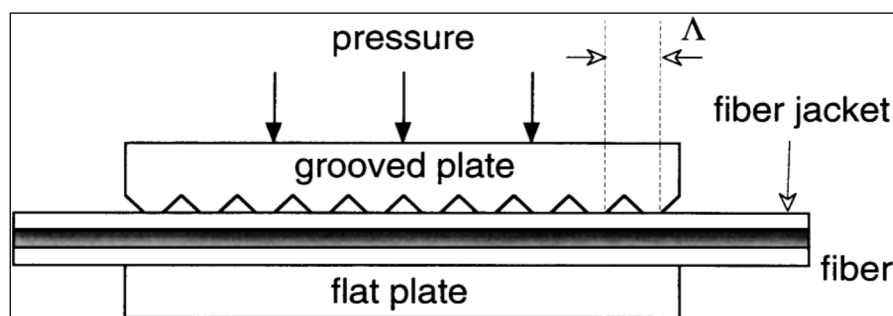


Figure 2.8: Side view of a mechanically induced LPG [16].

The advantage of using this technique is that a LPG can be formed in any section of the fibre as the plates can be moved and placed anywhere and at any time thus by using a mechanical control system the shape of the attenuation bands can be adjusted. The force applied between the plates has an effect on the transmission spectrum of the LPG.

## b. Deformation of the core or cladding of the fibre:

Although not originally destined to manufacture LPGs, a technique demonstrated by Poole et al. [19] in 1994 permits the creation of LPGs by deforming the fibre core periodically. This is done by first cutting a tiny section of a fibre by using a CO<sub>2</sub> laser beam with each localized heat above the silica melting point.

The next step involves annealing the fibre. This is done by heating the fibre locally using the arc produced by a fusion splicer. Elongation on the fibre surface into a sinusoidal deformation of the core and the process is shown in Figure 2.9. However, it is difficult to control the annealing process to ensure the repeatability of the LPGs created.

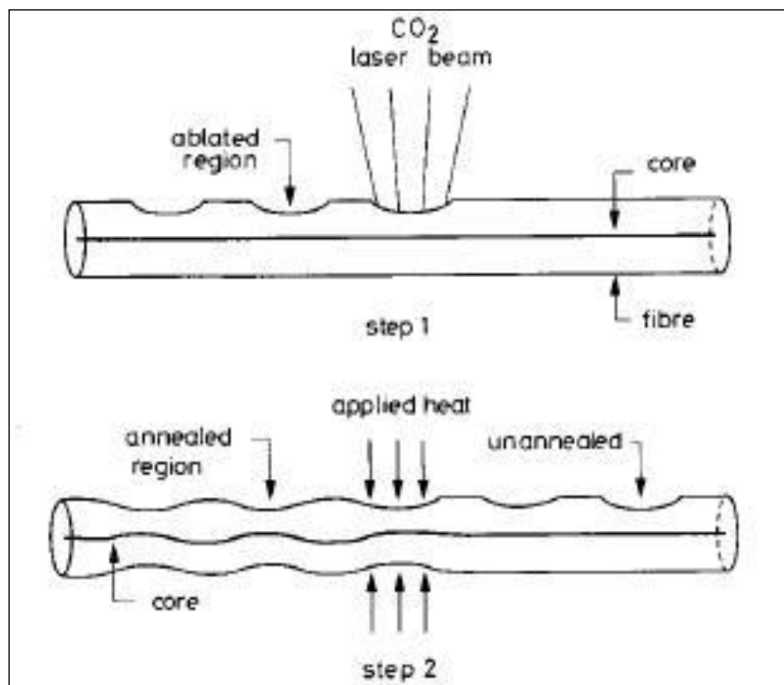


Figure 2.9: Two-step process for the deformation of the fibre core [19].

Lin et al. [16] created a corrugated structure in the cladding of a fibre which caused a periodic variation in radius of the cladding. This was created by periodically etching the cladding of the fibre.

### 2.4.2. Refractive index modulation

#### a. Irradiation using CO<sub>2</sub> Laser

Davis et al. [18] proposed the fabrication of LPGs using focused CO<sub>2</sub> laser pulses at a free space wavelength of 10.6 mm. The main advantage of this fabrication method is that the LPG can be manufactured using standard telecommunications fibre. The refractive index variation is thought to be based on the stress relief and/or densification of the glass of the fibre. This mainly appears at the first 10 to 20mm of the fibre and creates an increase of the refractive index of the cladding.

Using this point-by-point fabrication technique; the fibre has to be mounted onto a translation stage which can be moved in relation to the delivery of laser pulses. The duration of the pulses and the laser output power determine the strength of the LPG fabricated.

#### b. Electric arc discharge

A relatively inexpensive and simple fabrication method was proposed by Palai et al. [20]. It uses a commercial fusion splicer that creates periodic electric arcs along a fibre. These arcs are produced by generating a high voltage applied to the two electrodes which are very close to each other. The arc applied causes a change in the refractive index of the core of the fibre. In addition to the low cost, the possibility of writing LPGs into any type of fibres makes it a very attractive technique. The index modulation is created by local heating of silica of a fibre [21] whose jacket has been removed. The fibre was pulled by a translation stage controlled by a motor synchronised with the splicer. The required length can be achieved by repeating the procedure as many times as desired. This technique has limitations such as the potential variation in groove and depth due to the use of a fusion splicer and limited precision due to the precise movement of the fibre required to ensure a uniform period to be inscribed. In addition, the electric arc generated by the splicer is not always constant and this affects the depth of inscription for each period.

c. Femto second pulse radiation

A LPG can be written using the Ultraviolet light from a pulsed excimer laser. This was first proposed by Kondo et al. [22] in 1999. The fabrication process proposed was based upon a point by point technique. The drawback, however, is the irregular refractive index modulation. To overcome this limitation, researchers have proposed the use of a femtosecond laser for writing LPGs into pure silica [23], germanium doped and photonic crystal fibres [24], [25]. The femtosecond pulse radiation has received increased attention recently mainly for the inscription of LPGs into photonic crystal fibres as these fibres are primarily made of fused silica thus popular inscription methods such as UV radiations cannot be used for LPG fabrication [26].

d. Ion implantation

This LPG fabrication technique was proposed by Fujikami et al. in 2000 [27]. The advantage of this technique is that it uses standard telecommunications fibres and it is possible to write LPGs on virtually any type of silica fibres. The authors presented the inscription of an LPG in a single mode fibre using  $\text{He}^{2+}$  ion implantation. To do so, the fibre cladding was chemically etched to allow the fibre core to be exposed to the ions, thus creating an increase in refractive index. A large change in refractive index is highly desirable when using this technique. The main disadvantage of this technique however is the use of an expensive and very bulky piece of equipment such as a tandem accelerator. Thus this inscription technique is not very practical.

e. UV-radiation

The most popular method for the fabrication of LPGs in single mode fibres is the UV radiation method. It was first used by Meltz et al. in 1989 [28] to manufacture FBGs using the transverse holographic technique. The technique was improved by Hill et al. [29], [30] as they proposed the use of a phase mask to create FBGs. A similar UV inscription technique can be used for LPG fabrication using an amplitude mask or point-by-point technique.

Similar to FBG fabrication, the fibres used for the LPG fabrication are required to be photosensitive or to be made photosensitive. This can be achieved by using specially doped fibres (Boron-Germanium) or by hydrogen loading [31]. The most commonly used UV source for the LPG fabrication is a pulsed excimer laser source (248nm) [32].

The point-by-point technique requires the use of a translation stage that can move the fibre in synchronisation with the pulses produced by the laser. Figure 2.10 shows the fabrication setup using point-by-point based technique.

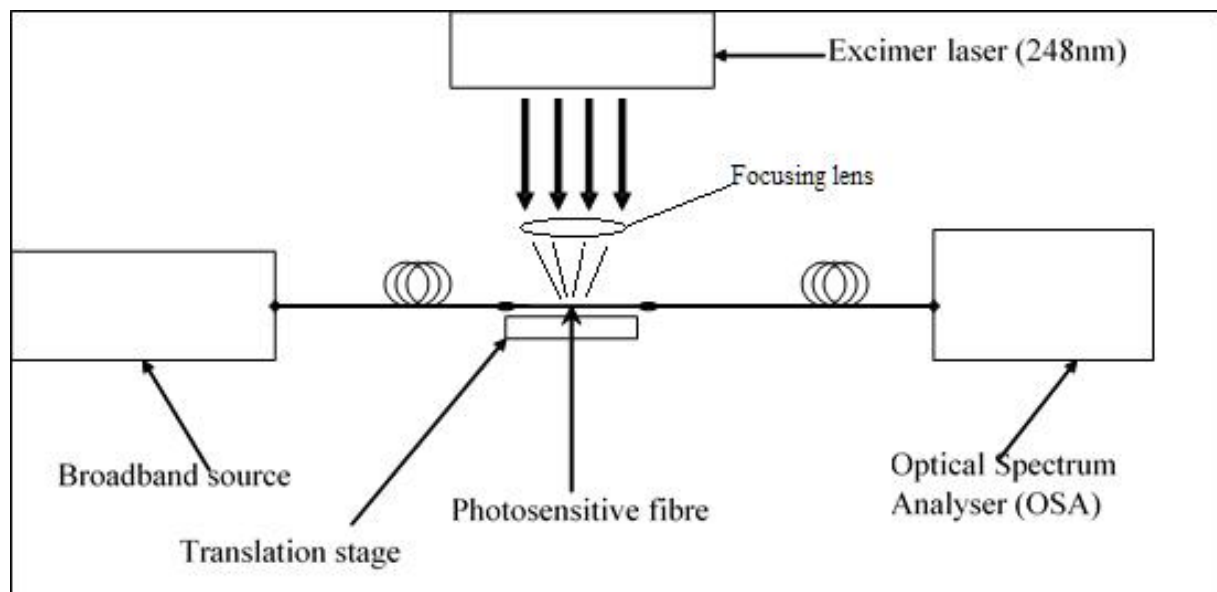


**Figure 2.10: LPG Fabrication setup using the point-by-point technique**

The main advantage of this LPG fabrication technique is that the length and the period of the LPG can be adjusted by setting up the translation stage. The fabrication process is however longer than using the mask technique.

The inscription of LPGs using an amplitude mask is the technique used at City University London with a metal mask being placed between the laser beam and the fibre to be inscribed. For comparison Figure 2.11 shows the picture of a phase mask and an amplitude mask. It can be seen that the phase mask is much smaller and has a shorter period than the amplitude mask. These masks do not have a particular windowing function, although windowing functions can be used for inscribing special FBGs, for example, in order to obtain a filter with specific characteristics or for improving the performance of Wavelength Division Multiplexing systems for example; however the use of windowing functions is not relevant to LPGs in this work.

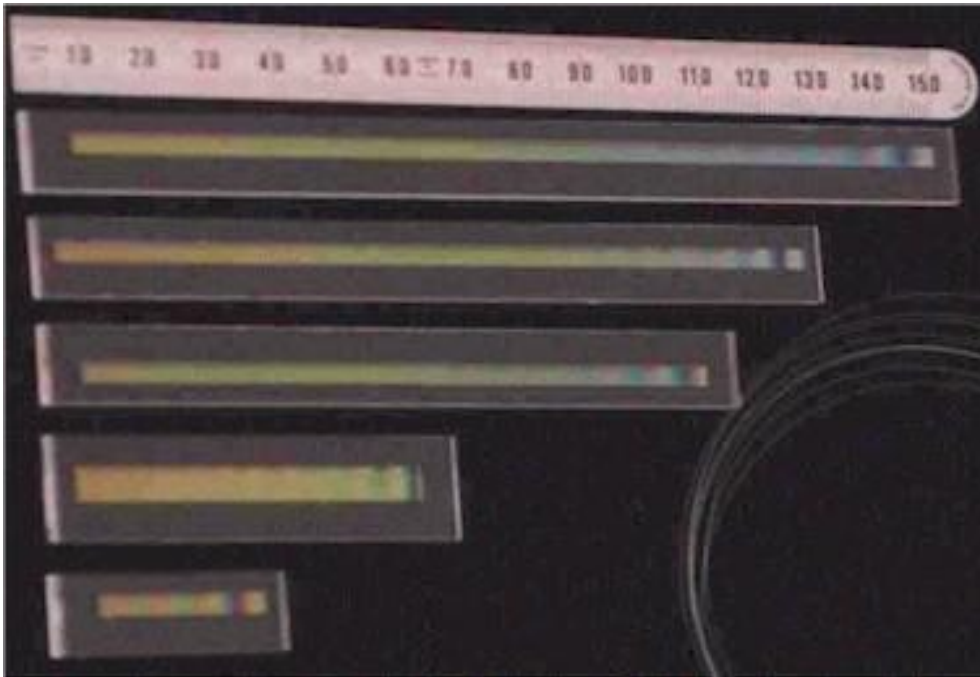


**Figure 2.11: Typical masks used at City University London for long period grating fabrication.**

LPGs are created by exposing the core of a fibre to an intense ultraviolet radiation through an amplitude mask, which is used to modulate the amount of ultraviolet light that is transmitted, thus allowing for a periodic refractive index change in the core of the fibre.

The setup for the inscription of LPGs in optical fibres using an amplitude mask is shown in Figure 2.12. Using this technique, a high level of repeatability in the characteristics of the LPGs fabricated can be achieved, subject to a very good alignment setup. In addition, the fabrication time taken using this technique, compared to that of the point-by-point fabrication method is much shorter (tens of seconds).

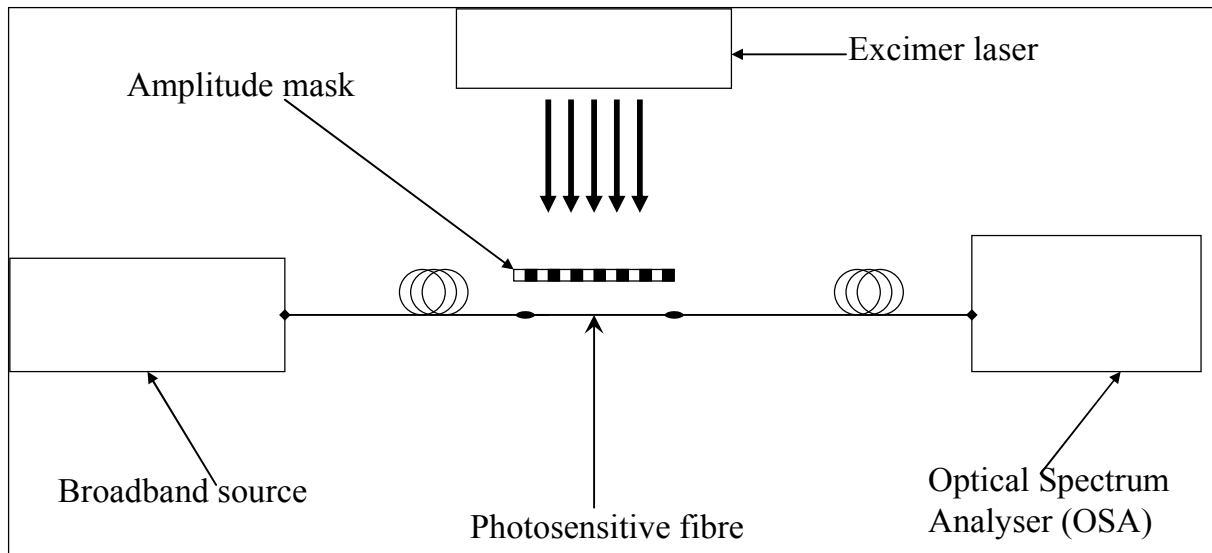


Figure 2.12: Fabrication setup of a LPG using an amplitude mask

## 2.5. Use of Long Period Gratings as sensors

Long period gratings have been used as temperature, strain, bend and refractive index, but they also have shown to be capable of simultaneously measuring these different parameters [13]. However in this chapter we will focus on each parameter independently.

### 2.5.1. Temperature sensitivity

LPGs are sensitive to different physical parameters and an important one is temperature, as discussed in [6] by Bhatia et al. in 1996, demonstrating the dependence of the resonant wavelengths of the attenuation bands on temperature. However as a LPG is also sensitive to other physical parameters, such as strain and bending, therefore under most circumstances, its cross-sensitivity is required to be compensated or to be eliminated if only one parameter is required to be measured.

The sensing mechanism of a LPG is based on the phase-matching condition resulting in a coupling wavelength  $\lambda$ , which is given by the following equation.

$$\lambda = (\delta n_{eff})\Lambda \quad (2.11)$$

where  $\Lambda$  is the grating periodicity and  $\delta n_{eff}$  the difference in refractive index between the core and cladding modes which can be expressed as,

$$\delta n_{eff} = n_{eff} - n_{cl} \quad (2.12)$$

where  $n_{eff}$  and  $n_{cl}$  respectively represent the effective refractive index of the forward propagated mode and the cladding modes.

The fibre parameters influence the effective indices of the core and cladding. But external variations in temperature or strain modulate the parameters of the fibre as well as the grating period and as a result changing the coupling wavelengths.

Assuming a perturbation  $\xi$  acting on a fibre on which a grating is inscribed with a period  $\Lambda$ .

Using the chain rule of derivative, the wavelength shift  $\frac{d\lambda}{d\xi}$  can be given by [5]

$$\frac{d\lambda}{d\xi} = \frac{d\lambda}{d(\delta n_{eff})} \frac{d(\delta n_{eff})}{d\xi} + \frac{d\lambda}{d\Lambda} \frac{d\Lambda}{d\xi} \quad (2.13)$$

By replacing  $\xi$  by T, the temperature sensitivity of a LPG can be described by the following equation [5]:

$$\frac{d\lambda}{dT} = \frac{d\lambda}{d\delta n_{eff}} \left( \frac{dn_{eff}}{dT} - \frac{dn_{cl}}{dT} \right) + \Lambda \frac{d\lambda}{d\Lambda} \frac{1}{L} \left( \frac{dL}{dT} \right) \quad (2.14)$$

Where  $\lambda$  represents a central wavelength of one of the attenuation bands, T the temperature and  $\delta n_{eff}$  the differential effective refractive index and L the grating length.

It can be seen from the equation that two factors have an impact on the temperature sensitivity of the LPG. The first one is the material contribution which is caused by a change in the differential effective refractive index due to temperature variations. The second is the waveguide effect which is a change in the grating periodicity, this effect can either be positive or negative depending on the order of the cladding mode [5].

The temperature sensitivity of LPGs is highly dependent on the type of fibres used, LPGs written in silica fibres tend to have a relatively low waveguide effect and this is mainly because the thermal expansion coefficient of silica is very small  $7.6 \times 10^{-6}/\text{C}$

A LPG written in a SMF 28 fibre with a period of  $210\mu\text{m}$  using a CO<sub>2</sub> laser, showed a temperature sensitivity of  $154\text{pm}/\text{C}$ . On the other hand LPGs written in B-Ge fibres have been reported as being highly sensitive to temperature. Sensors proposed by Shu et al. to measure temperature [33] showed a spectral shift of the wavelength of the attenuation band caused by temperature variations to be  $2.75\text{nm}/\text{C}$  over a range from 0 to  $10\text{C}$ . Venu et al. [34] proposed a temperature sensor with a sensitivity of  $1.4\text{nm}/\text{C}$  using a large optical band from  $1.2$  to  $2.2\mu\text{m}$ , thus allowing flexibility in the choice of light sources. For comparison the temperature sensitivity of FBGs is in the order of  $8.9\text{pm}/\text{C}$  [35].

One solution to overcome the temperature sensitivity is to make use of components that have the inverse effect. This is commonly used in electronics for example in oscillators and amplifiers, or in optical telecommunications by the use of dispersion compensating fibres. In effect this allows a linearization over a range of operation.

Temperature insensitive LPGs have been proposed by Jang et al. [36] by coating the LPG using a polymer showing a positive refractive index change with temperature. This would cause a blue shift in wavelength when the temperature increases, which is the inverse to the typical LPG's behaviour thus the effects would cancel each other. The problem is that most polymers show a negative refractive index change to temperature thus it is relatively difficult to find a polymer with a positive refractive index change to temperature [37]. Another

possibility is to choose the level of dopant (Boron and Germanium for example) to ensure that an increase in temperature would cause a blue shift, thus allowing for the use of a standard coating. This scheme can reduce the LPG temperature sensitivity down to 0.7pm/ C [36].

### 2.5.2. Refractive index sensitivity

The value of the refractive index directly outside the fibre cladding has a strong influence on the propagation properties of the LPG. The influence of the refractive index of the medium surrounding the cladding has been formulated by Bhatia in 1996 [5] and is given below:

$$\frac{d\lambda}{dn_{sur}} = \frac{d\lambda}{dn_{m,clad}} \frac{dn_{m,clad}}{dn_{sur}} \quad (2.15)$$

Where  $n_{sur}$  is the refractive index surrounding material and  $n_{m,clad}$  the effective cladding refractive index at the  $m^{\text{th}}$  cladding mode.  $d\lambda$  shows the shift in wavelength of the attenuation bands.

Figure 2.13 shows the transmission spectrum of a LPG immersed at different water levels. It can be seen that the higher the level of water the more the signal is shifted towards the shorter wavelengths.

The water level corresponds to the amount proportion of the LPG being immersed. Thus at 0% the LPG is surrounded by air and at 100% it is submerged, thus the external refractive index goes from about 1.5 to about 1.33.

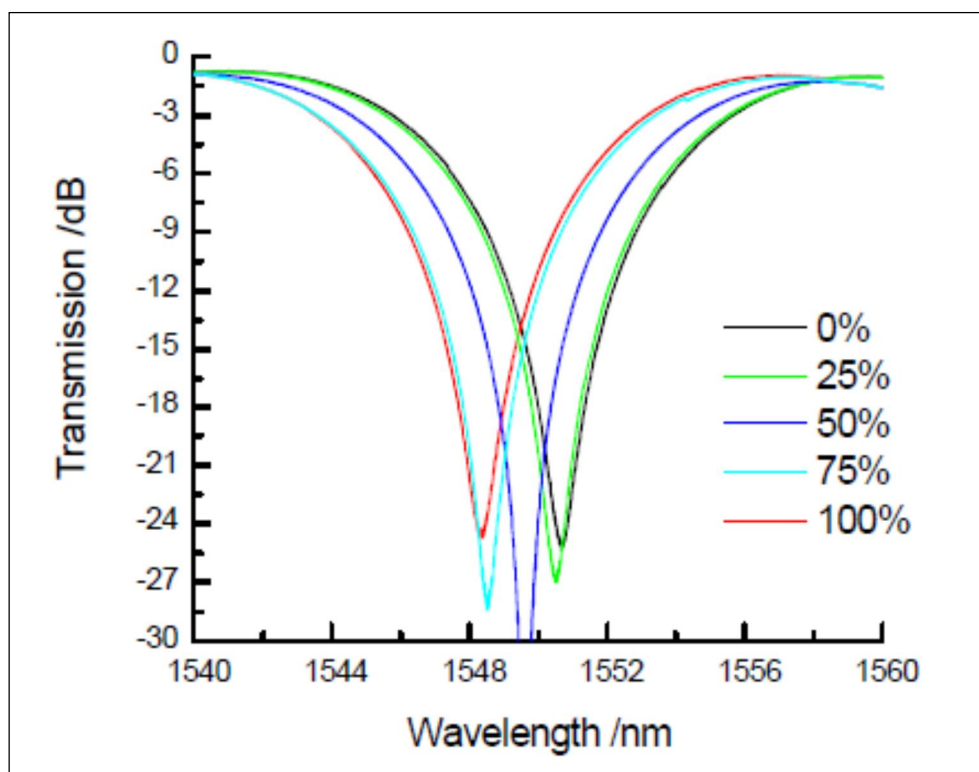


Figure 2.13: Transmission spectrum of a LPG depending on the amount of immersion of the LPG. [37]

Refractive index sensors based on LPGs have been proposed, by Keith et al. [38] for the measurement of refractive indices of different oils and mixtures. A potential application would be for use in aircraft fuel tanks, but this has not yet been reported.

Due to the length of LPGs and their sensitivity to the external refractive index they can be good candidates for level sensors, such a sensor was proposed by Grice et al. in 2009 [39]. They measured the level of water and fuel in a glass tube. The level of fluid causes a change in the attenuation peak of the LPG.

### 2.5.3. Strain sensitivity

The change in the attenuation wavelength of an LPG caused by an axial strain is given by the following equation: [5]

$$\frac{d\lambda}{d\varepsilon} = \frac{d\lambda}{d\delta n_{eff}} \left( \frac{dn_{eff}}{d\varepsilon} - \frac{dn_{cl}}{d\varepsilon} \right) + \Lambda \frac{d\lambda}{d\Lambda} \quad (2.16)$$

Where  $\lambda$  is the central wavelength of the attenuation band,  $\varepsilon$  the axial strain and  $\delta n_{\text{eff}}$  the effective refractive index.

The variation of wavelength caused by the strain is dependent on waveguide and material contributions. The material contribution is related to the change in differential refractive index of the core, cladding and geometrical changes in the fibre caused by the axial strain [5]. The waveguide change is related to the period of the grating as well as the order of the attenuation modes. For LPGs with a period longer than  $100\mu\text{m}$  written in standard single mode fibre, the waveguide and material contribution have an opposite effect on the wavelength, thus it is possible to create a strain insensitive LPG ( $4\text{pm}/\mu\varepsilon$ ) [40].

A high strain sensitivity using LPGs can be achieved ( $221.4\text{pm}/\mu\varepsilon$ ) by choosing a very short period ( $40\mu\text{m}$ ) as proposed by Bhatia et al. [5], while FBGs, tend to have typical strain sensitivities in the order of  $1.2\text{pm}/\mu\varepsilon$ . Recent work has shown that the cross sensitivity between strain and temperature can be achieved by using photonic crystal fibres written using  $\text{CO}_2$  laser beams [41], this is achieved by creating grooves on the fibre cladding by repeating the writing of each period leading to a gasification of the surface of the fibre. It is possible to separate the strain from temperature effect based on its birefringence variation [13]. The applied strain causes each attenuation band to be split into two components, corresponding to the two orthogonal polarisation states. The wavelength of attenuation is directly related to the birefringence, and the increase in load causes an increase in the separation between the wavelengths of the attenuation bands. A more practical way of inducing birefringence is to use a highly birefringent (Hi-Bi) fibre or elliptical core fibres [42].

#### 2.5.4. Bending sensitivity

In his original work, Bhatia [5] demonstrated that LPGs are extremely sensitive to small bends. The bend can cause the attenuation bands of the transmission spectrum of the LPG to shift [43] or split each of the attenuation bands into two [44], [45].

Bhatia reported that the shift in wavelength of the attenuation bands caused by the bend increases the bandwidth of each attenuation band and decreases their intensity. An explanation to this phenomenon was proposed by Vengsarkar et al [6].

Two reasons have been found to be correlated with the effect. The first is that bending the LPG is creating a change in the effective refractive index of the cladding which directly

changes the wavelength of the attenuation bands. The second is due to the amount of light that is leaked out of the fibre through the cladding-air (or other surrounding material) interface. This is causing a decrease in the amount of signal that is transmitted.

This sensitivity arises from a change in the cladding mode, assuming the fundamental guided mode is also confined in the core. When the bend arises the cladding modes are scattered out of the fibre, thus the coupling between the guided and cladding modes is changed. The perturbation due to the bend depends on different parameters such as the radius of curvature, wavelength, and order of the mode, the fibre refractive index as well as the refractive index of the material surrounding the cladding.

The measurement of the bend requires a pair of translation stages in order to control the amount of bend that is applied. Figure 2.14 shows a typical setup for the measurement of the bend. By moving one of the translation stages towards the other, the fibre is subject to a pressure forcing in to bend. The amount of curvature was measured using a surveying compass.

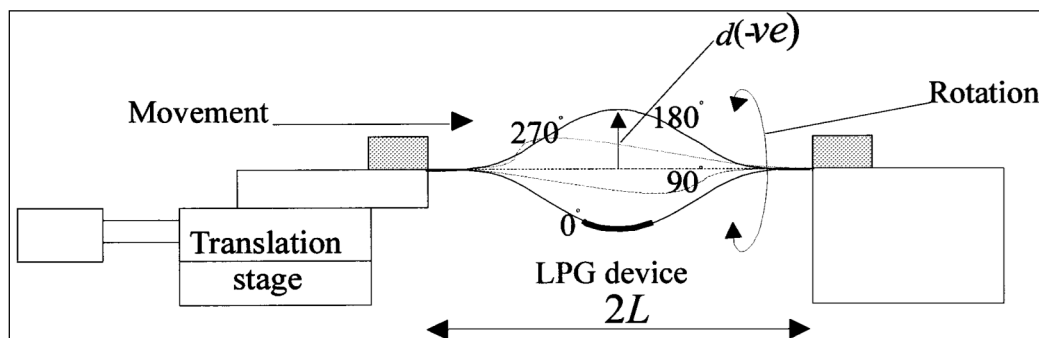


Figure 2.14: Setup for the measurement of the bending effect on a LPG [46]

The split of the attenuation bands was investigated by Liu et al. [47]. They found that when a LPG was subject to a bend, the attenuation bands of lower cladding modes were split into two. This phenomenon can be explained by the fact that the bending of a fibre causes a loss of symmetry in the spatial degenerate cladding modes, thus the fibre becomes non-degenerate. This is causing a polarisation mode splitting. Subsequently this causes 2 values of effective refractive index satisfying the core/cladding coupling conditions therefore leading to a resonance band splitting in the LPG spectrum.

The measurement of the separation between these two peaks gives a very good bending sensitivity (up to  $251\text{nm/m}^{-1}$ ) [48], much higher than that using a typical detection method

(14nm/m<sup>-1</sup>). The bending sensitivity can be increased by using higher order modes as discussed by Shu et al. [49] and Ye et al [50].

Another way of increasing the sensitivity of LPGs to bend is to create a rotation of the LPG, which was proposed by Patrick et al. [43]. This, however, generally requires the use of a highly Ge-doped fibre with a large core concentricity error [47].

In practice, the bending effect has been demonstrated as an efficient way to measure the dynamic process of structures, and their monitoring [51]. More recent work made use of the bending sensitivity of LPGs to create a vibration sensor [52]. The system shows a linear response to the amount of vibration that is generated by a piezo transducer.

#### 2.5.5. Sensitivity to other parameters

As discussed above LPGs are sensitive to different parameters such as bend, temperature, and refractive index. Some of these changes can be very useful for the detection of sound waves and this will be discussed in detail in the following chapters.

## 2.6. Summary

In this chapter the operating principle of long period gratings used as sensors is discussed in detail, following a review of the LPG fabrication techniques and wave guiding in both FBGs and LPGs.

To have a good grasp of the operating principles of light transmission mechanisms in optical fibres, this chapter started with the concept of modes and mode coupling leading to the use of FBGs and LPGs.

The reported fabrication techniques used for manufacturing LPGs have been reviewed. There are 2 main methods for the inscription of LPGs: one is through the physical deformation of the fibre, which can be performed using mechanical stresses and the other the index modulation, which modulates the core or the cladding of the fibre. Both can be realized by using CO<sub>2</sub> laser irradiation, an electric arc discharge, ion implantation or more commonly the UV irradiation using photosensitive fibres.

The sensitivity of LPGs to different parameters such as the temperature, strain, refractive index, and bending was discussed. Techniques reported to improve the sensitivity to these parameters and to eliminate the cross-sensitivity of LPGs have also been discussed.

# **Chapter 3**

## **Review of optical fibre based techniques for sound detection**

### **3.1. Introduction**

The first reported implementation of the concept of acousto-optic effect was proposed by Alexander Graham Bell in 1880 [53]. The system was called a photophone which used a selenium cell with its electrical resistance varying inversely with the level of light applied on it. Thus the light beam was modulated by a mirror made to vibrate by the voice of an operator.

This invention, however, was not practically viable due to its high sensitivity to interferences such as variations in luminosity caused by weather change or outdoor interferences. In 1935 Von Ohain [54] proposed an optical microphone using an interferometer. Since the end of the Second World War the research in optical detection of sound has been intensive. Following the development and use of optical fibres, the first optical fibre based microphone was proposed by Culshaw et al. in 1977 [55], whose fundamental principle was based on the sound-induced change of refractive index ( $n$ ) causing a shift in the frequency of the optical signal.

This chapter presents a review of a number of different fibre optic based techniques used for the detection of sound waves transmitted in different media. The industrial need for fibre optic based acoustic detection is constantly increasing. Industrial sectors, such as the oil industry, require the measurement of seismic waves using a more cost-effective approach to replace large arrays of geophones or hydrophones which are currently being used with high sensitivity, but coupled with high cost and high fragility. The optical fibre based acoustic sensors have demonstrated high versatility, low cost, high immunity to disturbance especially electromagnetic fields, therefore have shown promise. In the last section of this chapter discussions will be made in relation to the potential for sensor arrays and distributed fibre optic acoustic sensors.

## 3.2. Classification of optical fibre techniques for sound detection

There are different types of optical fibre detection systems available for sound detection, thus it is important to create a systematic classification. [55] Such taxonomy could be based on different approaches such as the fabrication method, the nature of the signal, the suitability for a particular application etc. The classification chosen here is based on the type of modulation. This is because the underpinning principle is similar given the same type of modulation.

The modulation of light in a waveguide can be undertaken in three major yet different ways, i.e. intensity, phase and polarisation modulations. It is important to note that if the phase or polarisation modulation technique is used, the light modulation will have to be converted from polarisation or phase to intensity, since photo-detectors can only detect intensity modulation.

### 3.2.1. Types of modulation:

**Intensity modulation:** This type of modulation acts on the optical power of the light source. There are two approaches to monitor the intensity modulation. The radiated waves method is based on the amount of energy that is sent out of the optical path. And the evanescent waves method is based on the mode coupling [56], [57].

**Frequency (or Phase) modulation:** These optical microphones can either use an interferometer or a grating to perform the frequency to amplitude modulation conversion.

**Polarisation modulation:** This technique is not very commonly used. Early devices were based on liquid crystals and differential index shifting. But more recent techniques involve the use of birefringent elements such as a polarisation maintaining fibre. The conversion from polarisation modulation to amplitude modulation is done by using a polariser.

### 3.2.2. Definitions

**Sound pressure:** The sound pressure is the pressure deviation from the ambient atmospheric pressure caused by a sound wave. In air the sound pressure is measured using a microphone and in water using a hydrophone. A measurement system is thus used to quantify the *sound pressure level*, which is a logarithmic measure (dB) of the sound relative to a value of reference. This value of reference has been defined to be 20  $\mu\text{Pa}$  RMS in air. This value was chosen because it is the threshold of hearing of humans at the frequency of 1 kHz. In the case of water the value of reference is 1  $\mu\text{Pa}$  RMS [58]. These values are defined by the American National Standard Institute (ANSI)

Equation (3.1) is used to calculate the sound pressure level given the acoustic power.

$$I_P = 20 \log_{10} \left( \frac{P_{rms}}{P_{ref}} \right) \quad (3.1)$$

With  $P_{rms}$  the sound pressure measured and  $P_{ref}$  the sound pressure of reference. It is critical to mention the distance between the measuring devices to the sound source. The standard distance is 1 meter from the acoustic source. Also in the case of measurements taking place in a closed room, it is preferable to use an anechoic chamber in order to avoid reflections and make the measurements comparable to a free field environment.

**Bandwidth:** It is the difference between the upper and lower frequencies in a single set of frequencies. In this work, the term bandwidth will be used to define the frequency range that the sound detection systems can detect.

### 3.2.3. Acoustic detection setups

Figure 3.1 summarizes different types of optical microphones that have been reported in literature:

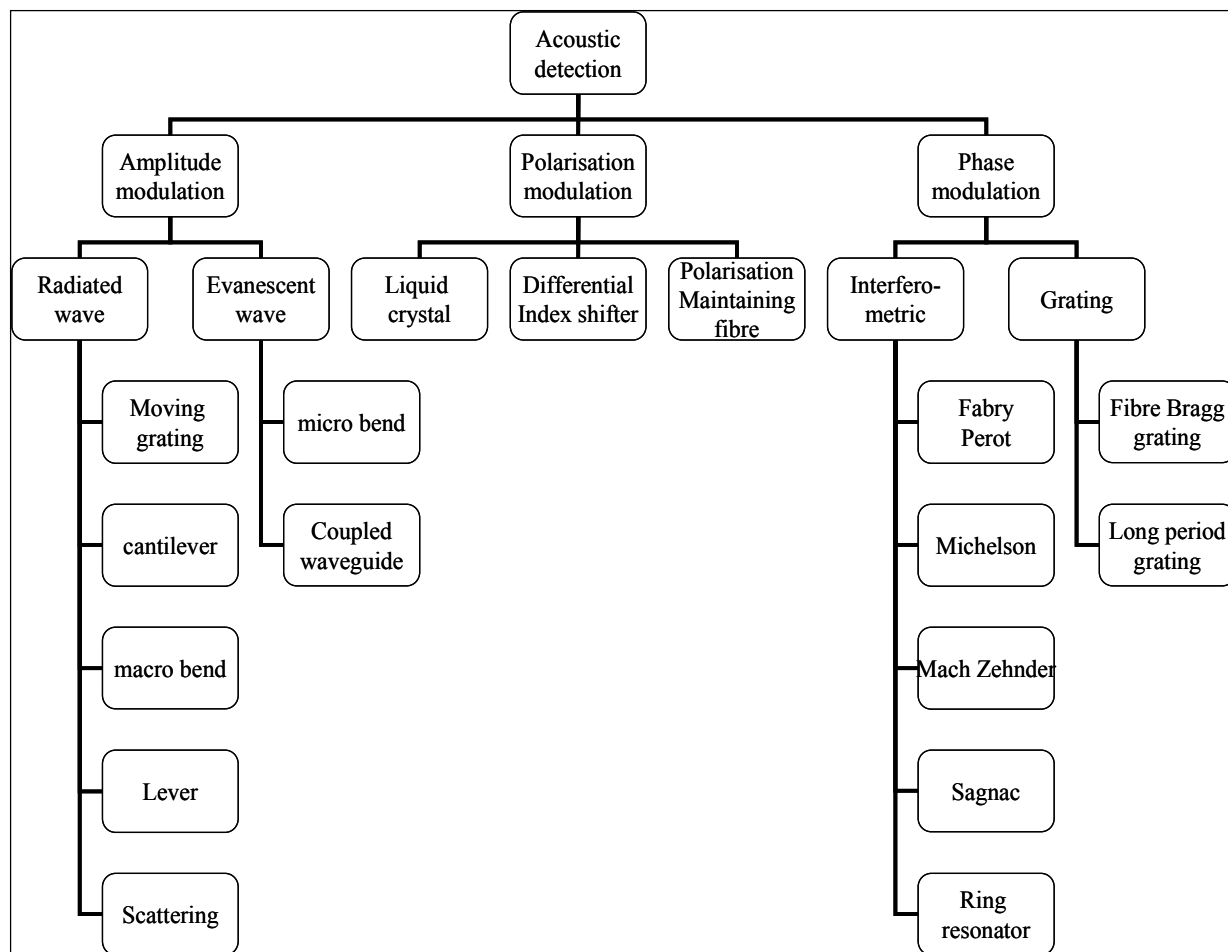


Figure 3.1: Operating principles of acoustic detection systems

Most microphones and hydrophones presented in this review are composed of two optical ports, one is the source (LED or Laser) and the other is a photodiode receiving the optical signal. Acoustic detection can be done in different environments such as air, liquids, gases and composite structures.

### 3.3. Intensity Modulation

#### 3.3.1. Radiated wave

In the radiated wave intensity modulation subgroup five different techniques to detect sound have been proposed. The principle for each of these systems and examples of practical implementations will be described in this section. The advantage of intensity based sensors is their simplicity together with the fact that they do not require the use of single mode fibres

and do not require a coherent source. However they tend to be dependent on the fluctuations in power from the light source which leads to errors in the measurement.

Moving Grating: A microphone system was proposed by Fulengwider and Gonsalves [56] in 1980 and later a fibre based hydrophone proposed by Spillman and Mc Mahon [57]. It involves the use of a grating attached to a diaphragm, as shown in Figure 3.2. The acoustic wave creating a periodic displacement of the grating modulates the amount of light that is transmitted. This setup could detect sound wave of 100Hz to 2.5 kHz with a minimum detectable acoustic pressure varying from 45 to 60dB ref  $1\mu\text{Pa}$ .

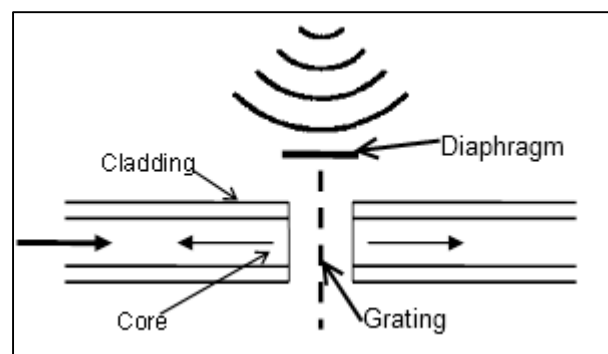


**Figure 3.2: Principle of the moving grating based sensor.**

The cantilever technique: It was first proposed by Fulhengwider and Gonsalves in their patent [56], the device uses a multimode optical fibre (for ease of alignment) one of the fibres is fixed and the other one attached to a membrane as shown in Figure 3.3. Each end of the fibre is polished and tapered for improved responsivity. Practical implementations have also been proposed by Spillman and Mc Mahon [59]. The authors reported a minimum detectable signal of about 55dB ref  $1\mu\text{Pa}$  over a frequency range of 100Hz to 10 kHz.

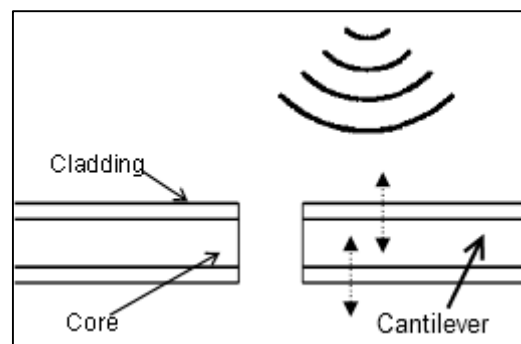


**Figure 3.3: Cantilever based setup**

Macro bending loss: Macrobend losses occur when a fibre is bent to a radius, also called critical radius ( $<10\text{mm}$ ), the light propagating through it experiences attenuation.

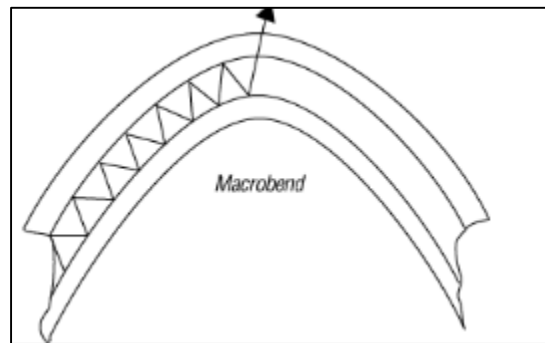


**Figure 3.4: Macrobend on an optical fibre**

As illustrated in Figure 3.4, the amount of power loss is related to the bend radius; the lower the bend radius the higher the loss. This property can be used to realize an acoustic sensor based only on a single loop of single mode fibre. The effect of bending losses in a coiled optical fibre was originally proposed for the design of a hydrophone by Giallorenzi et al. [60]. More recent work has been reported by Sun et al. [61] describing the device making use of the bending loss of the single mode-multimode-single mode (SMS) structure varied by the sound wave. In order to improve the sensitivity, the fibre was attached to an aluminium membrane and shows a resonant frequency that is dependent on its size. The bandwidth of the device ranged from 20Hz to 20 kHz; however the frequency response was not flat. In addition to macrobend acoustic sensors, microbend acoustic sensors have also been developed, which will be discussed later in this chapter.

Moving membrane: These sensors have been subject to intensive research, a microphone using a pair of single mode fibres was proposed by Garthe [62] in 1991. The original setup made use of step index single mode fibres but subsequently used lenses to couple the light from one fibre to the other however the noise level was still very high (62 to 64 dB). Improvements were made to the detection system by using a differential detector and in 1993, Garthe proposed a setup whose noise level was reduced to 38dB [63]. One issue with this type of sensors is that they can sometimes show a non-linear response and a solution to this has been provided by Hadjicoulas et al. [64] by using a force feedback transducer.

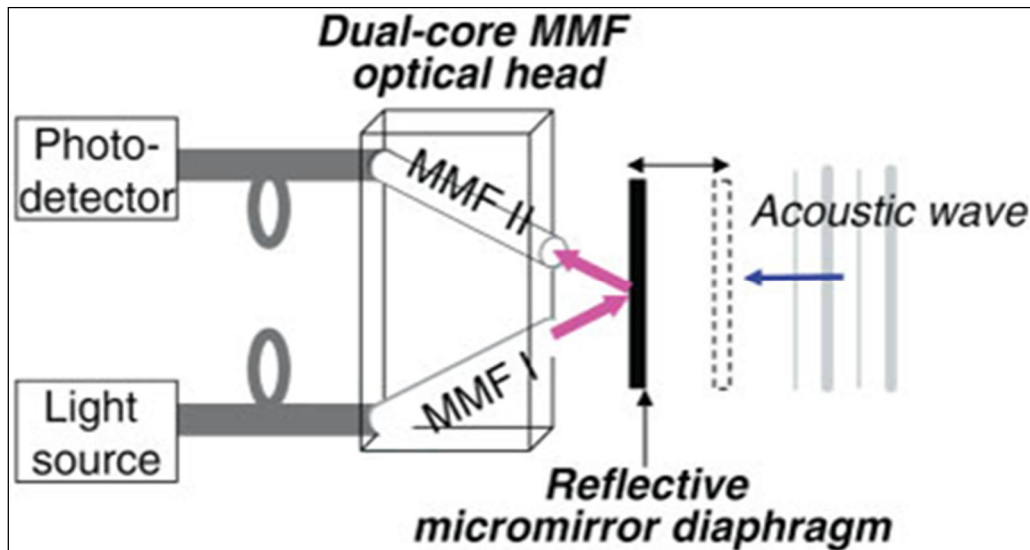


Figure 3.5: Schematic structure of the microphone based on a moving diaphragm. Song et al. 2007 [65]

More recent work was proposed by Song and Lee (2007) [65]. The device uses a multimode fibre combined with a micro-mirror based diaphragm. It exhibits a bandwidth of 3 kHz with a variation of about 15dB in the frequency response; the setup of the system is displayed in Figure 3.5. Based on a similar setup, Sun et al. proposed a microphone using a foil as a membrane [66], showing the advantage of being low cost thus disposable.

Scattering based: Scattering is the process that forces light to deviate from a straight trajectory. There are 3 different types of scattering, Brillouin, Rayleigh and Raman scattering, which are briefly described below.

- *Rayleigh scattering* is caused by the irregularities in the refractive index of the fibre core. These random variations of refractive index appear during the manufacturing process of the fibre.
- *Raman scattering* is caused by the molecular vibrations of glass fibre stimulated by incident light.
- *Brillouin scattering* arises when light in a medium interacts with time dependent optical density variations. These density variations can be caused by the light that is emitted in an optical fibre but also caused by external environmental changes such as temperature, strain or acoustic pressure etc.

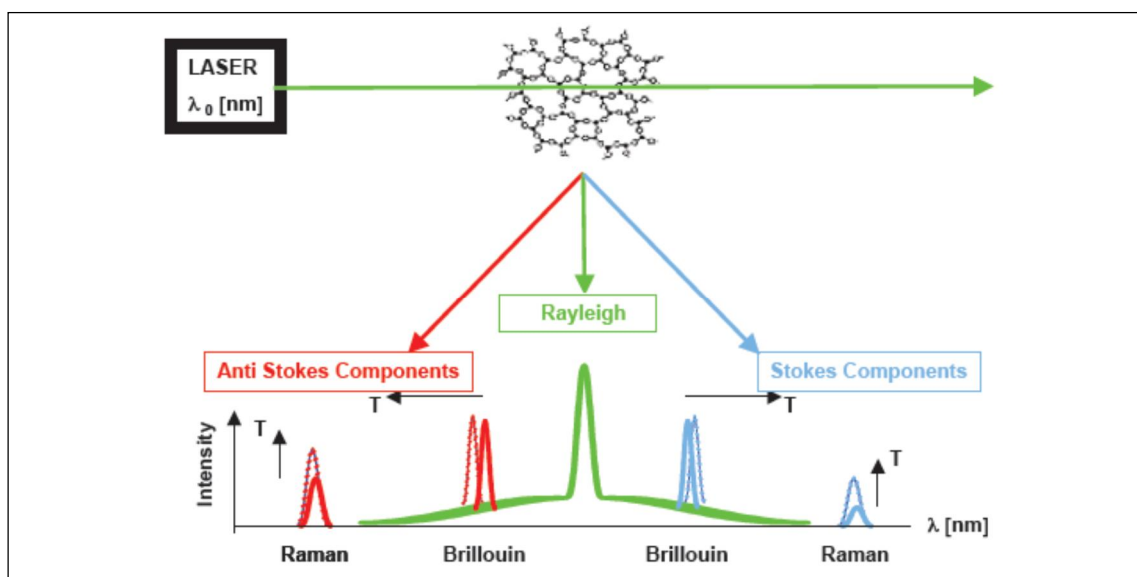


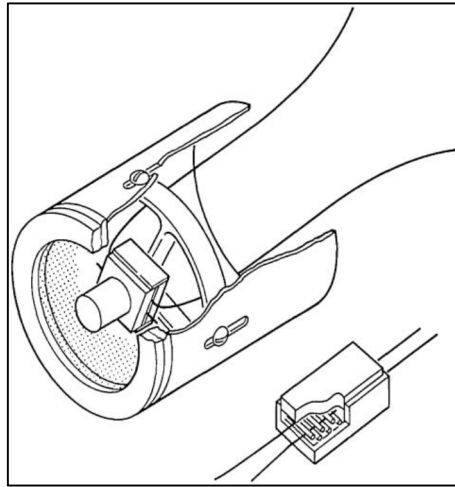
Figure 3.6: Spectrum of three different types of light scattering.

Figure 3.6 shows the three different types of scattering and their respective effect on the intensity and wavelength of the light. Building on this, the detection of strain variations using single mode optical fibres was proposed by Parker et al. [67], [68] in 1997. They used a series of long optical fibres each portion being subjected to different temperature or strain conditions. More recent work has been focused on the detection of dynamic strain and vibrations.

### 3.3.2. Evanescent wave based

Microbending: Acoustic sensors relying on the micro bending losses make use of the intrinsic bending losses in optical fibres. When a fibre is subjected to microbends, some of the light in the core of the fibre exceeds the critical angle causing some guided higher order core modes to couple to the cladding modes causing transmission losses. By monitoring the loss in light intensity, different types of microbend sensors can be designed. An early system proposed by Fields et al. [69] is composed of a bending loss modulator as shown in Figure 3.7. A hydrophone was proposed by Fields and Cole using a step index multimode fibre placed between a pair of ridged plates acting as the modulator. The minimum detectable acoustic pressure was reported to be of 95dB ref 1 $\mu$ Pa. The sensor proposed could detect sound waves from 100Hz to 2 kHz. A more recent acoustic sensor was proposed by Tsutsui et al. in 2004, [70] and it was used to monitor the deformation of composite materials. The

higher the deformation the higher the bend thus the lower the amplitude signal being transmitted to the photodiode.



**Figure 3.7: Fibre micro bend acoustic sensor. From Fields and Cole 1980 [69].**

Mode coupling: Another technique to monitor sound waves using intensity modulation can be done by using mode coupling in waveguides. Sheem et al. [71] reported on the sensitivity of optical couplers to acoustic signals. More recent work by Chen et al. (2006) [72] demonstrated that the incident strain field altered the length of the fused-tapered coupling region, resulting in a change in the coupling coefficient of the device.

### 3.3.3. Lock-in demodulation

If the signal to be detected is relatively noisy, it would be useful to use lock-in demodulation, which enables the effective extraction of a signal from a noisy background.

The type of detection, however, only works for AC signals and requires a reference signal frequency. It is composed of a multiplier with a reference input and a measurement input. The output of the multiplier is then integrated using a low pass filter whose time constant is greater than that of the signal. Assuming both the input and reference signals are sine waves, a signal will be present at the output only when the sine waves are at the same frequency based on their orthogonal property. Figure 3.8 shows a typical diagram of a phase sensitive detector. This type of demodulation offers a better noise performance than the standard rectifier technique and can be used for a wide range of applications. [73]

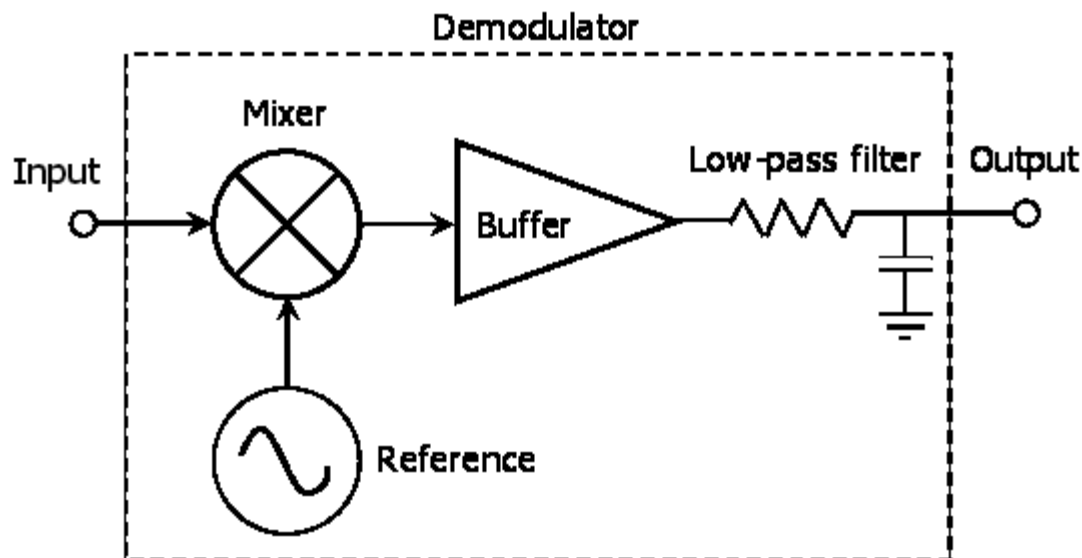


Figure 3.8: Phase Sensitive detector

In a practical experiment this would involve modulating the light emitted for example, by use of a chopper wheel, or an optical modulator at the frequency of the reference signal.

### 3.4. Phase modulation and demodulation

The literature on phase modulated optical fibre based acoustic sensors is extensive. This section includes two parts, i.e. the interferometric techniques which employ an interferometer to convert the phase shift into an amplitude variation and the grating based phase modulation which uses the wavelength shift induced by the strain variation on the fibre. Phase modulating optical modulators can be affected by optical phase noise and must use a coherent light source and also they should normally use single mode optical fibres.

Demodulation is required in order to retrieve the signal and the interferometer based technique can be classified into two types, i.e. homodyne and heterodyne approaches. The homodyne technique refers to a system where the interference between the two interfering beams has the same frequency whereas the heterodyne refers to the beams with different frequency. The frequency shift in one of the beams can be produced by acousto-optic modulation [74] for example. One advantage of using the interferometric technique is that it is capable of resolving variations many orders of magnitude lower than the wavelength of the light used in the sensors. In order to obtain high resolution it is necessary for the

interferometer to be operated at quadrature. It is thus necessary to control optimum operating point. A technique proposed by Dandridge et al. [75] is used to eliminate signal fading and environmental perturbations influencing the path length difference of the interferometer away from its quadrature state. The technique involves applying a sinusoidal modulation of known frequency and amplitude on the interferometer's phase difference. The signal is subsequently detected and the follow-up signal processing enables the separation between environmental perturbations and the relevant phase shift. The limitations of the sensitivity due to quantum noise of this scheme were analysed by Tayag et al. [76]

Another technique such as nulling configuration enables the blocking of light from a bright source to detect a faint source at its vicinity. It uses destructive interference between two coherent beams.

### 3.4.1. Optical fibre interferometers

Interferometer based modulators operate by changing the refractive index or the length of an optical test path. The signal is recombined with the signal from a reference path.

In an optical fibre of length  $L$ , the phase  $\varphi$  passing through it is given by:

$$\varphi = \beta L \quad (3.1)$$

With  $\beta$  the propagation constant given by:

$$\beta = n_{eff} k_0 \quad (3.2)$$

Where  $n_{eff}$  is the effective refractive index of the fibre core and cladding and  $k_0$  the wave number  $(\frac{2\pi}{\lambda})$ .

A change in phase causing a change in interference is required for use as a sensor. From equation (3.2) the change in phase can be performed either by changing the length ( $\Delta L$ ) or the propagation constant ( $\Delta\beta$ ). Thus:

$$\Delta\varphi = \beta\Delta L + L\Delta\beta \quad (3.3)$$

These two parameters, however, are not independent. For example stretching an optical fibre increases the length ( $L$ ).

The first optical fibre interferometer using single mode fibres reported for the detection of acoustic waves was proposed by Bucaro et al. [77] in 1977. The setup was used to detect ultrasonic waves (40-400 kHz) in water. It showed a relatively flat frequency response [78]

and the interferometer chosen for this purpose was a Mach-Zehnder interferometer with the setup being shown in Figure 3.9(a). Experiments focusing on the detection of sonic waves under water were later reported by Jarzynski [79]. A similar setup was presented by Cole et al. [80] but the sensor was able to detect sound waves of up to 100 kHz.

The use of multimode fibres as Mach-Zehnder interferometer for the detection of acoustic waves can be difficult due to the different phase modulations experienced by each mode in these fibres; a study of these phenomena has been done by Culshaw et al. in 1977. Another difficulty is the fact that the sound waves generate a very small strain which is intrinsically difficult to detect. Recent work by Zeng et al. [81] led to the development of a directional Mach-Zehnder based hydrophone using a diaphragm, the sensitivity level was reported to be -139 dB re V/ref 1  $\mu$ Pa from 100 Hz to 5 kHz.

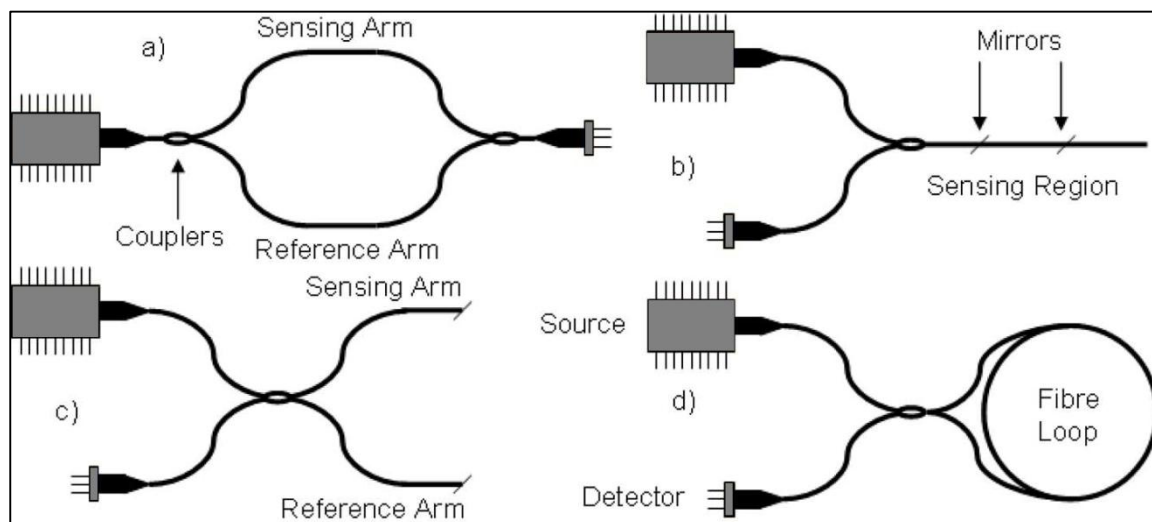


**Figure 3.9:** (a) Mach-Zehnder; (b) Fabry-Perot; (c) Michelson; (d) Sagnac. From Wild et al. [82]

Another type of interferometers is the Fabry Perot; it is based on the fact that the acoustic pressure changes the index of refraction of the core and cladding of an optical fibre, thus creating a variation in the optical path length of the guided light. But in order to have a Fabry Perot cavity in an optical fibre there is a need to build a pair of mirrors into the fibre, as shown on Figure 3.9(b). This can be done by using a coherent light source and cutting each end of the fibre used to measure the signal perpendicular to the fibre axis, this was proposed by Bucaro et al. in 1978 [83]. A practical implementation of an in-fibre Fabry Perot acoustic sensor for detection of acoustic waves in composites and plastic materials was proposed by Alcoz et al. [84] in 1990. The system is composed of a continuous length single mode fibre coated with a  $\text{TiO}_2$  film (acting as mirrors) on either end with one end being spliced to an

uncoated fibre using an arc fusion splicing method. It can detect ultrasonic waves from 100 kHz to 5MHz. More recent work proposed by Lima et al. [85] in 2009 makes use of Fibre Bragg Gratings (FBG) to create the mirrors of the Fabry Perot cavity. A diaphragm is attached to one side of the fibre, when the acoustic pressure causes the diaphragm to vibrate and this induces simultaneously a change in the grating spectrum (shift of the Bragg wavelength) and changes the length of the Fabry Perot cavity.

A different architecture of interferometer that can be used is the Michelson interferometer shown in Figure 3.9(c). It was first proposed by Imai et al. in 1980, [86] further work by the same author led to the development of a multimode fibre based microphone. In order to improve the sensitivity and reduce the noise level of optical fibres to acoustic waves in water, Garrett et al. [87] proposed to use both legs of the Michelson interferometer, each leg of the interferometer responding to the strain generated by the acoustic waves in opposite signs. Also the sensing section of the optical fibre can be turned into a coil or mandrel. Recent work based on this architecture has been proposed for the detection of sound along the littoral [88] sea bed and underground, an array of sensors based on a combination of Time Division Multiplexing (TDM) and Wavelength Division Multiplexing (WDM) is used to monitor the large area.

WDM allows the interrogation of different sensors simultaneously using a single optical fibre. This is done by emitting light at different wavelengths, there is however a requirement on the coherence of the light that the emitted wavelengths should not interfere with each other. Indeed the limitation on the channel density is limited by crosstalk between adjacent channels, thus potentially reducing the signal to noise ratio. Thus this technique requires highly stable light sources and narrow band filters and precise clocks. Research on techniques to monitor and reduce this phenomenon is ongoing [89], [90].

TDM normally requires the use of a switch that is used to interrogate the system; such a technique was used by Kersey et al. [91] to monitor several interferometric fibre sensors. This technique is also subject to crosstalk which can happen due to insufficient bandwidth, thus causing an overlapping between the pulses.

Other architectures have been proposed such as the Sagnac based interferometer as shown in Figure 3.9(d) and the main advantage of the Sagnac over the Mach-Zehnder interferometer is

the insusceptibility to polarisation induced signal fading [92]. This led to further research and the use of Sagnac interferometers in acoustic sensor arrays. [93]

### 3.4.2. Optical Fibre Bragg Grating sensors

As discussed earlier; the first in-fibre Bragg grating was demonstrated by Hill [7] in 1978. A Fibre Bragg Gating (FBG) can be fabricated by writing a periodic (or aperiodic) variation to the refractive index of the fibre core, which generates a wavelength specific mirror, thus induces a reflection. The reflection wavelength is called Bragg wavelength ( $\lambda_B$ ), it is determined by the period  $\Lambda$ , and the effective refractive index of the core of the fibre ( $n$ ).

The Bragg wavelength is given by the following formula:

$$\lambda_B = 2n\Lambda \quad (3.4)$$

In order to use a FBG as an acoustic sensor, its Bragg wavelength must be modulated by the sound wave. From equation (3.5), it can be seen that the change in wavelength can be caused by a change in the effective refractive index ( $\Delta n$ ) of the core of the fibre or by the change in the period of the grating ( $\Delta\lambda$ ). This is given by:

$$\Delta\lambda_B = 2n\Delta\Lambda + 2\Lambda\Delta n \quad (3.5)$$

Original work on the detection of acoustic waves using FBGs was performed in water and this first report related to the detection of acoustic waves using FBG's was proposed by Webb et al. [94] in 1996. The setup shown in Figure 3.10 is composed of a laser diode, a two by one coupler and the sensing FBG working in reflection mode. The FBG was placed in a water tank, and an ultrasonic piezo electric transducer placed near the fibre was used to produce the ultrasonic waves. The initial frequency of emission of the ultrasound transducer was 950 kHz and the power up to 30 Watts, but the data related to the sensitivity was not documented. The acoustic pressure creates a strain on the grating which subsequently causes a shift in the Bragg wavelength of the FBG. Since the reflection spectrum of the FBG is within one of the slope of the spectrum of emission of the laser diode, the conversion from wavelength shift to intensity variation is done directly as proposed by Fomitchov et al. [95]. In this work the authors found that the maximum detectable acoustic frequency was set by the length of the grating. Furthermore the length of the grating should be less than half the

acoustic wavelength in the fibre core. This is so that the grating is subject to a uniform strain [95]. Similar work was undertaken by Takahashi et al. [96] in Japan at around the same time but using signals at 20 kHz, the minimum detectable acoustic pressure was found to be 65.3dB ref. 1 $\mu$ Pa at a distance of a few centimetres. A numerical analysis of the response of a FBG to ultrasonic waves was undertaken by Coppola et al. [97] in 2001.

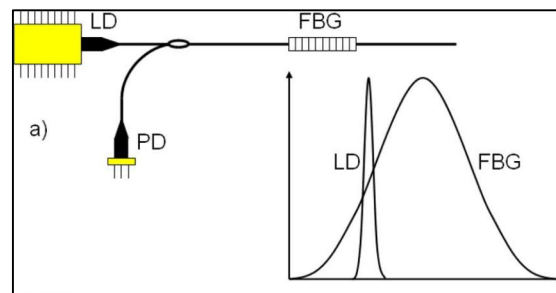


**Figure 3.10: FBG detection system using a narrow line-width laser diode.**

In order to detect the maximum signal intensity the wavelength of the laser should be locked to the mid reflection wavelength of the FBG. This can be done by using an electronic feedback system.

The temperature variation in a water tank for example can cause the Bragg wavelength to change, therefore in order to overcome this, there is a need to monitor the temperature and change the wavelength of emission of the laser or the Bragg wavelength of the matched FBG accordingly. A solution proposed by Tanaka et al. [98] is to make use of a shielded matched FBG, which is also placed in the water tank, thus a change in temperature will create a change in the Bragg wavelength of both FBGs thus making the sensor temperature-insensitive.

Perez et al. [99] proposed a system that uses a matched FBG acting as a frequency demodulator and the setup is shown in Figure 3.11. This allows the use of a broadband source, the main advantage of this system is the lower cost and the insensitivity to small wavelength shifts of the source power. The latter is achieved by using a pair of photodiodes to cancel the fluctuations in source power. In this setup the FBG was bonded on to an aluminium plate and the system proposed can detect ultrasonic waves generated at a distance of up to 30cm from the source.

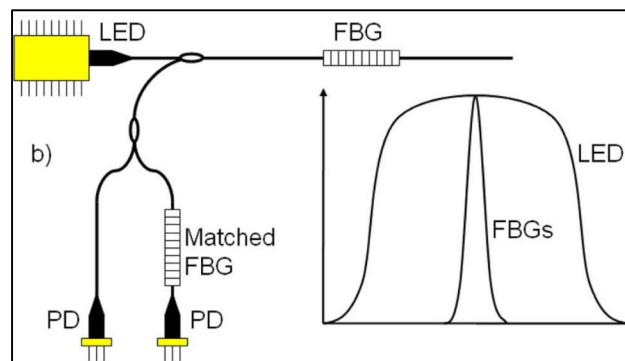


Figure 3.11: FBG detection scheme using a SLED source.

It was found that due to the impedance mismatch between air and the optical fibre the coupling of the sound wave to the fibre was inefficient. Work by Cusano et al. [100] led to an improvement of the sensitivity using plastic coatings, the minimum detectable acoustic pressure was 113.9dB ref  $1\mu\text{Pa}$ , at a distance of 1 to 2.2 meters. More recent work by Moccia et al. [101], [102] led to the development of an underwater resonant FBG as the resonance frequency depends on the size and geometry of the coating surrounding the FBG.

The detection of sound waves in air using FBGs was first proposed by Iida et al. in 2002 [103]. The sensing element was composed of a FBG attached to the membrane of a condenser microphone and a minimum detectable sound pressure about 50dB ref  $20\mu\text{Pa}$  was reported. It was also reported by Mohanty et al. in 2006 [104] that a system based on a membrane was able to measure the sound wave at a distance of up to 4cm from the acoustic source, although the minimum detectable acoustic pressure was not given.

### 3.5. Polarisation modulation

In an ideal single-mode fiber, two orthogonally and linearly polarized waves propagate at the same velocity. However when a sound wave is generated normally to the fibre, the fibre becomes anisotropic. The two polarizations in the fibre encounter different refractive indices and hence propagate at different velocities. Bending a fibre will also change the output polarization of the light thus a polarization controller should be used before the sensing part of the fibre. Polarization maintaining fibres can be used for the purpose. In order to measure the polarization state of the light it is required to use a polariser (also called analyser) or a birefringent element which converts the polarisation modulation into an intensity modulation that can be detected by a photodiode.

The first account of a polarimetric optical fibre acoustic sensor was proposed by Rashleigh [105] in 1980. An acoustic wave changes the phase velocities of the polarization modes in a tension-coiled fibre resulting in the polarization rotation of the transmitted light. The light was demodulated by using a Wollaston prism to obtain the phase delay between the two polarisation states, and thus the signal was subsequently detected using a pair of photodiodes. An advantage of using this technique is that it is independent from the fluctuation of the light source.

Work by Chan et al. [106] reported on an underwater ultrasonic fibre optic sensor based on a polarisation maintaining fibre and the setup is shown in Figure 3.12.

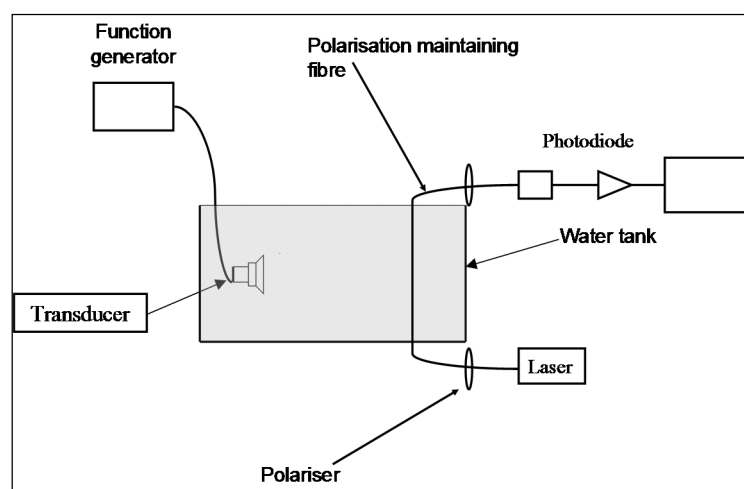


Figure 3.12: Setup for the detection of acoustic waves using the polarisation change.

Recent work reported by Thursby and Culshaw in 2010 [107] made use of the change in polarisation caused by ultrasonic waves on polyimide coated single mode optical fibres embedded in a carbon plate. The birefringence caused by the pressure was observed using a polarizer. The input light was linearly polarized thanks to a polarization controller. They could detect ultrasonic pulses of frequency 100 kHz.

The main disadvantage of polarisation based sensors is the need for polarisation maintaining components such as polarisation maintaining fibres which leads to an increase in the complexity of the sensing system. Also a drift in the state of the polarisation of the source over time can diminish the accuracy of the sensor.

## 3.6. Distributed acoustic sensors

The use of point sensors is useful for some applications but there are cases where the acoustic pressure over a long distance or a large area needs to be monitored such as along a pipeline, an oil or gas well, on or under a field, within the structure of a building...

### 3.6.1. Bragg Reflector based sensors

Thus making use of FBGs and the widely available WDM systems researchers have proposed multipoint and distributed acoustic sensors in water [108] and in air [104]. One of the major applications of FBG-based acoustic sensors is related to the monitoring of civil structures and aircrafts. Fomitchov [109] proposed the use of a FBG for the detection of ultrasonic waves in solid. The setup is similar to that reported by Webb et al. [94]. But the range of frequency detected was from 10 kHz to 5 MHz, making it very suited for the real time detection of cracks in buildings.

The detection of Lamb waves using FBGs has also been investigated by Betz et al. [110] in a Perspex plate, and in Aluminium plates [10], [111]. Based on the work by Mohanty et al. [104] Nakamura et al. (2007) [112] proposed an array of FBG-based microphones for the detection of audible sound waves.

### 3.6.2. Distributed sensing using Optical Time Domain Reflectometry (OTDR)

More recent developments based on spontaneous backscattering such as Rayleigh or Raman scattering have shown the potential to detect seismic waves [113], or for border monitoring [114]. But this requires a relatively high acoustic pressure and/or strain, involving the use of vibrotrucks or dynamite to generate seismic waves for example.

A limitation of this type of sensors is that only a portion of the light is reflected back to the detector due to backscattering [115]. Therefore the amount of light received is about 0.15%, thus causing a 28dB reduction in SNR. [116]. In addition, the maximum detectable frequency is directly related to the fibre length. Assuming a refractive index of the fibre is 1.5, it would take 10 $\mu$ s for a light pulse to travel to the end of a 10km fibre and back. Only one pulse can be sent at a time, thus according to Nyquist's theorem limiting the maximum measurable frequency to <50 kHz.

### 3.7. Summary of reported fibre optic based acoustic sensors

The table below gives an overview of different applications and optical techniques available to detect sound waves.

<b>Reference and Authors</b>	<b>Application</b>	<b>Sensing Principle</b>	<b>Light Source</b>	<b>Advantages/ Drawbacks</b>
Song and Lee [65]	Medical, industrial, Civil	Moving membrane	Laser	Involves the use of a membrane, fragile
Mohanty et al. [104]		Moving membrane & Fibre Bragg grating	Laser	Uses a membrane
Thursby and Culshaw [107]	Ultrasound detection	Polarisation	Laser	High complexity
Parker et al. [68],[67]	Oil, Gas, Security	Distributed, Rayleigh	Laser	Mainly detects strain variations, high complexity, expensive.
Betz et al. [111]	Detection of Lamb waves	Fibre Bragg grating	Tunable laser	Suitable for ultrasound detection
Tsutsui et al. [70]	Composite structure monitoring	Bending loss modulator	Unknown	Complex implementation

As can be seen from the table a lot of different techniques are available, each with its own benefits and drawbacks. Novel sensors relatively robust, stable and simple to implement are required.

### 3.8. Summary

Most reported intensity modulated acoustic sensors are using a simple and low cost sensor interrogation. Generally the sensor only requires a light source and a photodetector to detect the light intensity variations due to applied pressure caused by the sound wave. Their fabrication is often relatively uncomplicated. However their sensitivity to noise sources that are not related to the measurands demands a relatively complex compensation setup. Polarisation based acoustic sensors have the advantage of being immune to variations in the source power, but they require birefringent elements and polarisation maintaining fibres which do not make the implementation of such systems very practical. Interferometer based acoustic sensors are not sensitive to fluctuations of the source power however the very low level of photoelastic or stress-optic coefficients of the applied optical glass fibres make it necessary to have a long length of sensing fibre.

Fully distributed acoustic sensors have the advantage of using single mode fibres but require the use of complex optical and signal processing systems which drastically increase the cost.

Grating based acoustic sensors use short lengths of fibre and are immune to small variations of source power. Despite the fact that they are sensitive to changes in the environment such as temperature, humidity etc., it is relatively easy to discriminate different phenomena by using paired gratings.

The next chapter will discuss the Long Period gratings and the potential for use as acoustic sensors.

# **Chapter 4**

## **Properties and principles of LPG-based acoustic detectors in air**

### **4.1. Introduction**

The previous chapters have summarized fibre-optic techniques that have been developed for the measurement of acoustic vibrations, using different types of optical fibres. The key advantage of this type of sensors is their immunity to electromagnetic interference, and the possibility to use the same component either in air [104],[117], solids [118] or fluids [119].

This chapter outlines the work carried out to investigate the potential of using long period gratings (LPGs) for acoustic detection and the setup used to monitor the sound waves. Based on the detailed discussions made on the sensing principle of using LPGs for acoustic detection, and the improvement of the detection sensitivity through the variation of several key parameters, a simple model will be proposed describing the way the sensor is operating.

The first part of this Chapter is focused on the description of the physical principle and this is followed by a detailed description of different elements used for the detection of sound waves both in air and in water. Following the illustration of the measurement and mechanical setups, discussions are made based on the experimental results obtained.

## 4.2. Operational Principle

### 4.2.1. Long Period grating as a sensing element

In Chapter 2, discussions have been made in relation to the fabrication and sensitivity of LPGs to different parameters such as temperature, strain, refractive index and bending. The focus of this Chapter, however, is on the LPG bending effect as it underpins the design of a novel LPG-based acoustic pressure detector.

Figure 4.1 illustrates an experimental setup with a LPG being placed between two pillars. One pillar is screwed directly onto an optical table and the other fixed onto a translation stage. When a sound wave is produced and propagated in the transverse direction of the LPG, the properties of the LPG change because of the variation in the acoustic pressure in air, at the frequency of the sound. Thus the bending curvature of LPG is to be modulated as a result of the variation of the acoustic pressure applied on to the LPG.

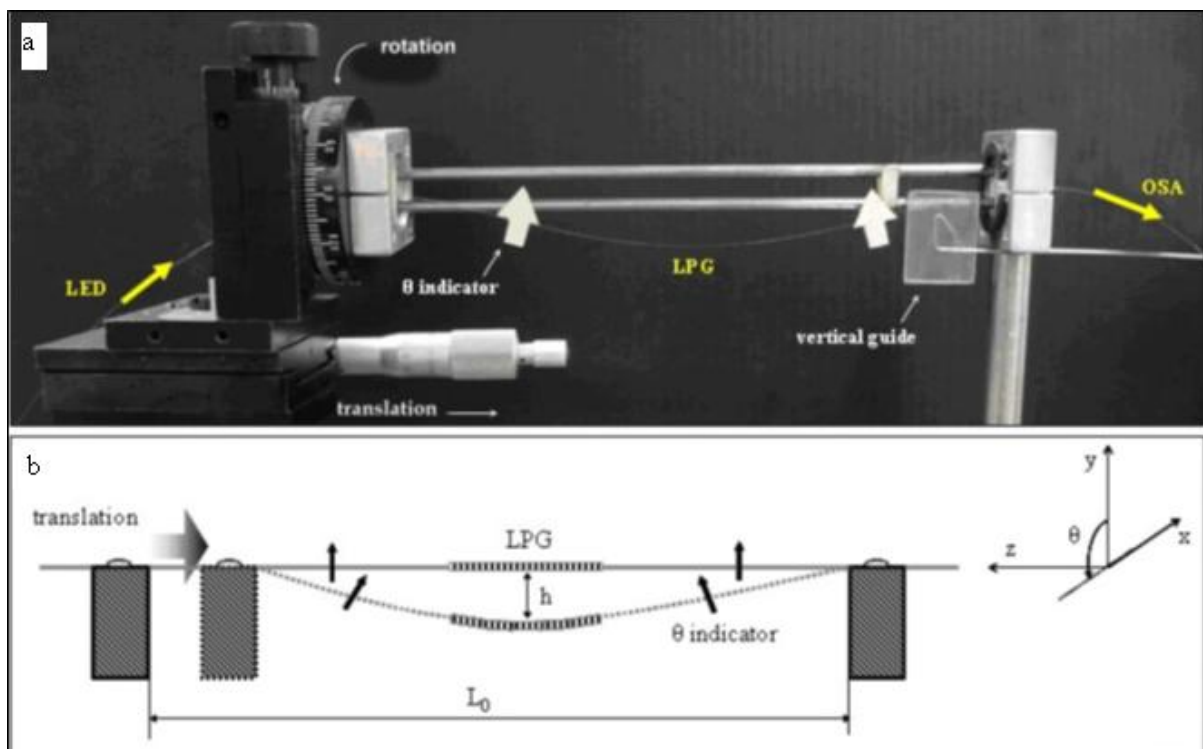


Figure 4.1: Setup of the curvature and bend measurement. (a) schematic diagram of the LPG sensor setup; (b) the magnified fibre with a LPG in the middle [120]

LPGs have been demonstrated as extremely sensitive to small bends [52]. When a bend arises the cladding modes are scattering out of the fibre, this changes the coupling between the

guided core mode and cladding modes. The perturbation due to the bend depends on different parameters such as: the radius of curvature, wavelength, and order of the mode, fibre refractive index as well as the refractive index of the material surrounding the cladding.

Ideally the sensitivity of the LPG should be as high as possible in order to detect variations of pressure causing small bends. There are different ways of improving the bend sensitivity of optical fibres, as discussed by [49] the higher the mode, the more sensitive the system will be, but this was limited by the type of LPG and the source available. The sound pressure is causing a minute bend variation which needs to be converted from the wavelength shift of the attenuation bands to an amplitude variation. This requires the source to be very stable and also a relatively high amount of signal to be received.

Another technique as proposed by Patrick [45] is to rotate the LPG, however this would require the use of a fibre with a high core concentricity error.

The length of the LPG is also critical as the longer the LPG the deeper and narrower the attenuation bands will be. However the length of the LPG is usually limited by the grating fabrication facility and/or the length of the amplitude mask used.

In this work, different LPGs have been used, with the period varying from  $\Lambda=400$  to  $550\mu\text{m}$  and the length from 6 to 16mm. The LPGs fabricated had to fulfil criteria both in terms of the wavelength of the attenuation bands and their attenuation depth and they are specifically chosen for the measurements planned.

#### 4.2.2. Modified string theory

In light of the above, an LPG can be used for detection of acoustic waves taking advantage of the bending effect discussed. To do so, as shown in Figure 4.2, a LPG-based acoustic sensor system was set up. A piece of fibre with a LPG written into it was placed between two solid pillars, where the distance between the pillars,  $2L$ , can be adjusted by placing one of the pillars on a translation stage. Initially, in the set up created, the fibre was straight and the distance between the pillars was set to be 100mm.

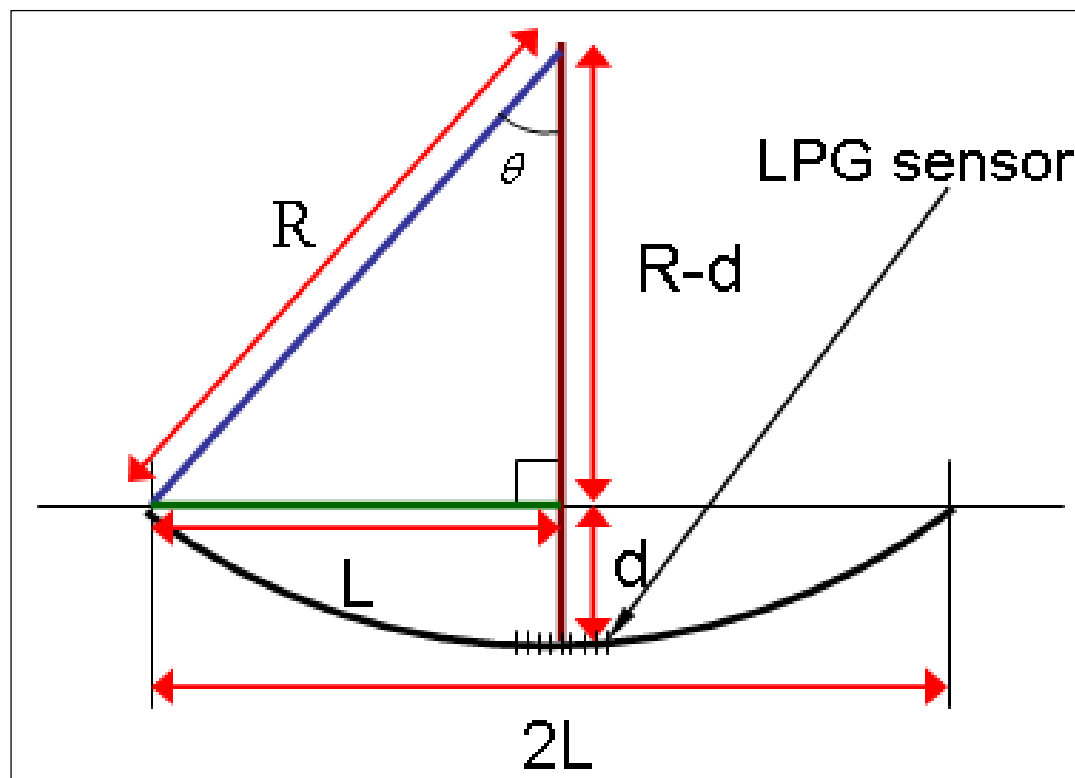


Figure 4.2: Setup of a LPG-based acoustic sensor.

As indicated in Figure 4.2, the bending radius of the LPG can be reduced by shortening the distance between the pillars, (in this case  $2L$ ). This was achieved by adjusting the translation stage and therefore increasing  $d$  the lowering distance at the centre. From this we can calculate the bending radius  $R$  of the LPG as defined by equation (4.1) [121].

$$R = \frac{(d^2 + L^2)}{2d} \quad (4.1)$$

Where  $L$  shows the half distance between the pillars.

The curvature,  $C$ , of the LPG can thus be defined as the reciprocal of the radius [121]:

$$C = \frac{1}{R} = \frac{2d}{d^2 + L^2} \quad (4.2)$$

The spectral sensitivity of the attenuation bands of the LPG is defined as a function of the LPG bending curvature  $C$ , thus be described as  $\frac{d\lambda}{dC}$ . Figure 4.3 shows the transmission

spectra of the LPG when the LPG bending curvature,  $C$ , changes by varying the distance between the pillars,  $2L$ , without changing the fibre length.

The inset diagram in Figure 4.3 shows clearly the linear characteristics of the attenuation band wavelength shift as a function of bending curvature. Therefore  $\frac{d\lambda}{dC}$  can be determined to be  $+13.5\text{nm/m}^{-1}$ , based on the experimental data obtained and this is in good agreement with that reported by other research groups [44].

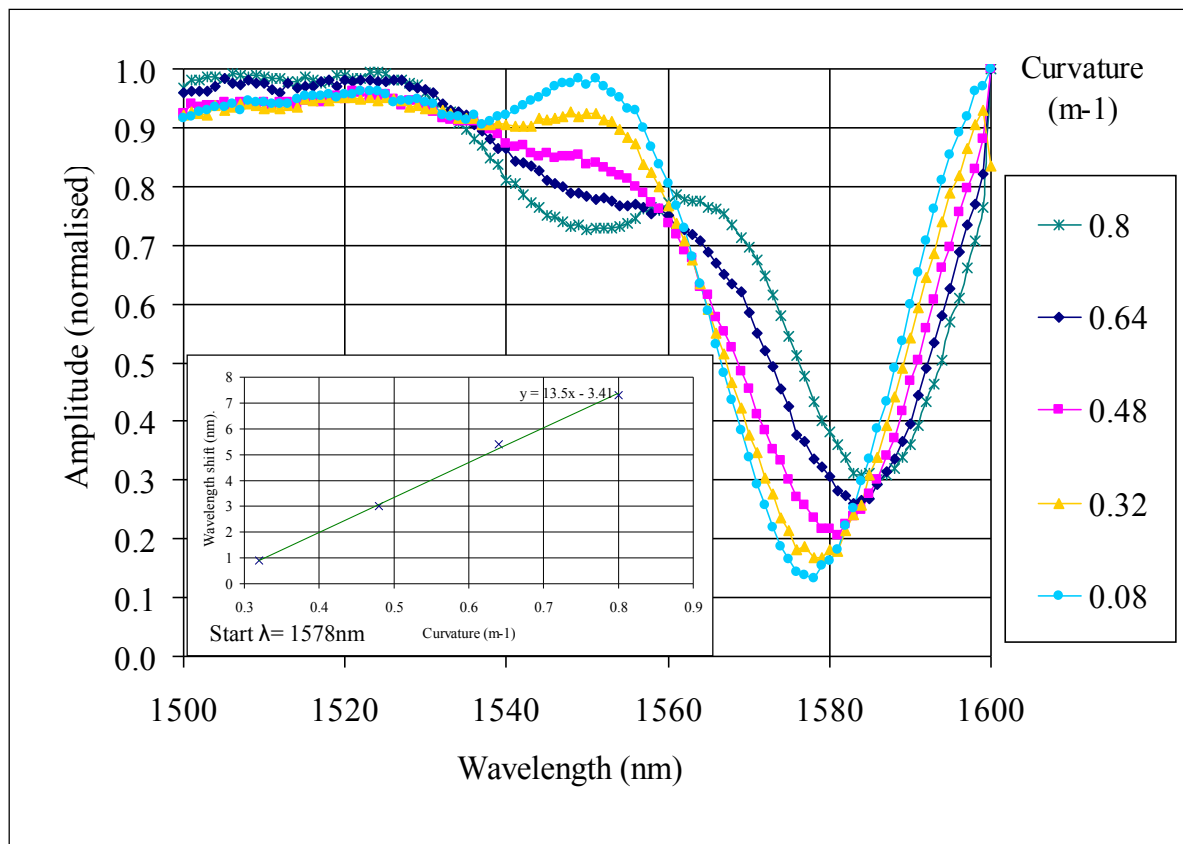


**Figure 4.3: LPG transmission spectra when LPG bending curvature changes. The inset shows the attenuation band wavelength shifts as a function of bending curvature  $C$ .**

When the LPG is exposed to a sound wave, the acoustic pressure of the sound is able to modulate the physical situation of the LPG, i.e. modulate the bending curvature of the LPG at some specific frequencies. In order to describe the performance of LPG when it is exposed to sound waves, a modified elastic string theory is proposed in this work to explain the frequency response of the LPG. As illustrated in Figure 4.2, if the pillar distance is fixed, but the fibre length is seen to be varying, the LPG can be considered to behave as an elastic string and its resonance frequency can thus be described using theory associated with a simple string and thus [122]:

$$f_n = \frac{nv}{2l}, n = 1,2,3,4 \dots \quad (4.3)$$

Where  $f_n$  shows respectively the  $n^{\text{th}}$  harmonic frequency produced,  $l$  is the fibre length between the pillars and  $v$  represents the speed of the sound wave. Equation 4.3 explains the relationship between the frequency response of the LPG and the fibre length change, i.e. the grating bending curvature change.

In this work, however, the distance between the pillars is allowed to vary, but the fibre length is fixed, therefore equation 4.3 can be modified as follows to relate directly the frequency response to the LPG curvature. As illustrated in Figure 4.2, angle  $\theta$  can both be described as:

$$\frac{l}{2\pi R} = \frac{\theta}{2\pi} \Rightarrow \frac{l}{2} = \theta R \quad (4.4)$$

$$\sin\theta = \frac{l}{R} \quad (4.5)$$

Through the elimination of  $\theta$  by combining equations (4.4) and (4.5), the fibre length  $l$  in equation 4.3 can thus be described as follows.

$$l = 2R \cdot \arcsin\left(\frac{l}{R}\right) \quad (4.6)$$

Subsequently when  $R$  in equation 4.6 is replaced by LPG curvature  $C$ , as described in equation 4.2, equation 4.6 can be changed to become

$$l = \frac{2}{C} \cdot \arcsin(LC) \quad (4.7)$$

Further, replacing  $l$  in equation (4.3) with that in equation (4.7), a modified theory for the string can be defined using equation (4.8) below

$$f_n = \frac{nv}{\frac{4}{c} \arcsin(LC)}, n = 1, 2, 3, 4 \dots \quad (4.8)$$

This formula can be used to relate clearly the frequency  $f_n$  to the LPG bending curvature, irrespective of the bending procedure, either through the change of the pillar distance or through the change of the fibre length.

When the fibre is loose the cavity effect due to the pillars has a greater importance. It must be noted that even though the distance between the pillars is changing the length of fibre is constant, thus the resonance frequency is supposed to remain constant, making the assumption that for a certain mode the LPG is behaving as a string, therefore the expressions derived above can be used for a constant length of fibre.

#### 4.2.3. Sound pressure

The sound pressure of an acoustic wave is applying a strain on the fibre although this strain is extremely small.

It is expected that the Young's modulus of the fibre (e.g. glass) has a direct impact on the vibration.

The Young's modulus can be calculated by dividing the tensile stress ( $\sigma$ ) by the extensional strain ( $\epsilon$ ) and is given by the following expression:

$$E = \frac{\sigma}{\epsilon} \quad (4.9)$$

However, when it is compared to the bending effect of a LPG, which is written into a fibre as a function of vibration, this effect is negligible.

This change in bending creates a change in the optical properties of the LPG. This phenomenon is having a higher importance when the fibre is tight; as it cannot move thus the bending has little effect therefore the sound pressure variation caused in the air by the sound wave causes a slight variation in the transmission spectrum of the LPG. Overall the effect of the sound pressure is minimal since LPGs are mainly sensitive to the change in bending.

### 4.3. Measurement system

This section describes different elements required to detect the sound wave in air using the LPG technique described above. A set of experiments was performed to allow a better understanding of the frequency response of a LPG, depending on the amount of bending applied, as well as the range of frequencies applied. All the following experiments were fully automated; and the instruments were controlled using LabVIEW.

The sensor system configured in this way has been designed to overcome the limitation of the low frequency response of commercial Optical Spectrum Analysers (OSAs). There have been a number of techniques reported to demodulate signals at high frequencies, such as the interferometric wavelength shift detection method [1], but this usually requires the sensor to work in a reflection mode.

Another fast interrogation technique is to use a light source whose emission spectrum matches closely with one of the attenuation bands of the LPG. All experiments were performed in a laboratory environment, where the temperature fluctuation is not significant. However the light source is temperature compensated as the emission spectrum is temperature-dependent and would have an impact on the measurements.

By using a FBG, whose Bragg wavelength is positioned within the slope of the LPG attenuation band, the wavelength shift of the LPG attenuation band can thus be converted into an intensity change which can be detected by a photodiode. Figure 4.4 shows the layout of a LPG-based sensor system created and evaluated in this work.

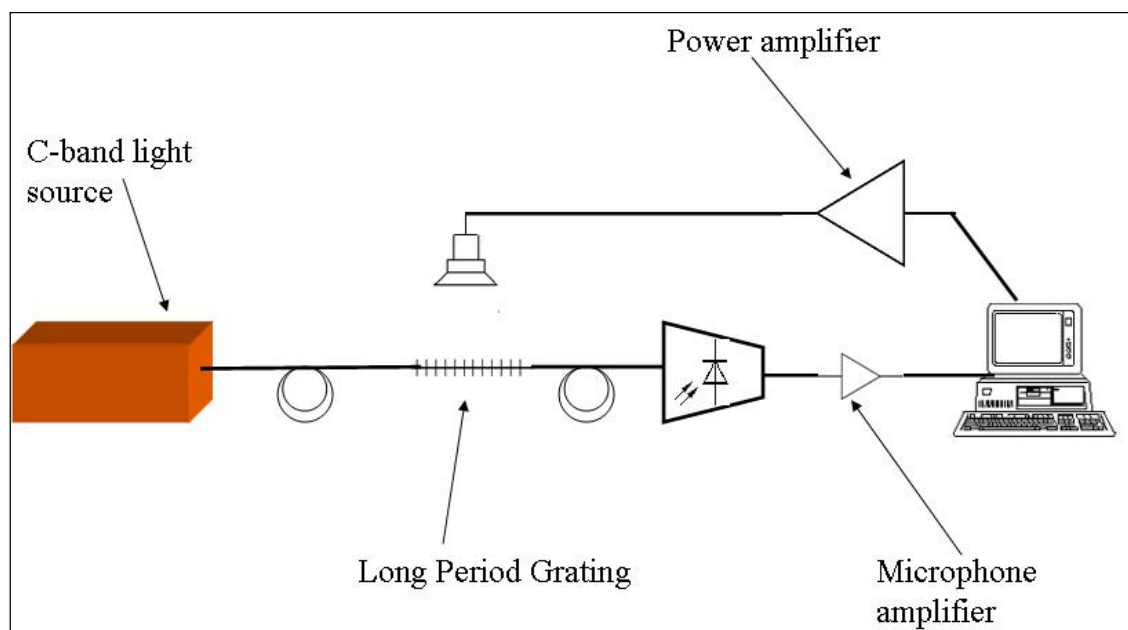


Figure 4.4: Setup of a LPG-based acoustic detector

#### 4.3.1. The light source

The first requirement for these sources is that their spectrum of emission has to be overlapping with one of the attenuation bands of a sensor LPG. It is important to note that the source power has an influence on the amount of signal detected as well as the signal to noise ratio. This is due to the fact that the amount of optical signal modulated by the sound wave and detected by the photodiode is determined by both the optical spectrum and the optical power of the light source. Given the small induced shift in wavelength of the optical spectrum of the LPG, the light source is required to be stable both in terms of amplitude and wavelength; indeed a change in either of these factors would have an impact on the detected signal and generate an error in the measurement.

The different criteria to choose the source are:

- *Output power*: The power needs to be high enough to allow the signal to be detected by the photodiode, and differentiate the noise from the signal. The output power of optical sources used in the experiments varies from a few hundreds of  $\mu\text{W}$  to a few tens of  $\text{mW}$ .
- *Bandwidth*: The band of emission has to be wide enough to compensate the wavelength instabilities and cover one of the attenuation bands of the LPG.
- *Stability*: The shape of the source has to be constant over a long time and independent of variations arising from the environment such as temperature, humidity...
- *Noise*: The optical signal from the light source carries a certain amount of noise; this can be due to the intrinsic characteristic of the source. But in the system used in this work, the noise is mainly caused by intensity and wavelength shift of the source.
- *Variation of the power of the source*: Since the optical signal is directly converted from wavelength shift to intensity change, the amplitude of the light source has to be stable to allow a reliable measurement of the frequency response of the system to be made.

### 4.3.2. Choice of the light source

Four different light sources have been used and evaluated. Each of them has its own characteristics in terms of bandwidth stability and output power.

#### a. S-LED at 1550nm and 1580nm

The main advantages of SLED light sources are the low cost and relatively small size. The main drawback is that they have a relatively broad band spectrum; which is problematic in the setup used for this experiment since we make use of the direct conversion from wavelength shift to intensity variation thus there needs to be a sharp edge on either side of the transmitted power. In addition the output power of the sources available was about 1mW which is relatively low. The optical spectrum of a S-LED source at 1550nm reference: DL-CS5037B is shown in Figure 4.5.

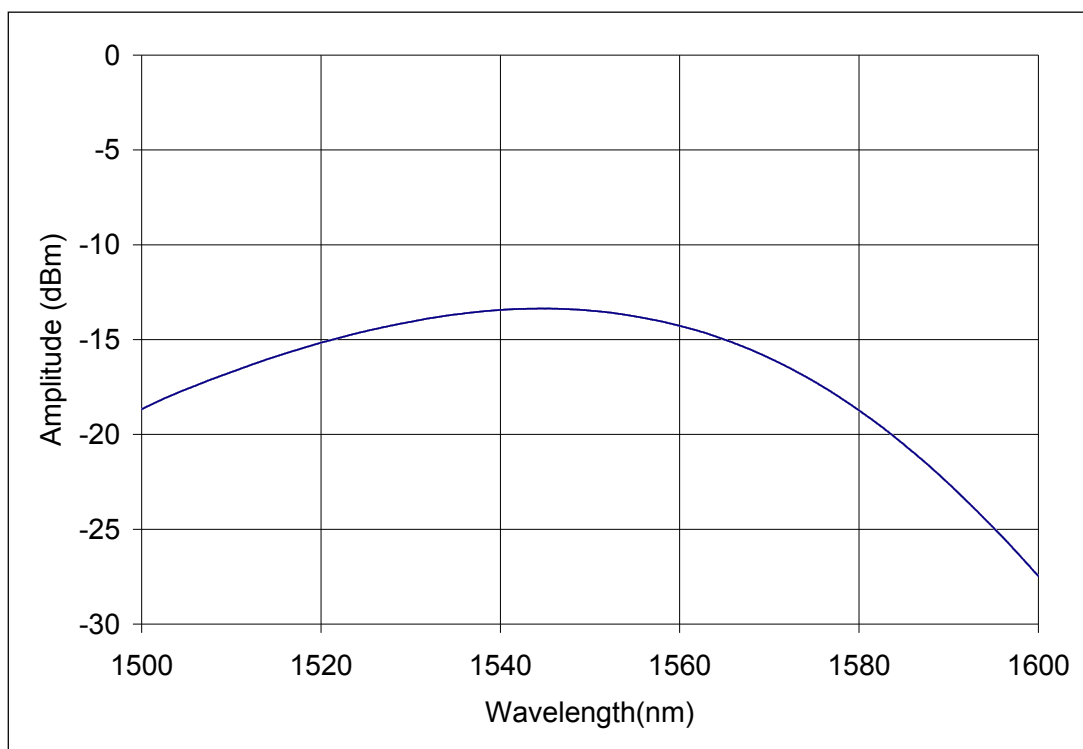
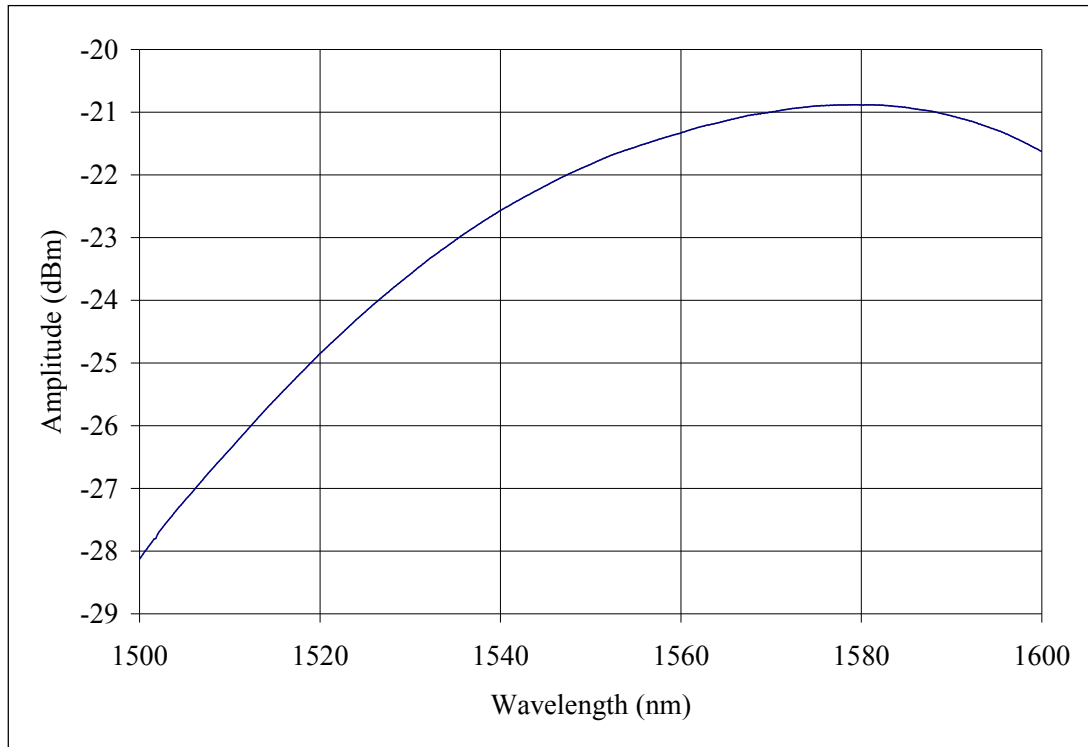


Figure 4.5: Spectrum of a 1550nm source

Figure 4.6 shows the output spectrum of a 1580nm S-LED reference DLCS58L9B. The output optical power measured was 1.8 mW



**Figure 4.6: Spectrum of a 1580nm S-LED light source**

As can be seen in Figure 4.5 and Figure 4.6 the slope of the emission spectrum is not sharp thus a change in the wavelength shift of the attenuation band of the LPG cannot be transformed into a large intensity variation. The output optical power measured from both S-LEDs was about 1 mW.

## b. S-LED source with FBG

In order to overcome the issue related to the fact that the S-LED has a broad spectrum. A setup using a FBG was proposed. This setup shown in Figure 4.8 is using a broadband light source and a FBG in reflection mode. It is composed of a light source, a circulator and a FBG used in reflection mode.

This mode of operation is made possible by using a circulator which is a passive non-reciprocal device. It takes the light from one port to the next with a minimum loss. As illustrated in Figure 4.7, the light goes from port 2 to port 1 and from port 1 to port 3. In order to perform this; the light coming from the port 1 is split into 2 beams with orthogonal polarisation states, the light polarisation is then rotated using half wave plates and Faraday mirrors so that the light transmitted to port 2. The light coming from port 2 to port 3 is sent to port 3 this happens due to the non-reciprocal property of Faraday rotators.

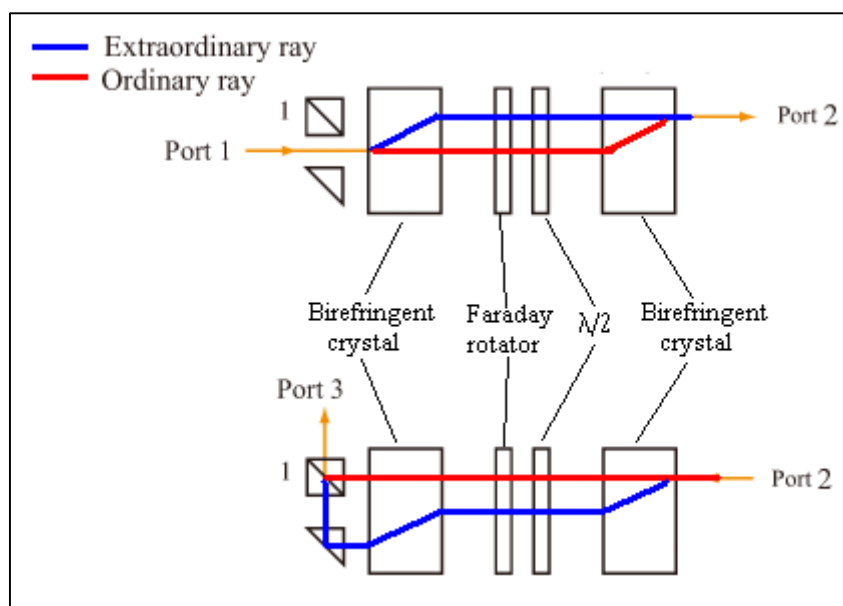
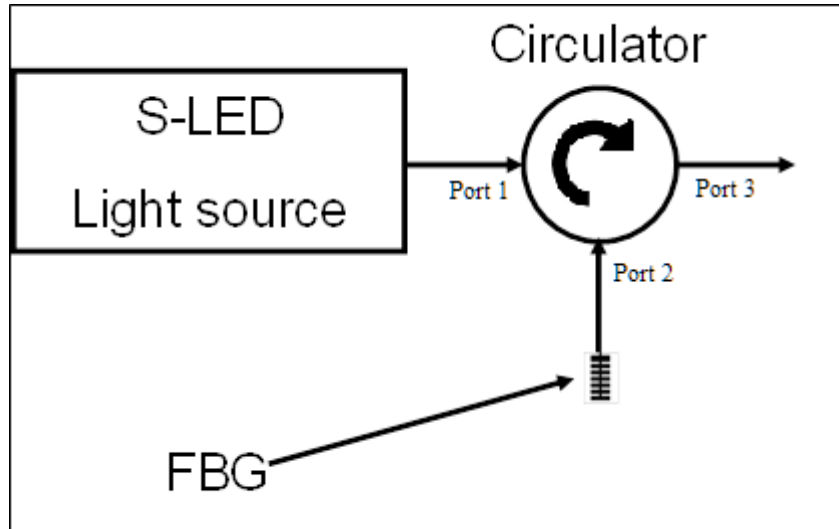


Figure 4.7: Principle of operation of a circulator, upper Port 1 to Port 2 lower, port 2 to Port 3

By doing so, the output signal has a very narrow bandwidth and if the FBG is placed in a protective environment, this combination produces a very stable and narrow-band source.



**Figure 4.8: Diagram of the FBG – broad band source.**

The main advantage of this setup is the high stability in terms of frequency as the FBG is fixed on to a piece of Perspex and protected from the surrounding environment therefore there is no wavelength shift. However one drawback is that the output power that is reflected is only a fraction of that of the source due to the narrow-band FBG being used. In addition, the FBG used is required to be fabricated in such a way that its reflection wavelength (Bragg wavelength) is near the highest emission wavelength of the source to ensure a high reflected signal and its reflectivity to be as high as possible to ensure enough light to be coupled into the sensor. Figure 4.9 shows a typical spectrum of a FBG used, showing the Bragg wavelength to be 1548nm and the reflectivity 90%.

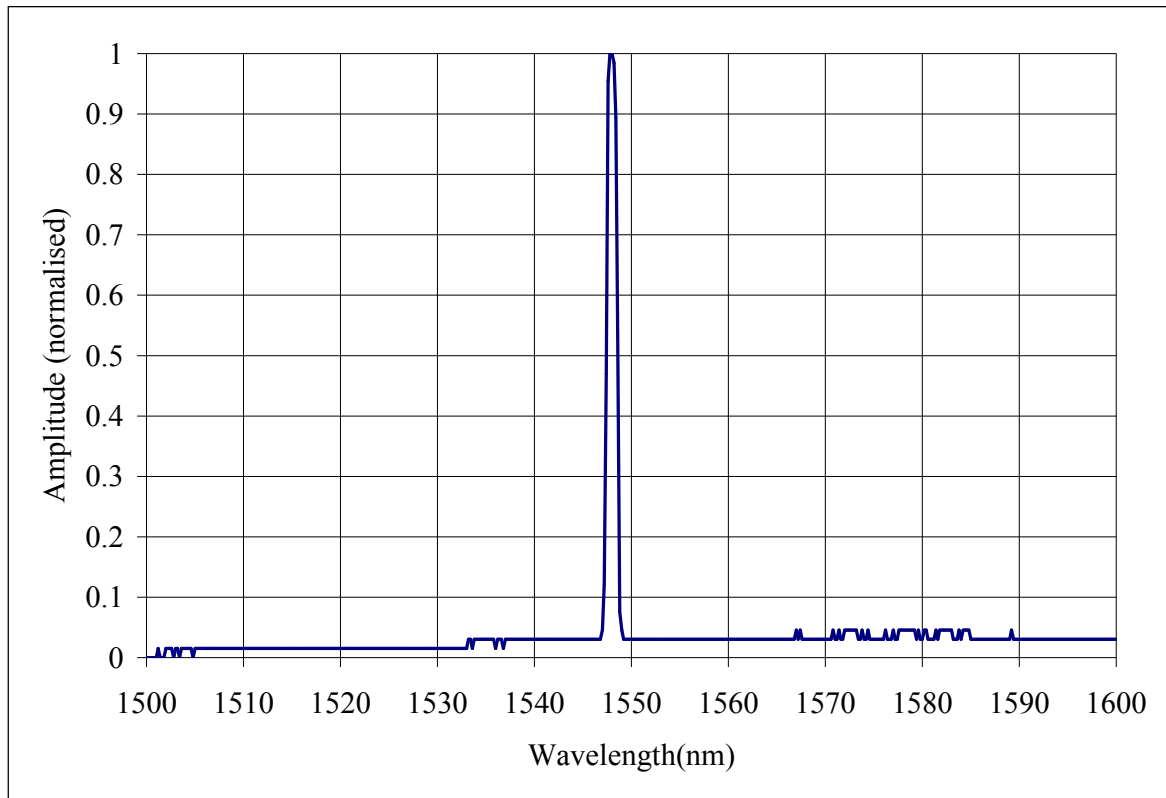


**Figure 4.9: Reflection spectrum of an FBG used with the broad-band 1550nm S-LED.**

c. Tunable Laser Source

The main advantage of using a tuneable laser source is that it gives more flexibility in the fabrication of the LPG, as it can be tuned over a relatively wide range at the near-infrared band. The emission spectrum of the light source can be adjusted easily to be located at the middle of one of the attenuation bands of the LPG being tested. The output power can be of up to a few milli-watts. However the narrow wavelength makes it difficult to measure very small wavelength shifts (i.e. in the order of a few tens of pm). Figure 4.10 shows the optical spectrum of a tunable laser source. The line width is much narrower than what is displayed but the limit for display of the linewidth is given by the Optical Spectrum Analyser used (20pm resolution).

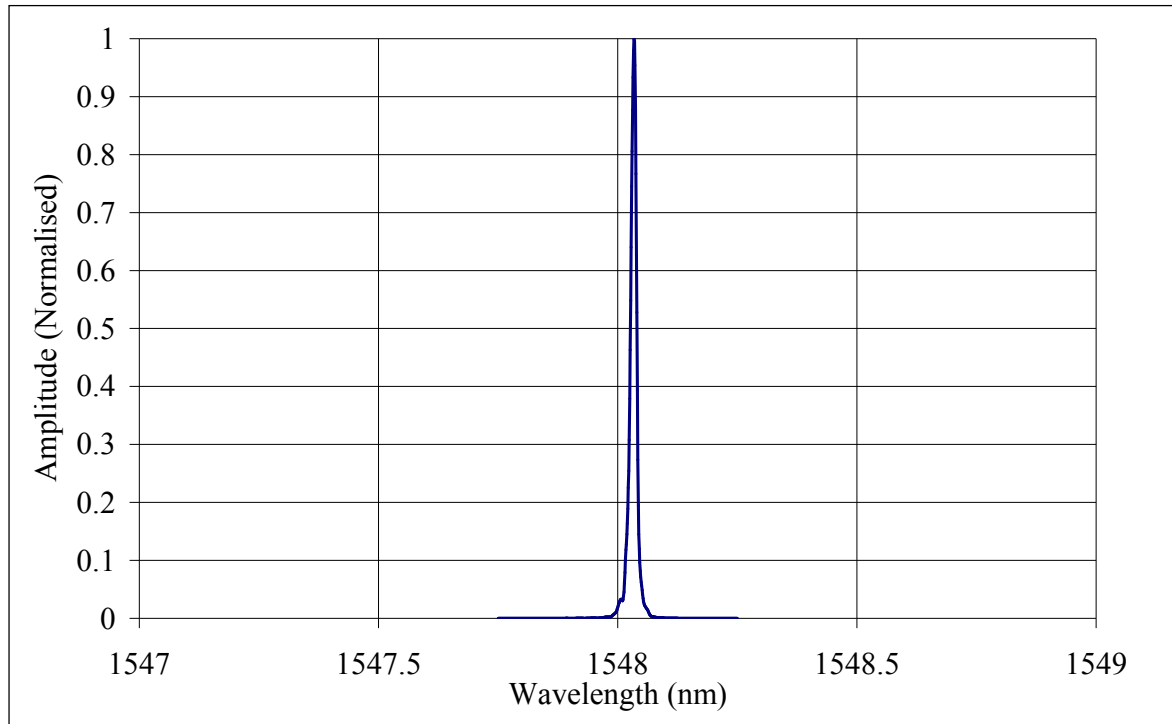


**Figure 4.10: Spectrum of a tuneable laser at 1548nm**

Further experiments using the Santec TSL-210L have confirmed the assumption made earlier, despite a relatively high stability, the jitter does not allow a suitable measurement. The datasheet of this tuneable laser source states a shift in wavelength of  $\pm 10$  pm which is relatively high given the width of the laser source which is of a few pm at 1550 nm. This causes a huge variation in intensity at the output of the LPG, thus this does not allow a consistent measurement of the frequency response of the LPG based sensor.

Recent work carried out by Tanaka et al. [6] made use of a tuneable laser for the detection of vibrations caused by a PZT directly touching the fibre. This wavelength shift caused by vibration is much greater than that of a loudspeaker at a distance of the fibre. Thus the error caused by a variation in the laser beam's wavelength is relatively small.

## d. C-band light source

Another experiment was undertaken by using a more powerful source. This is an Amplified spontaneous emission (ASE) source (OLS15C) with a maximum output power of 14.4dBm (26mW) over a range of 40nm between 1525 and 1565nm.

Based on the data provided by the manufacturer, the source is supposed to be stable and its wide spectrum allows the use of different types of LPGs. Its high power should allow a very good detection of the acoustic signals. Figure 4.11 shows the optical spectrum of the source and it can be seen that the edges of the emitted signal are very sharp, showing a major advantage of this type of sources over the S-LED as it would allow a better conversion from the wavelength shift to intensity change since the gradient is higher.

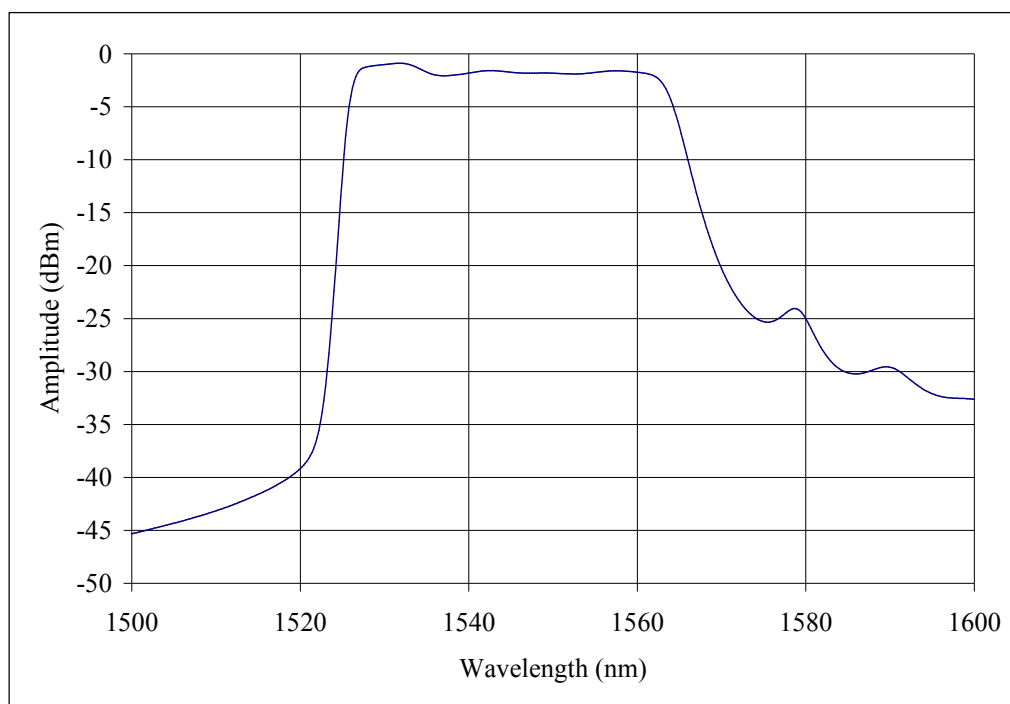


**Figure 4.11: Transmission spectrum of a C-band light source.**

As discussed earlier, it is very important for the source to be stable over time, thus the source was monitored over a long period to verify its stability. The Optical Spectrum Analyser was controlled using LabVIEW software and a computer was connected to the OSA using the Ethernet port. The automation of the measurement ensured consistent and reliable

measurements to be made once every 10 minutes. A set of 15 measurements was made so the whole experiment lasted for a total of 2 hours 30 minutes.

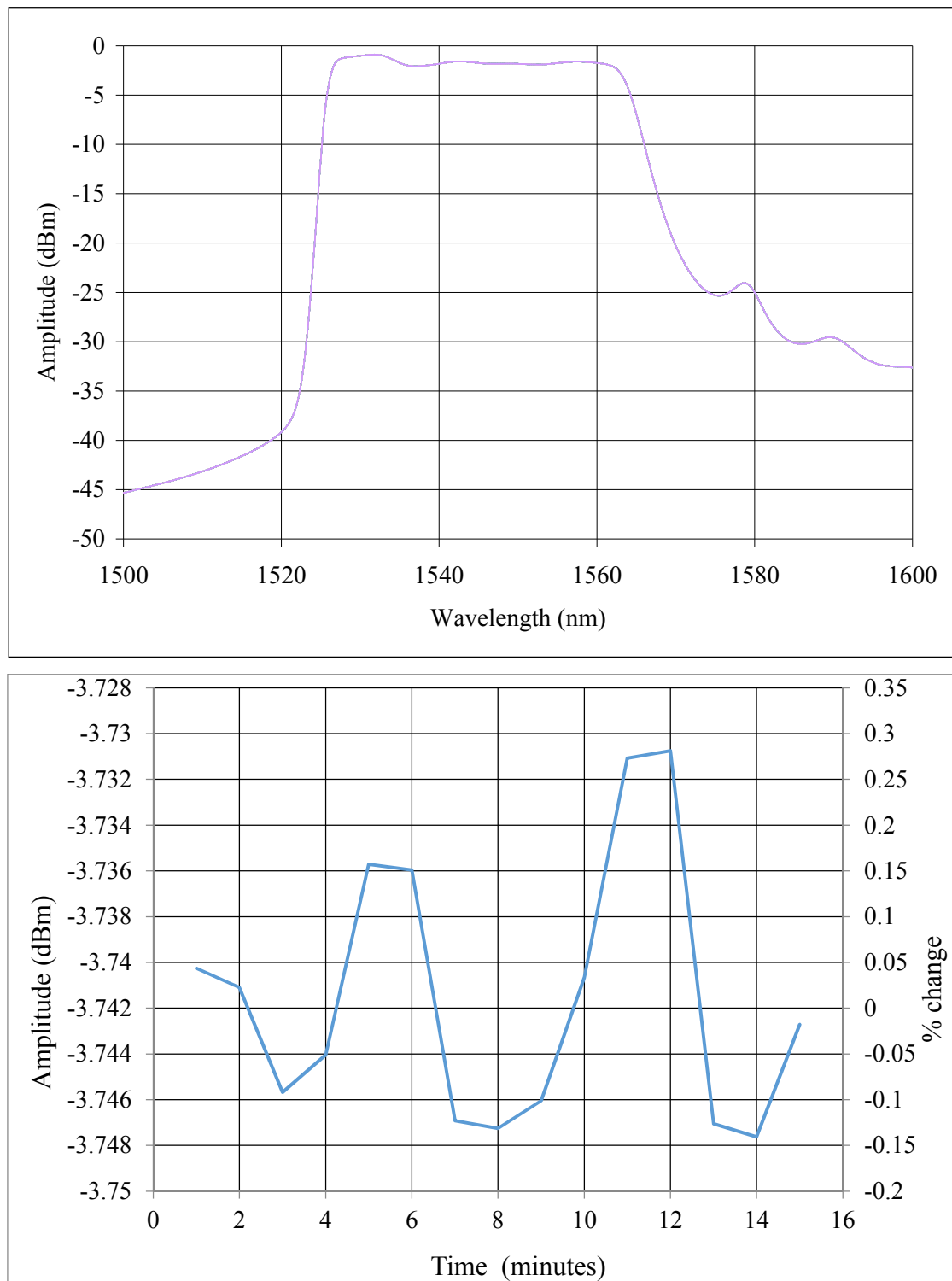


Figure 4.12: Spectrum of the C-band source measured every minute (Top), Amplitude of the signal at 1550nm measured every minute (Bottom).

The results obtained and shown in Figure 4.12 confirm that the output signal of the source is relatively stable.

e. C-band light source with FBG

Since the ASE source (OLS15C) has a higher output power and a narrower emission spectrum than the S-LED source, the use of a FBG following this source should give a relatively high output power. This combination is shown schematically in Figure 4.13.

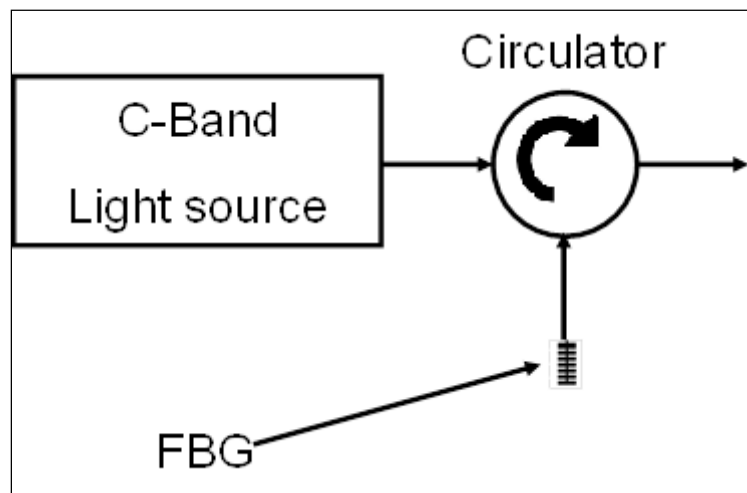


Figure 4.13: Setup of the C-Band source followed by a FBG.

The stability of the C-band source measured after a FBG glued on a piece of Perspex and used in reflection mode can be seen clearly in Figure 4.14.

As with the C-band source on its own, the stability of the source and FBG setup had to be verified, changes in physical parameters such as temperature, strain or humidity variations may cause a change in the spectrum [8], [35]. A set of 15 experiments performed with 10 minutes intervals was done. It can be seen in Figure 4.14 that the signal is very stable; showing that the FBG is well protected since it is not influenced by the external environment.

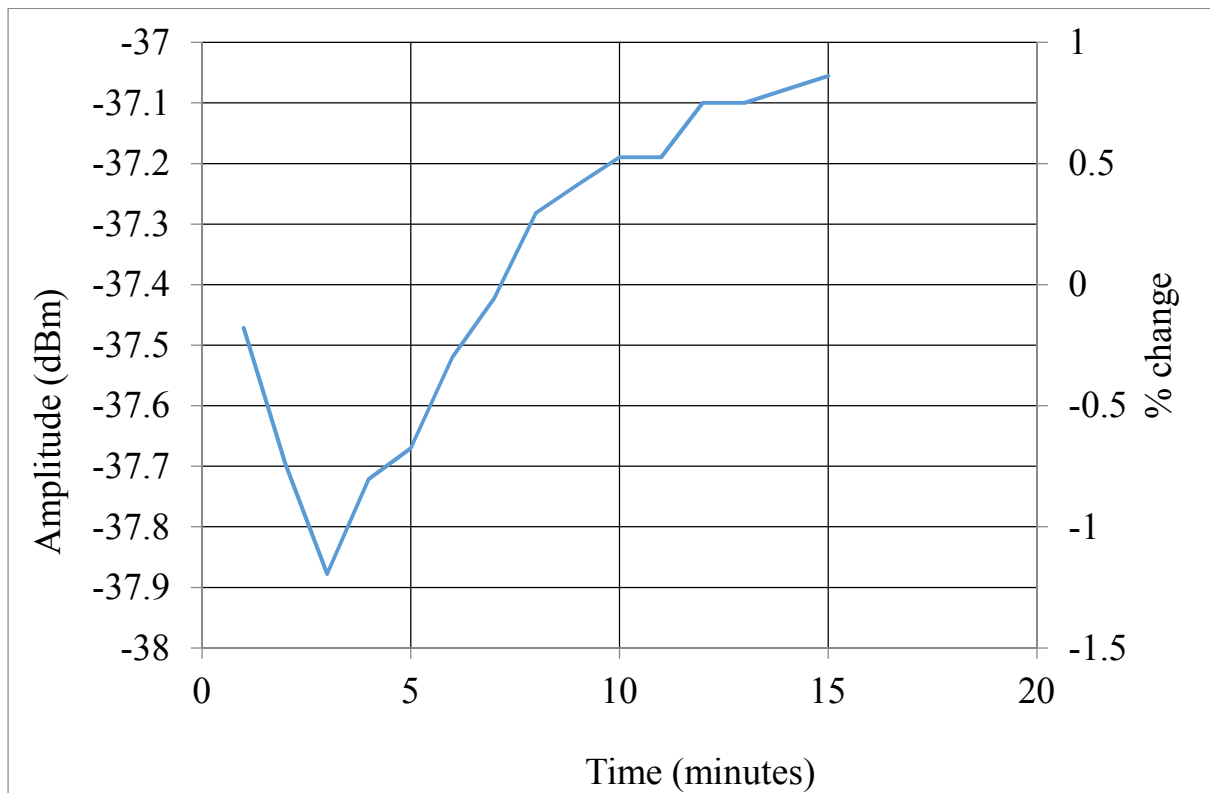
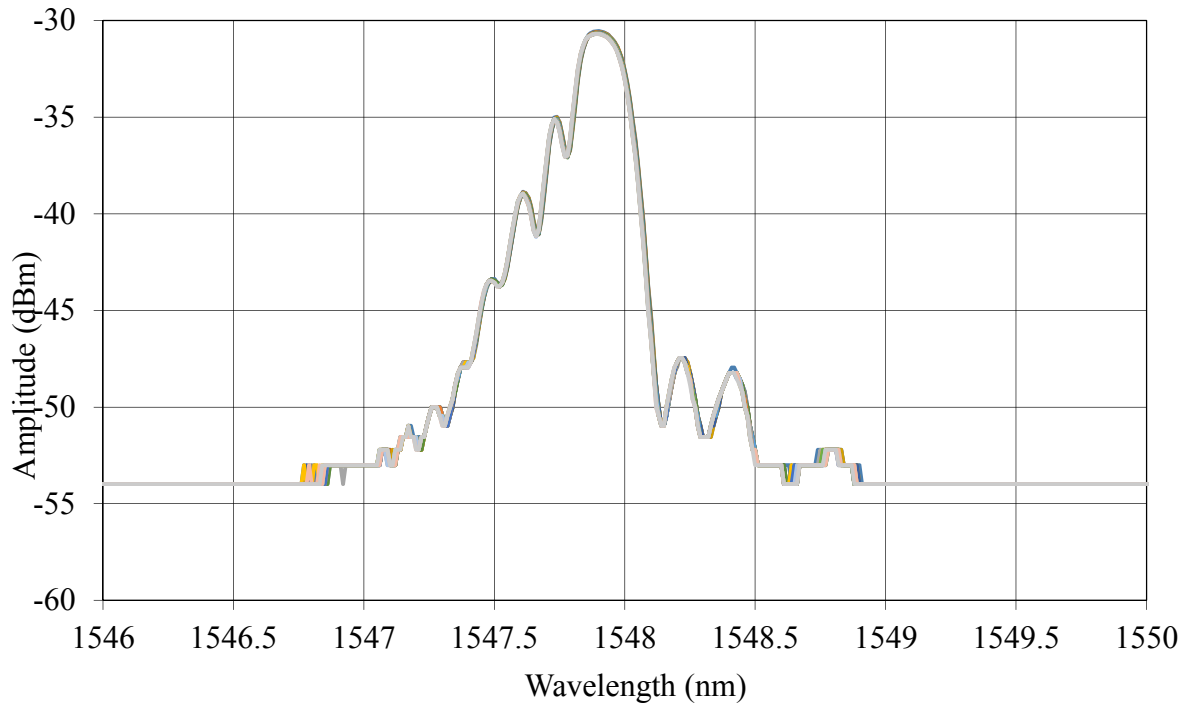


Figure 4.14: Spectrum of the C-band source after an FBG measured every minute (Top), Amplitude of the signal at 1547.7nm every minute (Bottom).

#### 4.3.3. Discussions

This section discussed different types of sources that have been evaluated. Many compromises had to be considered both in terms of available equipment and time. The light source had to have an optical power high enough to allow the signal to be transmitted to the LPG and detected by the photodiode. It is also important to take into account of the effect of the stability, the emission spectrum and the noise level. The band of emission has to be wide enough to compensate the wavelength instabilities and background noise.

## 4.4. The detection system

One of the problems commonly found with the usage of LPGs is the difficulty in interrogating its spectral response due to the large bandwidth of its resonant bands. In addition the measurement of dynamic response makes it difficult to use some measurement equipment such as OSA. Indeed the frequency of sound waves is generally too high compared to the sweep frequency of the OSA. There have been a number of techniques reported to demodulate signals at high frequencies, such as the interferometric wavelength shift detection method [123], but this usually requires the sensor to work in a reflection mode. As discussed earlier in this chapter another fast interrogation technique is to use a light source whose emission spectrum matches closely with one of the attenuation bands of the LPG. The use of a FBG, whose Bragg wavelength is positioned within the slope of the LPG attenuation band is thus able to convert the wavelength shift of the LPG attenuation band into an intensity change which can be detected by a photodiode, but this requires a relatively high source power.

Another method for the detection of the wavelength shift of the peak wavelength of LPG's is to use the fact that when an LPG is bent, the attenuation bands tend not only to shift but also to be divided into 2 smaller attenuation bands: a phenomena that have been discussed in Chapter 2 and reported by Liu et al. [35] and Block et al. [124]. They reported that an increase in bending curvature caused the split peaks to be separated further. Although the measurement of the wavelength shift between the peaks was successfully implemented by Liu et al. [47] for static bend measurements using an Optical Spectrum Analyser, the monitoring of very small wavelength shifts at audio frequencies would be very difficult to do. It would involve the use of a spectrum analyser with peak detection able to sample the signal at least twice the highest frequency to be measured, thus at least a few kHz.

The detection technique chosen here is to use a photodiode and an amplifier, allowing the conversion from the small variations caused by the modulation of light in the photodiode and the amplification of the signal. The photodiode's purpose is to convert the modulated optical signal into electrical signal over a period of time  $T$ , which is the inverse of the sampling frequency of the Data Acquisition Card (DAQ) in this case, 22.05 kHz. The sampling

frequency is suitable for the current application as only signals with a frequency component below 10 kHz are being measured.

#### 4.4.1. Photodiode selection:

The photodiode had to fulfil different criteria such as high linearity, low noise, robustness and compactness. It is also required to have a detection range covering the spectrum of emission of the source, thus the wavelength range had to be comprised between at least 1520 and 1580nm. This response depends on the material used as shown in Figure 4.15.

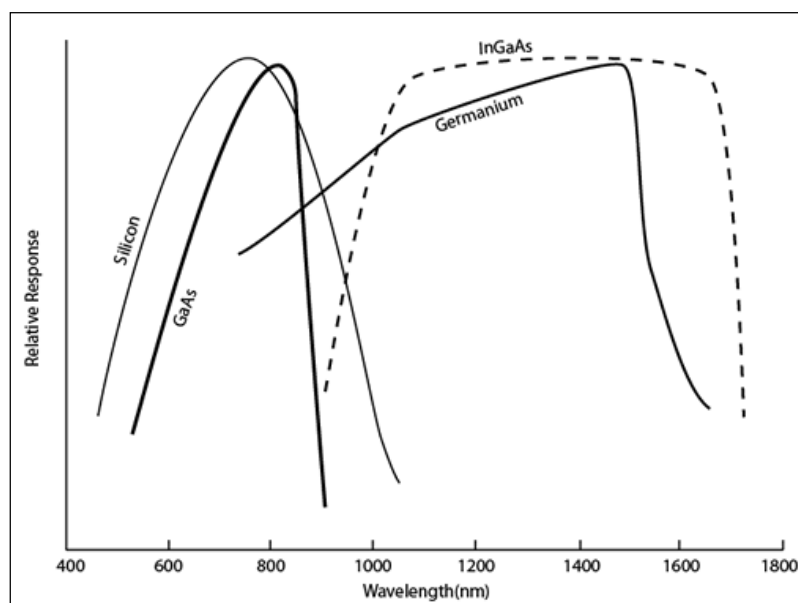


**Figure 4.15: Detector response curve for different materials**

It can be seen that only Germanium (Ge) and Indium Gallium Arsenide (InGaAs) based photodiodes can detect light at the wavelengths of interest. This graph also shows the limitation for the mode of the attenuation band of the LPG. As indicated in Chapter 2, the higher the mode, the higher the sensitivity to bending but in practice a compromise needs to be done both in terms of source and in terms of photodiode. If the mode is too high the photodiode might not be able to detect the light. Although it is not so critical in this application, it is important to take into account of the bandwidth, which must ideally be much higher than the maximum frequency that needs to be demodulated.

Since the photodiode had to be connected to an optical fibre, the packaging is very important. Thus it is required for the photodiode to either be pigtailed or have a FC-PC connector for

direct connection. The final choice was a PIN photodiode (3CN00019AA) manufactured by Alcatel. With a responsivity of  $0,9\text{A/W}$  and a detection range of 1260 to 1580nm it was found to be a suitable candidate for this application.

#### 4.4.2. Transimpedance amplifier

The requirements for the amplifier were to have the lowest possible noise, a bandwidth of up to 10 kHz bandwidth, and relatively high gain. Two types of transimpedance amplifiers have been considered and evaluated. They are either based on the photoconductive or photovoltaic mode. Figure 4.16 shows a typical circuit design for these two types of amplifiers.

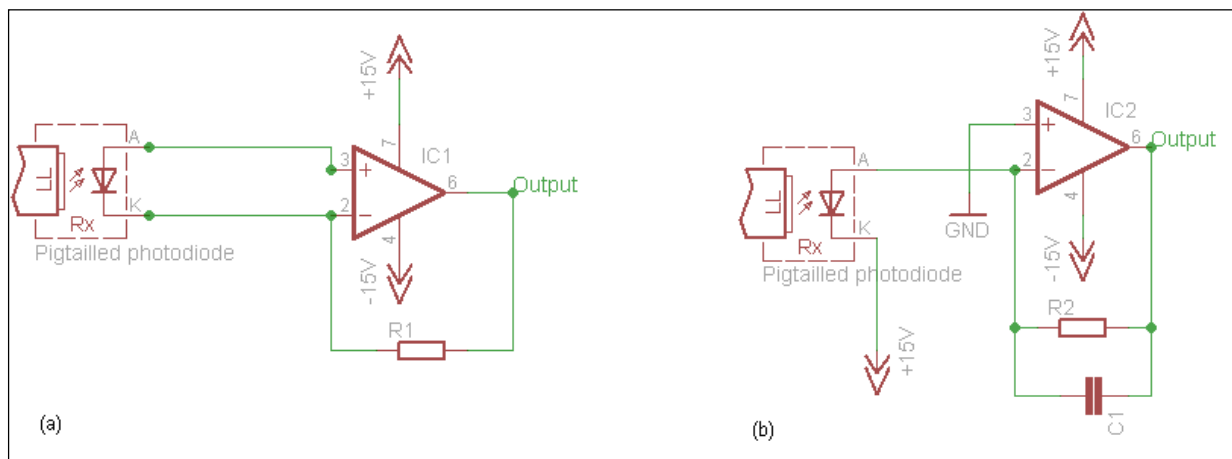


**Figure 4.16: Photodiode amplifier used in photovoltaic mode (a); and photoconductive mode (b).**

In photovoltaic mode (Figure 4.16 (a)), no bias voltage is used to polarise the photodiode thus the photodiode is used as a direct energy conversion device. It can be considered as a very small solar panel. Thus one can either measure the output voltage in open circuit or the output current in short circuit. It is important to note that these circuits make use of operational amplifiers to perform the transimpedance conversion. These components have different parameters limiting their performance, such as unity gain bandwidth, slew rate...

## 4.4.3. Noise considerations:

An operational amplifier has been used in this work to amplify the signal obtained from the photodiode. Noises in the system, however, can either be generated by the operational amplifier or by its associated passive components, superimposed on to the circuit by external sources. Therefore it is important to keep the noise level as low as possible as it is one of the key parameters that limits the performance of the sensor.

There are different types of noises and sometimes it is difficult to separate them, although each type does have its own specific spectrum (or frequency content). The noise is normally described by colour, i.e. *white noise* represents a flat spectrum whereas *pink noise* for example corresponds to a frequency-dependent noise following a 1/F rule, with F being the frequency of the noise; thus the higher the frequency the lower the noise level. It is always useful to determine what type of noise might be having the greatest impact in a circuit so that its mitigation would be the most efficient.

Below describes various types of noises as categorised in operational amplifiers and their associated components:

**Johnson noise (or thermal noise):** This type of noise is unavoidable; it is generated by the random thermal motion of electrons, in a conductor.

For frequencies lower than 100MHz; the value of thermal noise voltage can be calculated using Nyquist's equation:

$$E_{th} = \sqrt{4kTRB} \quad (4.10)$$

With

k= Boltzmann's constant ( $1.38 \times 10^{-23}$  Joules/K)

T= Absolute temperature in Kelvin

R= Resistance in Ohms

B= Noise bandwidth in Hertz

This type of noise is temperature dependent, thus one way of reducing it is to lower the temperature of the circuit. The other way is to lower the value of resistors as this thermal noise level is also associated with the resistance.

**Shot noise:** Sometimes it is also referred to as quantum noise. It is caused by random fluctuations in the motion of charge carriers in a conductor. It occurs when the number of electrons in an electronic circuit is small enough to give rise to detectable statistical fluctuations in a measurement. Unlike thermal noise, it is temperature independent. This type of noise is spectrally flat.

The average shot noise is given as follows:

$$E_{sh} = kT \sqrt{\frac{2B}{qI_{dc}}} \quad (4.11)$$

With

k = Boltzmann's constant ( $1.38 \times 10^{-23}$  Joules/K)

q = Electron charge ( $1.6 \times 10^{-19}$  coulombs)

T = Temperature in K

$I_{dc}$  = Average dc current in Ampere

B = Bandwidth in Hz

From the equation above, it can be seen that increasing the current has an effect on the decrease of the shot noise.

**Flicker noise:** This type of noise is mainly found at low frequencies and so is often called 1/f noise. It is caused by material defects for example related to imperfections in crystalline structure of semiconductors.

**Burst noise:** this type of noise is related to imperfections in semiconductor material and heavy ion implants. It can be described as step-like transitions between discrete voltage or current levels these transitions happen randomly.

In photoconductive mode (Figure 4.16 (b)), a bias voltage is used to polarise the photodiode in reverse mode. The current proportional to the amount of light is converted into a voltage by the resistor  $R_F$

For this work high linearity is required thus it was decided to use the photoconductive mode. After different experiments an amplifier of gain 500 (53.5dB) was used and connected to the

photodiode. This gave a good compromise between high signal to noise ratio and dynamic range.

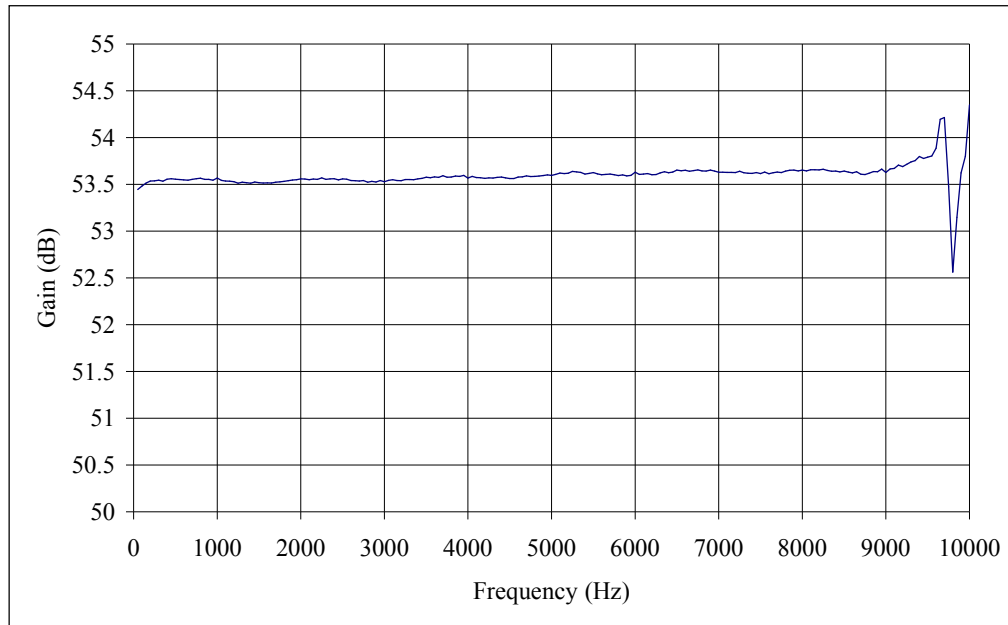


**Figure 4.17: Frequency response of the amplifier used after the photodiode.**

From Figure 4.17, it can be seen that the signal is amplified by 53.5dB with a very small variation through the band from 20 Hz to 10 kHz.

#### 4.4.4. Processing of the signal:

Once amplified the signal was sent to the computer, via a DAQ card. As the signal detected and amplified is an analogue signal, it was required first to be sampled using the Analogue to Digital Converter (ADC), a 14 bit ADC. An important factor in the selection of a right ADC is that it should have the right number of bits, termed as the Least Significant Bit (LSB), which indicates the smallest level of a signal that an ADC can convert. LSB is required to be low enough to allow the detection of any variation in acoustic pressure applied on the LPG. Once the digital signal was sent to the computer, a Fast Fourier Transform (FFT) operation was done with the results obtained being displayed on the computer in real time before being stored into Excel.

#### 4.4.5. LabVIEW based control software

In order to be able to conduct consistent experiments, the setup was fully automated using LabVIEW software and the signals were sent and received using a DAQ card. It is necessary

to generate audible single tone sound waves and the lack of an anechoic chamber requires all the experiments to be performed when no one was present in the lab. Thus most of the experiments were taking place at night; this also had the advantage of reducing the level of interferences caused by the surrounding noise. Thus the software included an experiment planning function that would start and stop the experiment as planned in advance.

The program was composed of one main function called Virtual Instrument (VI) and a multitude of sub functions called Sub VI's. The first step was to define the parameters such as the starting time, the starting and stopping frequency, the frequency step, the amplitude of the signal and the number of experiments to be done.

Once the program was started it would measure the background noise by measuring the signal at the output of the photodiode without any sound signal emitted. The following steps were to generate the sound and concurrently measure the amount of signal detected.

The flow chart of the program is shown in Figure 4.18.

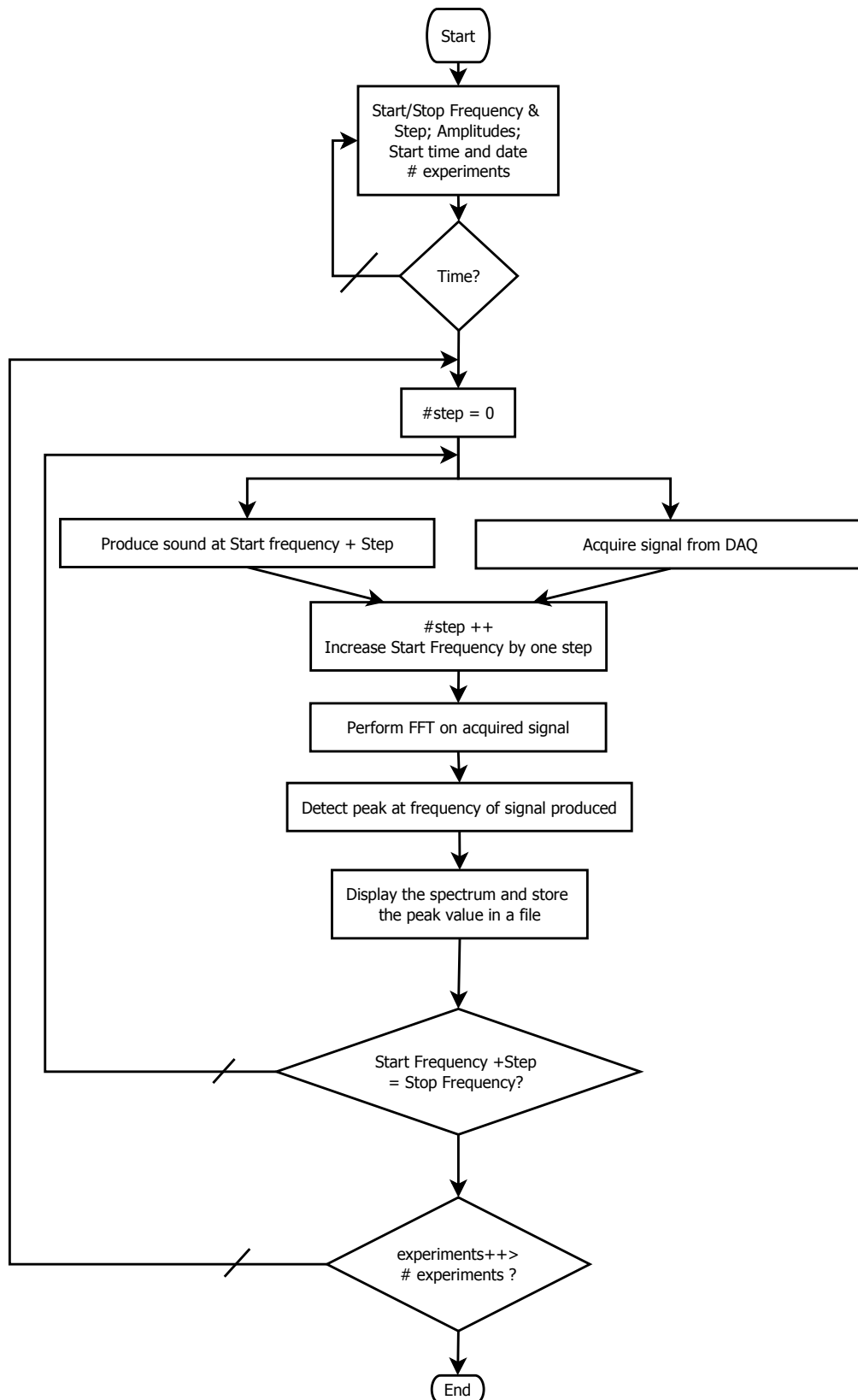
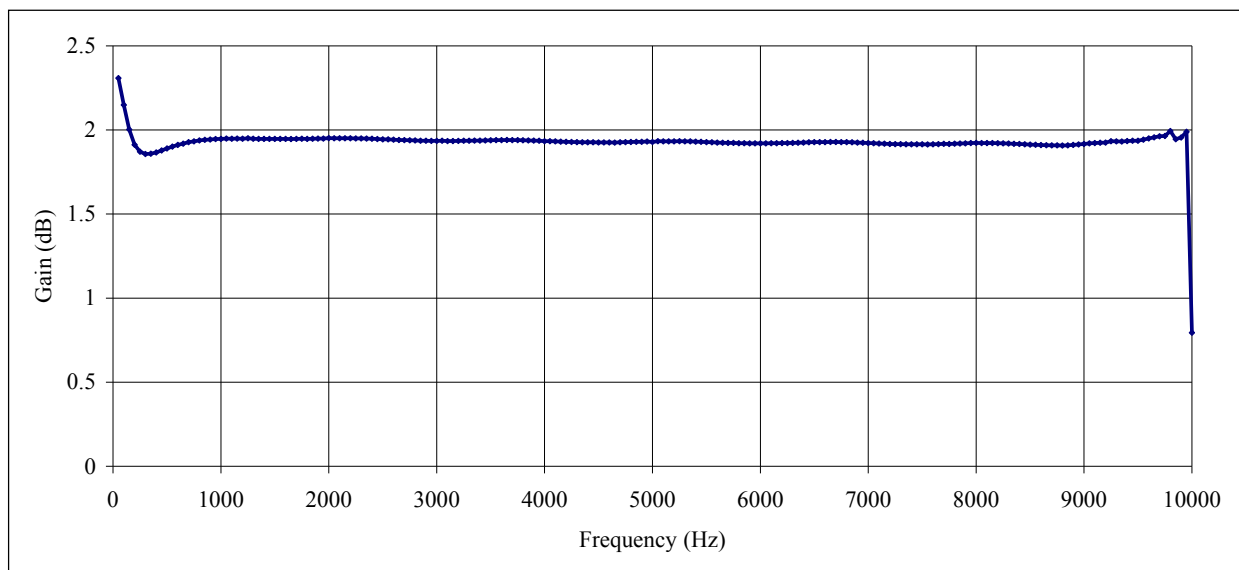


Figure 4.18: Flow chart of the LabVIEW based control software.

## 4.4.6. The sound generation

The measurement of the frequency response required the generation of a single tone signal. In order to produce a single tone of the right form, amplitude and frequency a LabVIEW sound generation sub VI was developed. The VI produced a sine wave sampled at 22 kHz, for 1 second and sent the signal to the DAQ card. Before being amplified using a power amplifier (Denon PMA-100m) and sent to the loudspeaker, the frequency response of the power amplifier was captured using the LabVIEW based software and can be seen in Figure 4.19.



**Figure 4.19: Frequency response of the power amplifier**

From Figure 4.19 it can be seen that the response is relatively flat and the role of the power amplifier is to adapt the impedance from the relatively high output impedance of the DAQ card to the low impedance of the loudspeaker. The frequency response was measured up to 10 kHz since the sampling rate was just over 20 kHz thus any signal above that frequency would create aliasing.

The detailed data showing the emitted acoustic pressure and the applied power to the loudspeaker are given in Table 4.1 and illustrated in Figure 4.20. The first column gives the power applied to the loudspeaker and the second column gives the amount of signal detected by the DAQ card. Finally the third column gives the sound pressure level measured using a dB meter (reference: DT-805) at a distance of 1 meter from the loudspeaker. The measurement of the acoustic pressure level was performed several times in order to verify the consistency of the results obtained.

Power (mW)	Signal amplitude from DAQ (Volts)	Sound pressure level in dB ref 20 $\mu$ Pa
2	0.09	66.8
15.6	0.25	76.6
42	0.41	81
83.4	0.579	83.8
136	0.738	86.3

Table 4.1: Power emitted by the loudspeaker.

The frequency was increased by steps, of 10Hz and this gave a good precision and allowed each experiment to have a reasonable amount of time to perform.

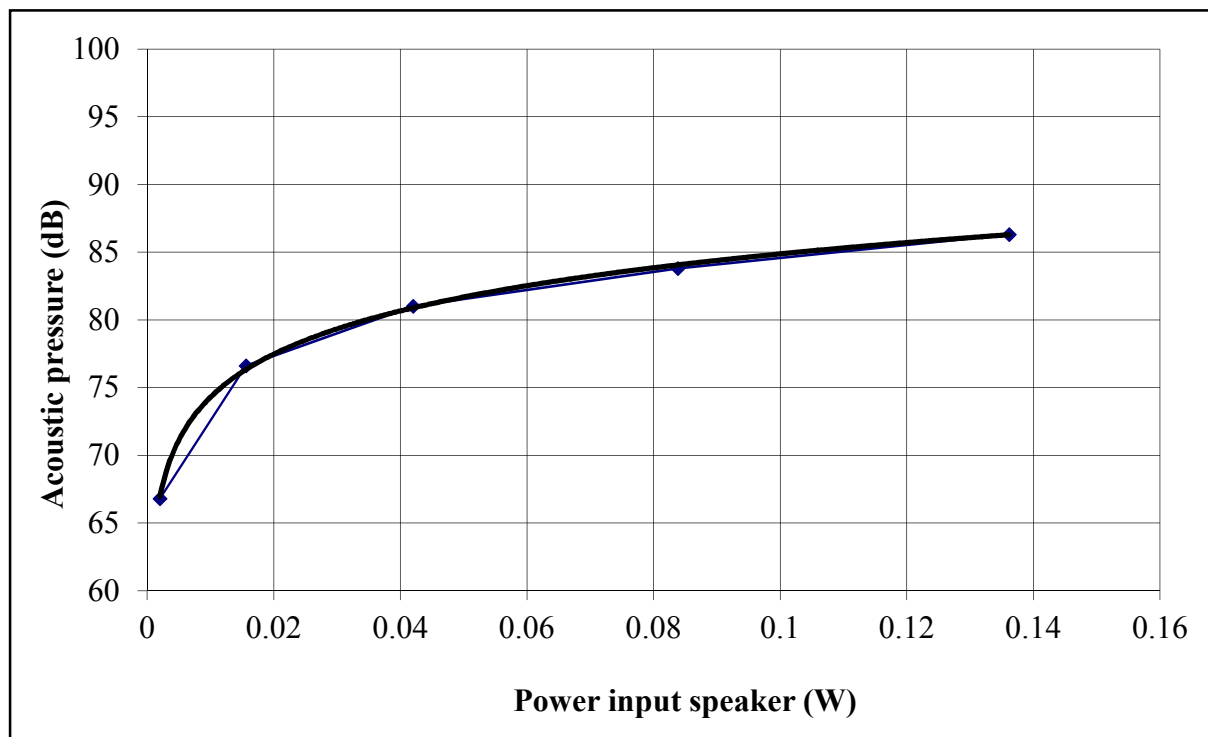


Figure 4.20: Power vs. acoustic pressure.

#### 4.4.7. Choice of the loudspeaker

Different loudspeakers and their frequency response were tested and the finally selected loudspeaker for the detection of sound in air was Eurotec 100mm speaker. It demonstrates a flat frequency response from 20 Hz to 20 kHz, making it a very good fit for the application

The quality of a loudspeaker is directly related to the magnet's quality, the coil and the diaphragm. In order to improve on this, the modulus of the diaphragm material should be as high as possible in order to provide a wider range of frequency responses and lower distortion. The density of the material used should be as low as possible in order to increase fidelity. Research on the improvement of diaphragms is still on-going. [125]

The production of sound waves in water required the use of an underwater loudspeaker, these types of loudspeakers are not very common, and so the ADS Neptune loudspeaker was chosen and found to be the most suitable for the measurement of sound waves in water.

## 4.5. Summary

This chapter discussed the principle of operation of the LPG based acoustic sensor, the process is relatively complex but a theoretical model has been established based on the bending effect of the LPG, modulated by the acoustic pressure applied on to the sensor. In order to set up a LPG-based sensor system, different components required for system have been considered, tested and evaluated, with an aim to have the best possible results from the sensor.

## **Chapter 5**

# **Experimental results obtained from a novel LPG-based acoustic detector.**

### **5.1. Introduction**

In this section a detailed discussion is made based on the results obtained from a novel LPG-based acoustic detection system discussed in detail in Chapter 4, when it was used for the measurement of sound waves both in air and in water. As a result, different setups and experiments have been performed with an aim to achieve the best possible results.

## 5.2. Detection of sound in air

### 5.2.1. Grating connected to the membrane of a loudspeaker.

One of the setups proposed, as illustrated in Figure 5.1, involved gluing a LPG and passing it through the membrane of a loudspeaker on one side and adding a small weight on the other side. This was done by piercing the membrane of the loudspeaker using a needle and passing the fibre through before fixing it to the wheel on the other side.

The LPG had to be used in transmission mode as the propagation of the light caused by the change in bend is causing the wave propagation from the core mode to the forward propagating cladding modes, thus almost no signal is reflected back.

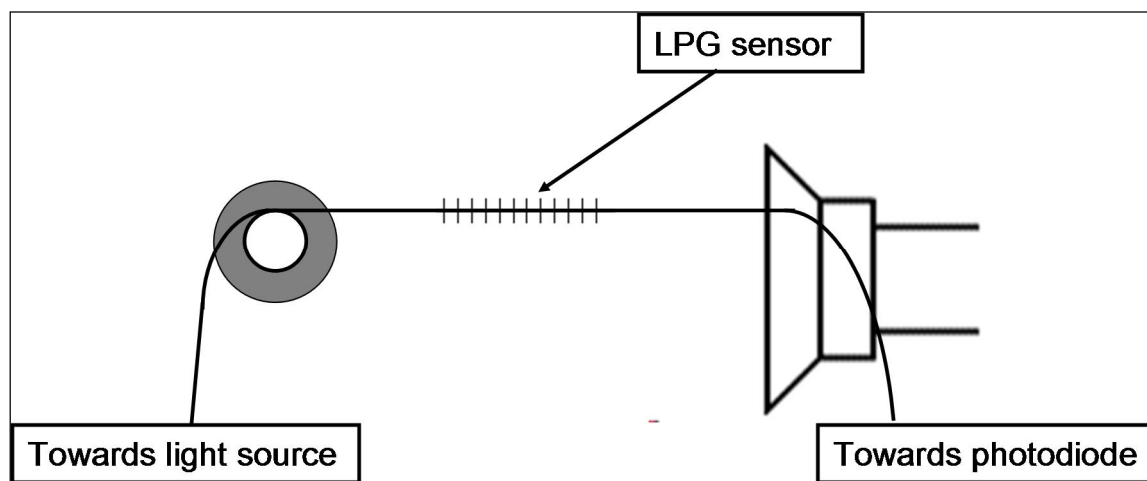
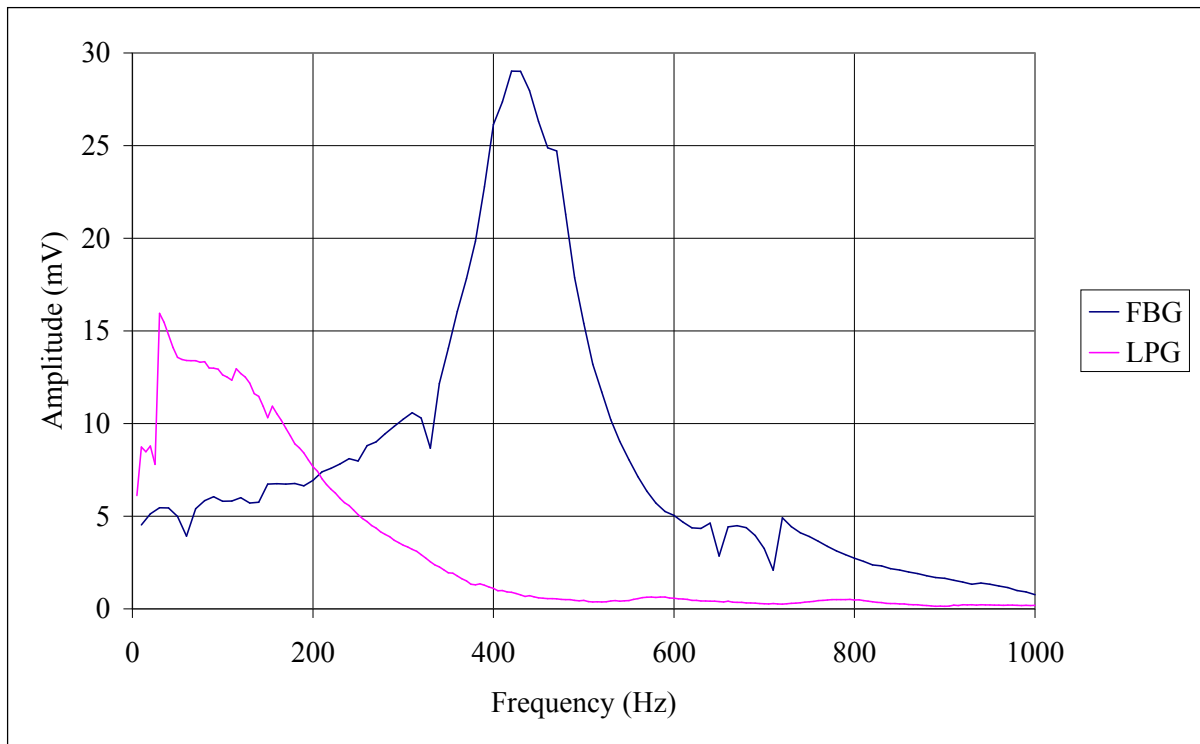


Figure 5.1: Mechanical setup of the LPG connected to the membrane of a speaker

This experimental arrangement was based on the work reported by Mohanty et al. (2006) [104], in which a FBG based acoustic detection system was created and evaluated by using a tube and a membrane.

A set of measurements was made using the sensor system shown in Figure 5.1 and the grating sensor can either be FBG or LPG. The experimental results obtained by using LPG are cross-compared with those using FBG and Figure 5.2 shows the frequency response of these two sensors. The acoustic pressure was 63.7 dB ref 20 $\mu$ Pa, giving a sensitivity of up to 979mV/Pa for the FBG and 490mV/Pa for the LPG sensor



**Figure 5.2: Frequency response of the LPG and FBG-based sensors**

### 5.2.2. Grating between 2 pillars

This setup was based on the measurement of bending discussed in detail in Chapter 4. The system used in this work for sound detection in air is composed of a light source, a pair of pillars in between of which the sensing LPG was fixed as shown in Figure 5.3.

The signal is detected using a photodiode amplified by 54dB and sent to the DAQ card for the input into a computer for further data analysis.

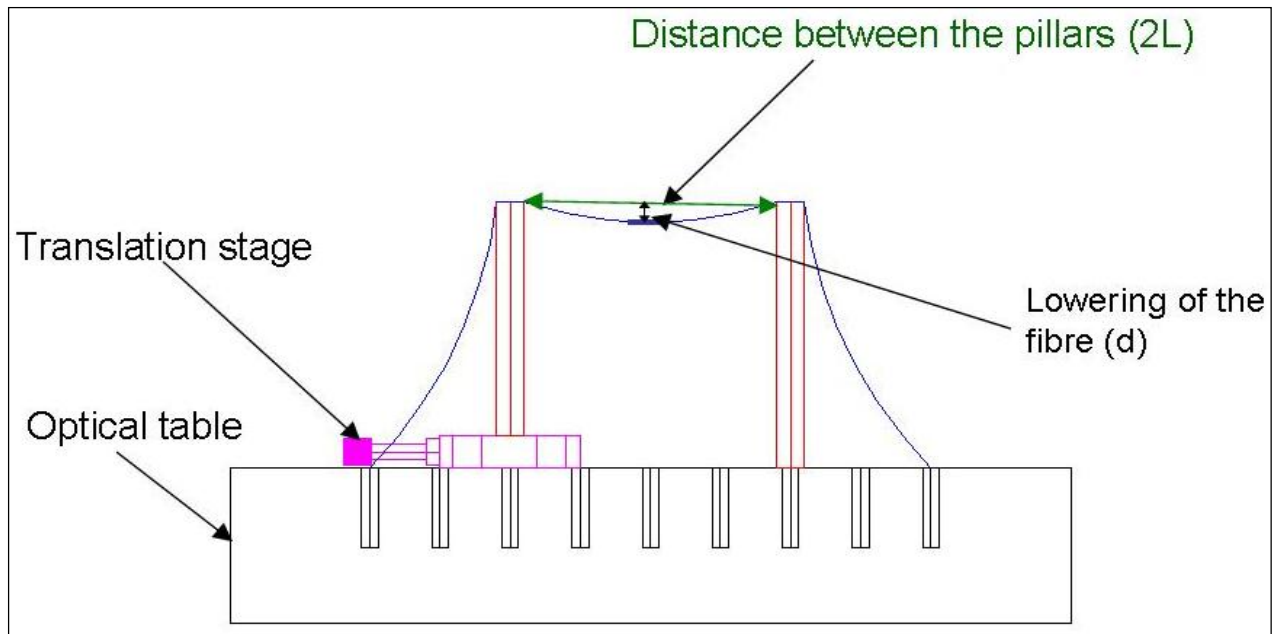


Figure 5.3: LPG-based sensor system with the LPG being fixed between two pillars.

### 5.2.3. Frequency response

In order to evaluate the sensor system shown in Figure 5.3 and its response to various acoustic signals, a loudspeaker of a diameter of 100mm was placed at a distance of 300mm from the fibre and produced a sound wave with different amplitudes and tones. It is orientated towards the middle of the fibre.

The experimental results obtained and shown in Figure 5.4 confirm that the frequency response of the LPG sensor fixed between two pillars is confined between 1000 and 2200Hz and the sensitivity of the sensor at lower and higher frequencies is difficult to measure as it is buried in the noise. The frequency step of 10Hz allows a good compromise between resolution and time to perform each set of experiments.

The pulse duration of 1 second is specifically chosen as a compromise between the speed of the experiment and the time needed for the LPG to detect the sound so that the detection system can detect the signal.

For each value of the bend of the fibre, the amplitude of the loudspeaker was varied between 66.8dB ref 20 $\mu$ Pa and 86.3dB ref 20 $\mu$ Pa. In order to eliminate any fluctuation caused by the amplifier, the signal was measured on the pins of the loudspeaker and recorded.

## 5.2.4. Amplitude response

Figure 5.4 also shows clearly the overlay of spectra of the LPG when it is exposed to various acoustic pressures, through the change of both the amplitude of the sound wave from 66.8dB to 86.3dB in 5 steps and the frequency of the sound from 1000 to 2200Hz by steps of 10Hz.

The fibre length was 100mm and the curvature set at  $0.48\text{m}^{-1}$ , the intensity variation of the sound produced by the loudspeaker does not cause any changes in the pattern of the frequency response of the LPG and the LPG has demonstrated a wide frequency response over the whole spectrum, although much higher sensitivities have been identified at frequency bands of around 1210Hz, 1340Hz and 1490Hz respectively.

The minimum detectable acoustic pressure was found to be 37dB; this figure could be reduced through the optimization of the experimental setup, for example using an embedded system rather than a computer. An embedded system could use a more advanced scheme for Analogue to digital conversion, but also the smaller size and lower amount of connectors and cables makes it less susceptible to noise and interferences.

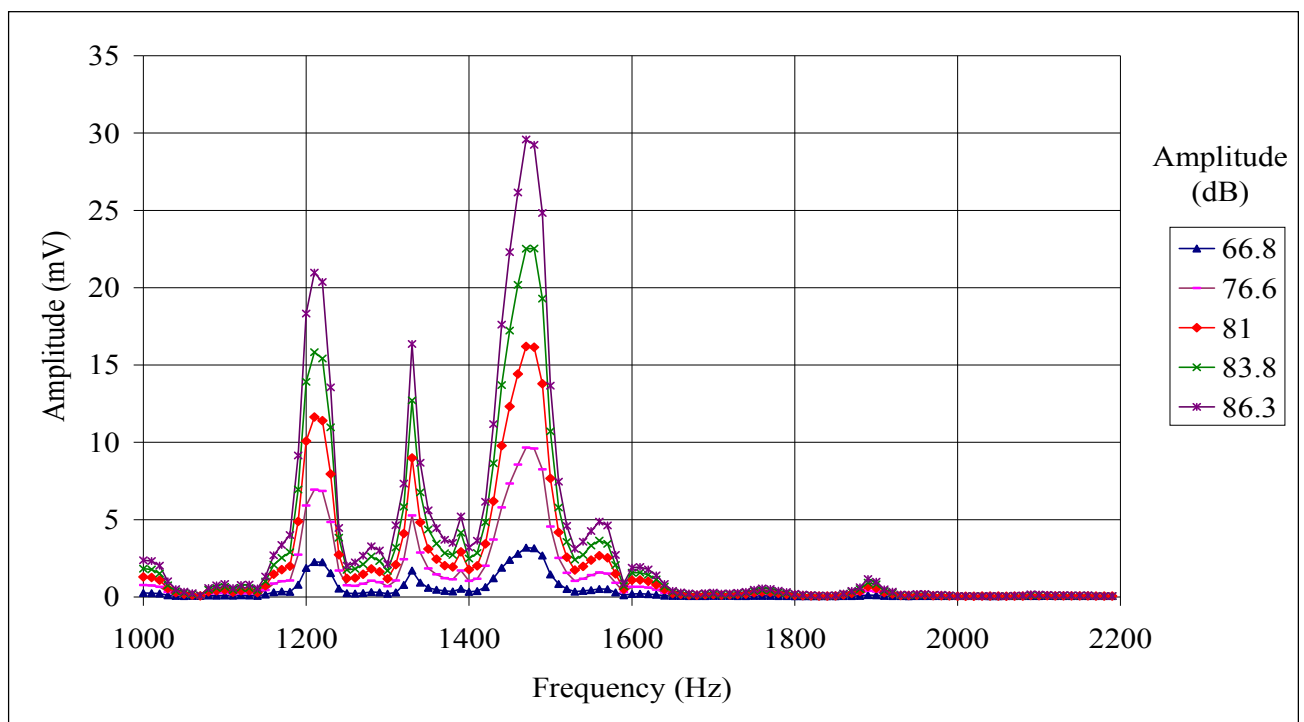


Figure 5.4: Frequency response of the LPG sensor fixed between two pillars when it is exposed to various acoustic pressures.

### 5.2.5. Curvature

In Chapter 4 the effect of the bending curvature on the frequency of the signal detected was discussed in detail and the equation derived was:

$$f_n = \frac{nv}{\frac{4}{c} \cdot \arcsin(LC)}, n = 1, 2, 3, 4 \dots \quad (5.1)$$

Based on this, a cross-comparison, showing both the theoretical values derived from equation (5.1) and the experimental values of the frequencies detected as shown in Figure 5.4, can thus be made and shown in Table 5.1

Curvature $m^{-1}$		$f_n$	$f_{n+1}$	$f_{n+2}$	$f_{n+3}$	$f_{n+4}$
0.08	<b>n</b>	6	7	8	9	10
	<b>Theory</b>	1132.22	1320.93	1509.63	1698.34	1887.04
	<b>Experiment</b>	1130	1330	1460		1900
0.32	<b>n</b>	12	13	14	15	16
	<b>Theory</b>	1138.10	1232.94	1327.78	1422.63	1517.47
	<b>Experiment</b>	1140	1250	1330	1410	1500
0.48	<b>n</b>	11	12	13	14	15
	<b>Theory</b>	1214.31	1324.70	1435.09	1545.48	1655.87
	<b>Experiment</b>	1210	1330	1450		
0.64	<b>n</b>	12	13	14	15	16
	<b>Theory</b>	1350.30	1462.83	1575.35	1687.88	1800.40
	<b>Experiment</b>	1340	1450			1840
0.8	<b>n</b>	12	13	14	15	16
	<b>Theory</b>	1350.80	1463.37	1575.93	1688.50	1801.07
	<b>Experiment</b>	1350				1840

Table 5.1: Comparison between the theoretical and experimental values of the frequencies detected.

There is a good correlation between theoretical and experimental data, however some of the frequency peaks are not detected, and this is due to the fact that the grating not being completely free to move at these frequencies.

Figure 5.5 shows the sensor response when the bending curvature changes and the peak frequencies at each curvature value can be identified and are shown in Table 5.1.

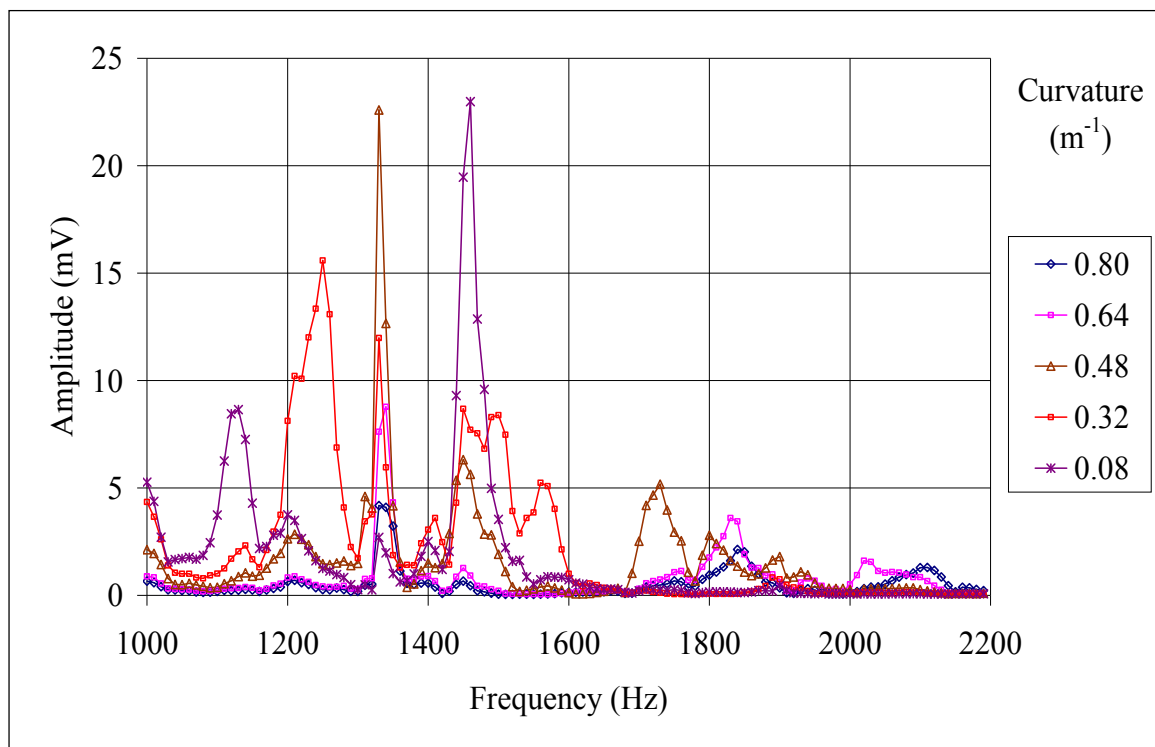


**Figure 5.5: Frequency response of the LPG when the bending curvature changes**

The close match between the theoretical and experimental data shown in Figure 5.5 further confirms that the resonant frequency detected by the LPG is closely related to the bending effect of the LPG, should this be caused by the fibre length change or the pillar distance change. The detected frequency peaks are harmonics of the fundamental frequencies. It was observed that with the increase of the bending curvature, the change of the fundamental frequencies becomes smaller. There are some ‘missing’ frequencies in the set of experimental data especially when the curvature value becomes larger. This may be due to the fact that when the bending curvature is larger, the fibre is more loosely placed between pillars and conditions hold for the modified elastic string theory may no longer be valid.

#### 5.2.6. Standard deviation (consistency of the results)

In order to ensure the reliability of the measurements, each frequency response was measured for 100 times. For each set of the data obtained, both the average and the standard deviation are calculated. As shown in Figure 5.6. When the volume of the sound is increased, the standard deviation is diminishing.

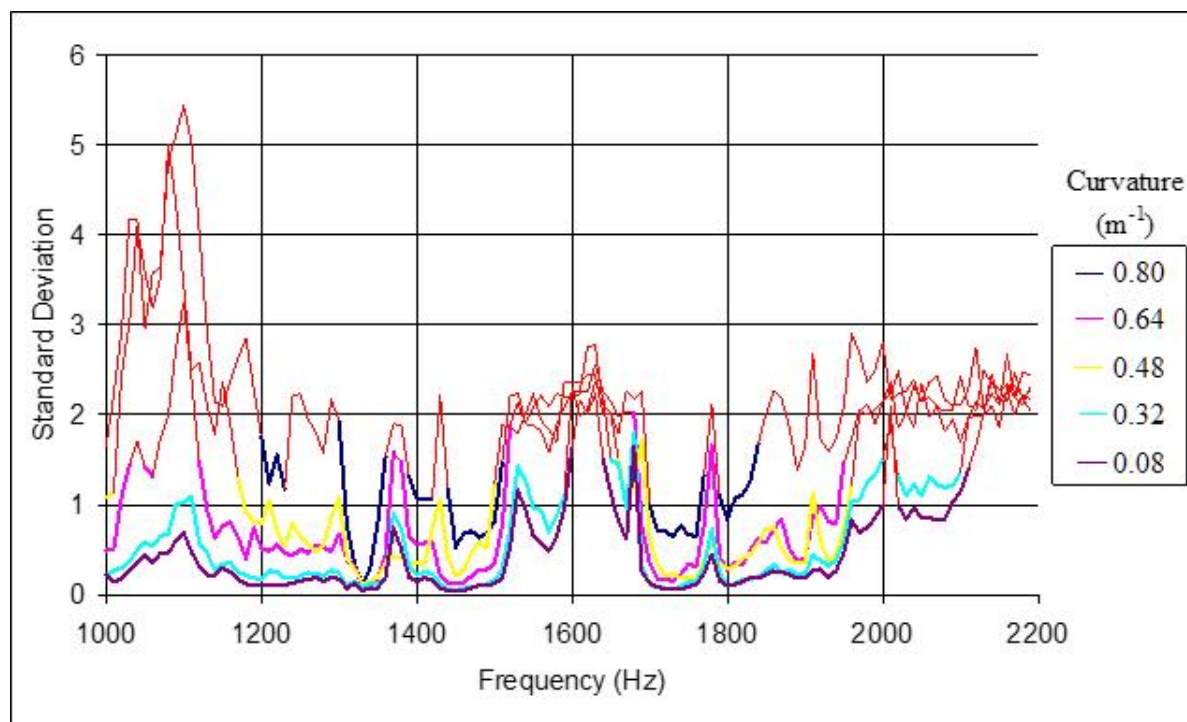


Figure 5.6: Standard deviation depending on the radius of curvature.

On this graph we can see the influence of the bend on the standard deviation (The intensity of the sound was 86.3dB).

Both the mean value and the standard deviation derived are very important as they show the repeatability of the experiments and allow for the differentiation between the signal and the noise.

The formula of the standard deviation is given below.

$$\sigma = \sqrt{\frac{1}{N} \sum_{i=1}^N (x_i - \bar{x})^2} \quad (5.2)$$

Where  $\bar{x}$  represents the arithmetic mean of the set of values  $x_i$  ( $i = 1, 2, \dots, N$ ) and is defined as:  $\frac{1}{N} \sum_{i=1}^N x_i$ .

Figure 5.7 shows standard deviation calculated when the volume of the sound is increased, where the decrease of the standard deviation shows clearly the increase of signal/noise ratio.

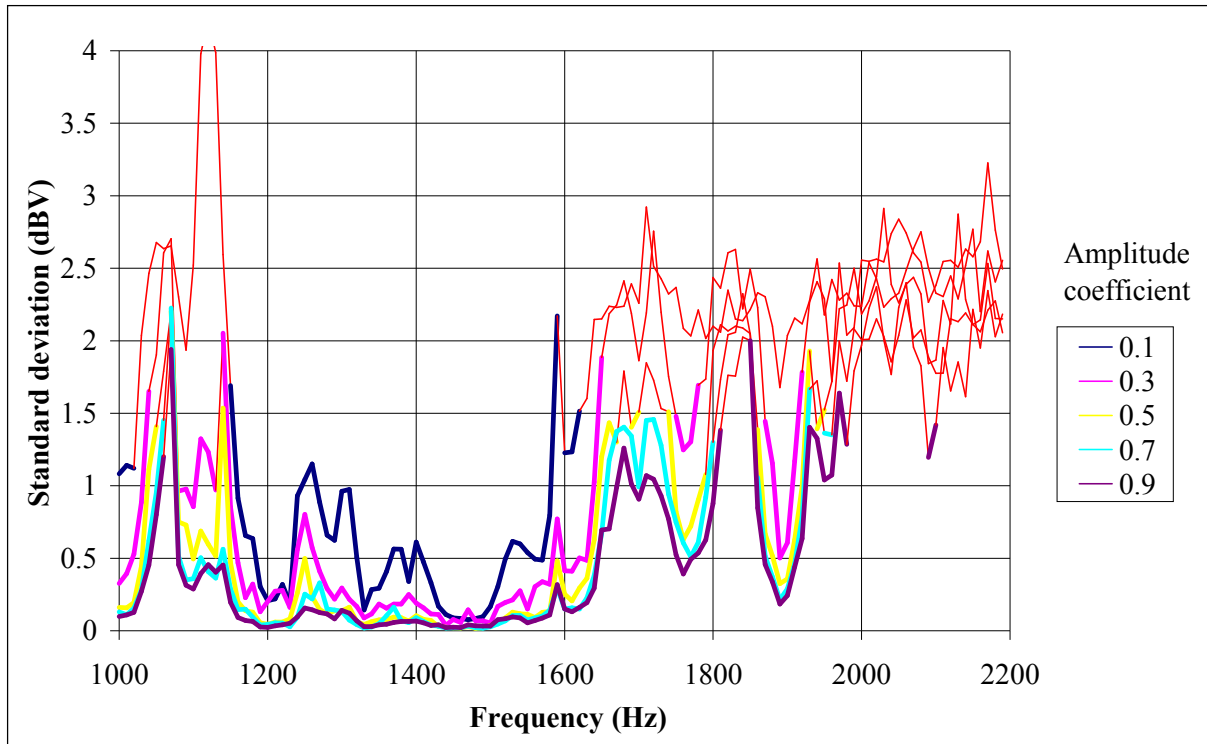


**Figure 5.7: Standard deviation as a function of the frequency of sound wave when its amplitude varies (the bending curvature of the LPG is 0.4mm)**

## 5.3. Detection of sound in water

The measurement of acoustic pressure in water was first proposed by Fessenden in 1912 [126]. It was operating at frequencies from 500Hz to 3 kHz.

### 5.3.1. Frequency response

The detection of sound in water is based on the bending effect of LPG in response to the frequency variation from 10Hz to 3000Hz by a step of 10Hz. The duration of the pulse of 1 second is chosen as a compromise between the speed of the experiment and the time needed for the LPG to detect the sound using the detection system used in this work.

For each value of bend of the fibre, the amplitude of the loudspeaker was varied between 92.8dB to 112.3dB ref  $1\mu\text{Pa}$ , these values were chosen as they give a relatively large acoustic pressure range. In order to eliminate any fluctuation caused by the amplifier the signal was measured on the pins of the loudspeaker and recorded.

At each of these sound pressures, the frequency of the sound was increased from 10 to 3000Hz by steps of 10Hz. The amplitude of the signal was monitored with each process being repeated 20 times. The minimum detectable sound pressure was found to be 63 dB ref  $1\mu\text{Pa}$ . The LPG was placed at a depth of 170mm under water.

### 5.3.2. Amplitude response

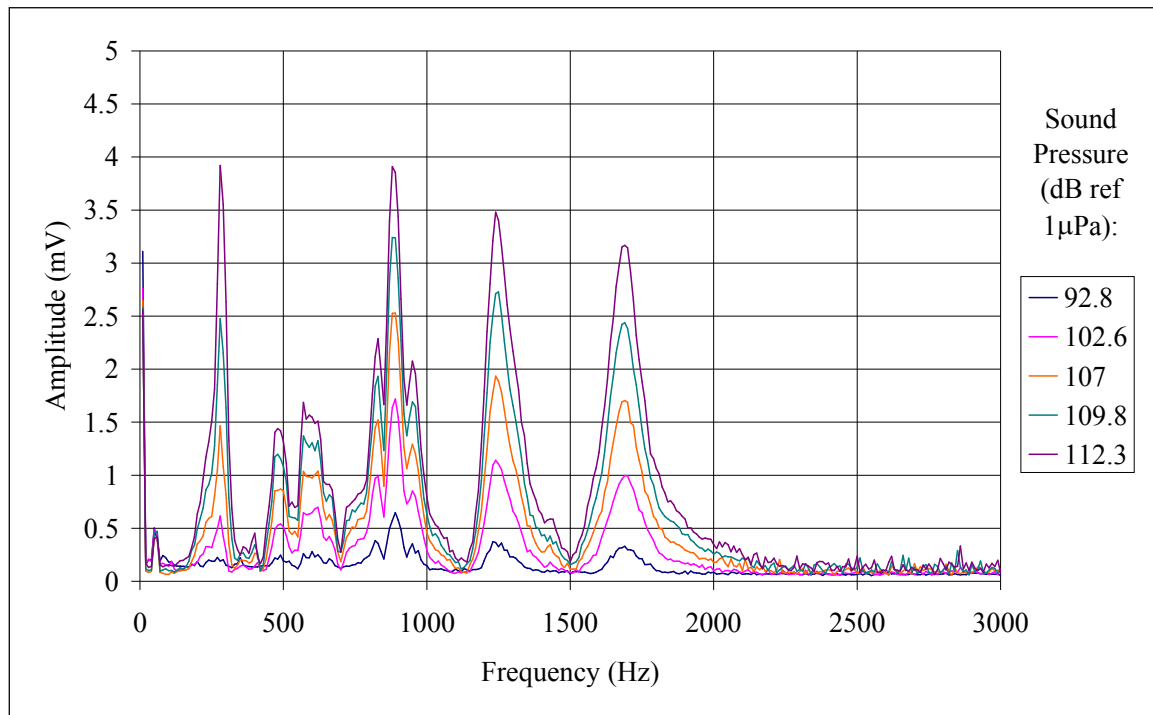
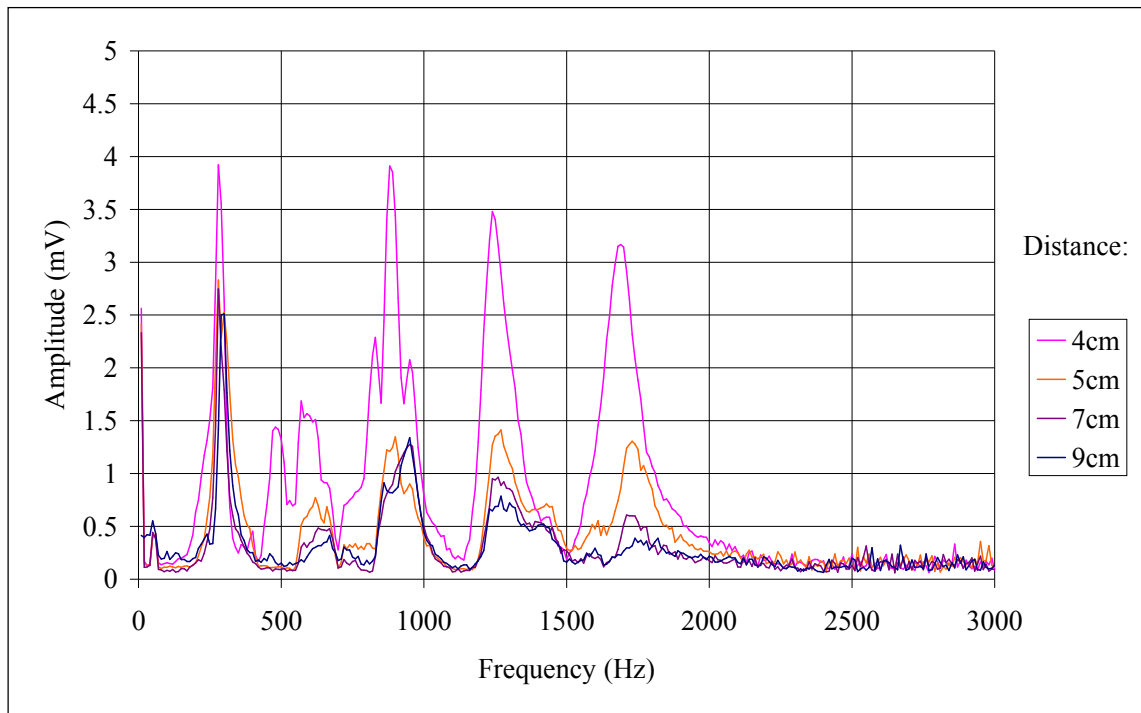


Figure 5.8: Amount of signal detected in relation to the acoustic pressure variation

The shape of the frequency response as shown in Figure 5.8 does not vary with the amount of signal generated by the loudspeaker and this means that the sensor works in a linear regime for this set of acoustic pressures.

### 5.3.3. Distance variation

In order to identify the sensitivity of the sensor as a function of the distance between the sensor and the loudspeaker, sound waves were generated at an acoustic pressure of 112.3dB ref 1 $\mu$ Pa. Figure 5.9 shows that the amount of signal detected decreases with the increase of the distance between the sensor and the loudspeaker. This behaviour is expected as the wave is spreading and scattered due to the surrounding environment [127].



**Figure 5.9: Response of the LPG as a function of the distance from the acoustic source.**

It was found that the maximum distance for a signal to be detected was 120mm. This is mainly caused by the fact that the bending effect of the LPG cannot be detected below a certain acoustic pressure.

#### 5.3.4. Water level effect

Figure 5.10 shows the amount of signal detected by the LPG as a function of its depth under water. The loudspeaker was placed at a distance of 4cm from the LPG, the sound pressure was 112.3dB ref.  $1\mu\text{Pa}$ . It can be seen that the depth of the water has an influence on the amount of signal that is detected. When the level of water is relatively low the pressure applied on the LPG allows it to move more freely than in the case of deep water level.

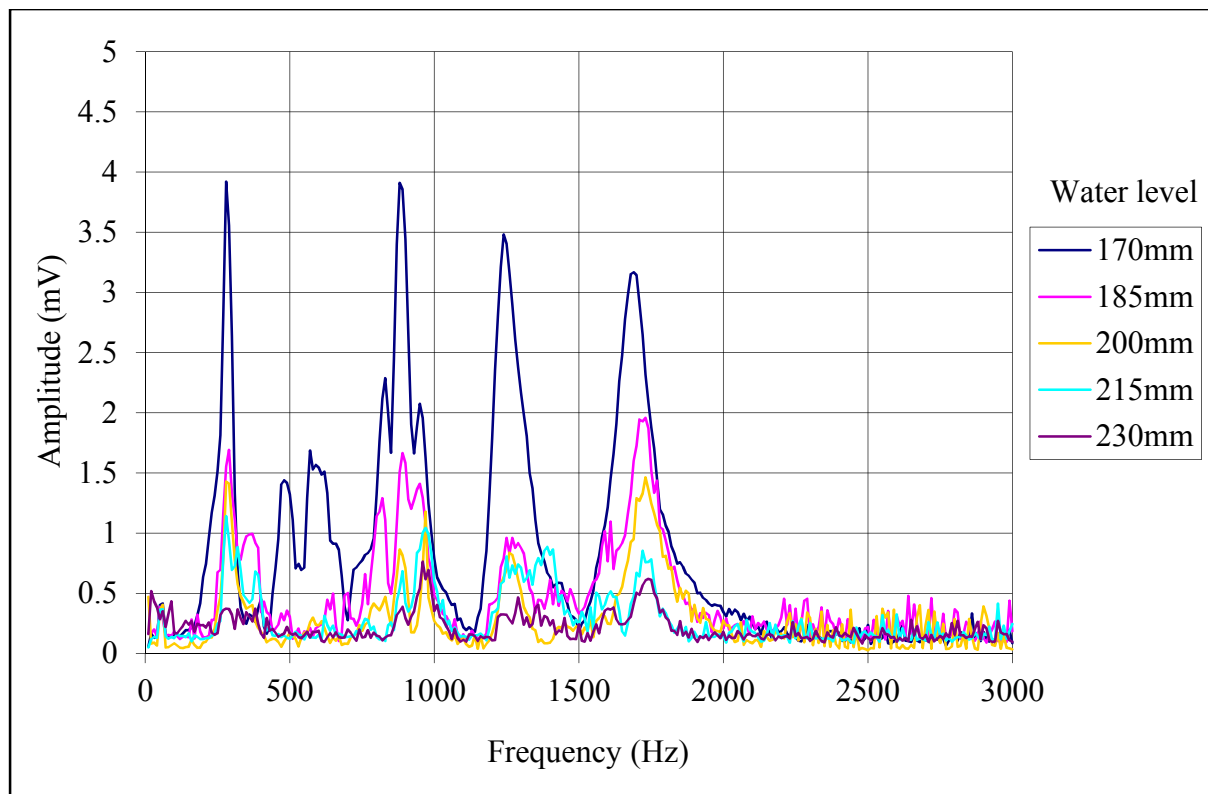


Figure 5.10: Response of the LPG at as a function of the depth of the water level.

## 5.4. The sensor system architecture

### 5.4.1. Mechanical setups

This section is to discuss different mechanical setups used for the acoustic wave pressure detection. Key issues in relation to the sensor system configuration and their related system performance are to be discussed in detail.

### 5.4.2. Setups for measurement of sound in air

Most of the experiments that were performed in air were based on the setup shown in Figure 5.11, where the LPG is placed between 2 identical pillars with a lowering distance of  $d$ . The height of the pillars is 80mm and the diameter of each is 7.5mm. The grating was positioned on the top of the pillars and fixed using blue tack. The advantage of using blue tack compared to glue is that it allows the LPG to be removed and replaced easily.

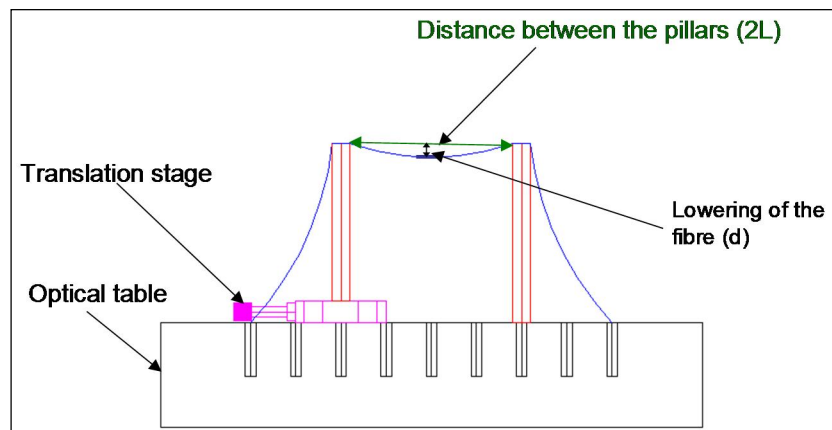


Figure 5.11: Fibre positioned between 2 pillars

One of the pillars was mobile and this was performed by using a translation stage which enables the fibre either to be bent or to remain straight with a slight tension. This setup is relatively bulky as it requires the whole setup to be mounted onto an optical table however it is very convenient to make measurements and characterise the LPG.

Different setups using membranes or diaphragms made of different materials such as paper, laminates or paper composites as used for loudspeakers and polymer materials were also tested, each with a different membrane dimension. It was found that the type of membrane used is critical. Since LPGs work in transmission mode, the fibre used in this work has to go through the membrane which reduces its strength since it has to be pierced. The signal detected using these setups was not very strong since the vibration of the membrane caused by the sound pressure was very small thus it created a wavelength shift that was not very significant.

#### 5.4.3. Setups for measurement of sound in water

When the under-water test is required, materials such as plastic or Perspex are usually preferred. It is also very important to ensure the easy removal and/or replacement of the fibre or adjustment. The setup shown in Figure 5.12 was built at City University and it was used to perform the experiments in water. It gave a good mechanical stability and allowed for some flexibility to conduct different types of experiments.

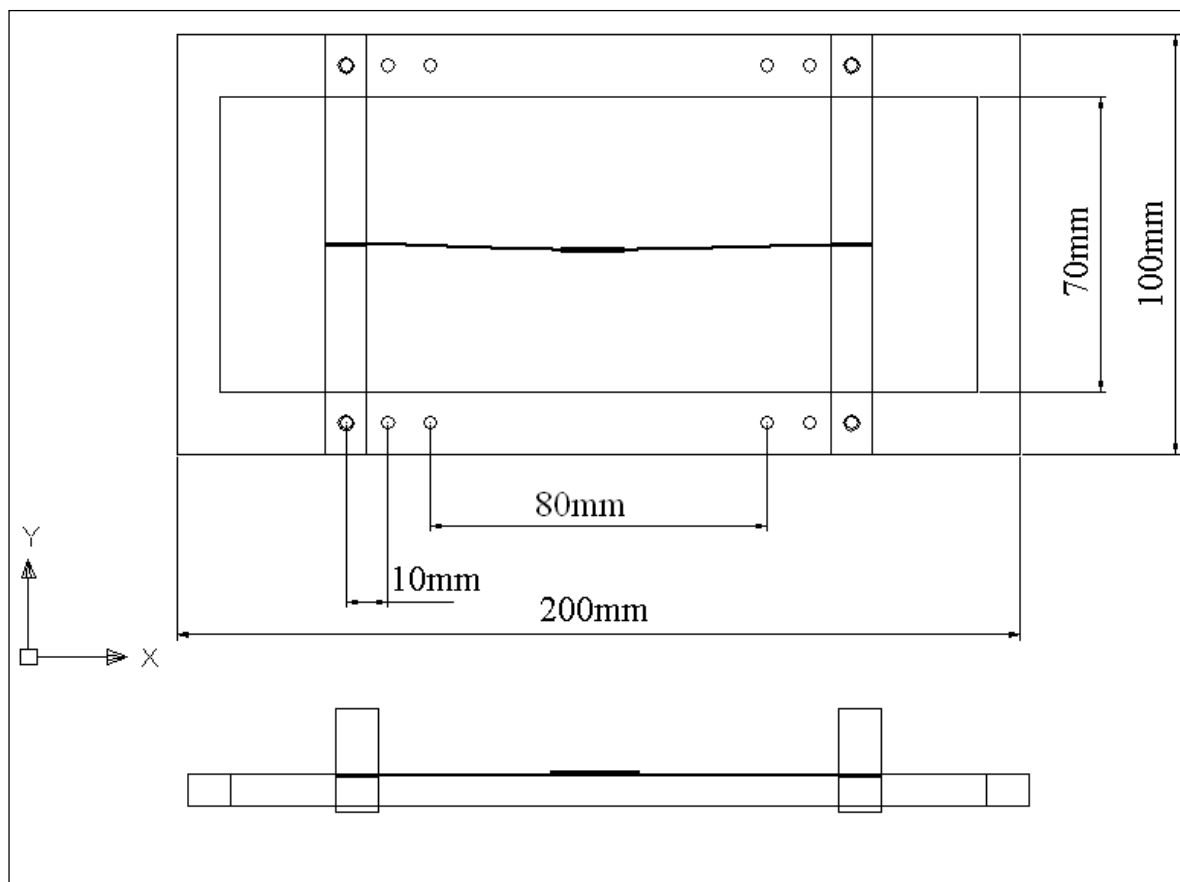


Figure 5.12: Mechanical setup of the underwater system

## 5.5. Summary

A novel method for the detection of acoustic wave pressure induced by a loudspeaker using a long period grating has been discussed and demonstrated. Through monitoring the variation of the transmission signals of the LPG, when it is exposed to various acoustic pressure conditions generated by a loudspeaker placed at a certain distance to the sensor, an effective spectrum of frequency response has been successfully obtained and analysed. The sensor has demonstrated a high level of selectivity to specific frequencies

regardless of the amplitude change and the frequency sensitivity can be tuned by varying the LPG bending curvature, which either can be achieved by varying the distance between the two pillars where the sensor is placed with a fixed fibre length or changing the fibre length with a fixed pillar distance. This dynamic response of the LPG sensor demonstrated was verified successfully by using a modified theory associated with a simple string.

It is important to note that these positive characteristics which have been demonstrated have made the LPG technique very attractive for measurements of acoustic signals over any specific frequency range through an appropriate control of the LPG curvature.

## Chapter 6

### Conclusions and future work

#### 6.1. Conclusions

The work carried out in this thesis is primarily focused on the development of a novel LPG-based sensor for acoustic signal detection. Based on the results obtained from this research and the achievements made, the conclusions of the work carried out in this thesis are drawn below:

- Chapter 2 starts with an introduction to the sensing mechanisms of long period gratings, highlighting their corresponding sensitivities to different physical parameters, such as temperature, strain, refractive index, bending and other parameters, based on the fundamental principles behind the propagation of optical waves in gratings. This is followed by discussions about different methods for inscription of LPGs into optical fibres with a particular focus on the experimental setup used for the fabrication of LPGs used in this work.

- Chapter 3 gives a comprehensive review of different optical fibre based techniques reported for sound detection, based on the classification of the modulation mechanisms used, i.e. intensity, frequency (or phase) and polarization respectively.
- Chapter 4 details the experimental setup used for the creation of a LPG-based acoustic sensor system. This includes evaluation and selection of suitable light sources, based on their stability, output power, wavelength of emission and overall complexity. The optical demodulation system has also been carefully designed and tested in order to provide a good quality signal with a high signal to noise ratio. A computer software based on National Instruments' LabVIEW has been developed and optimized to ensure the measurement accuracy and consistency. The Chapter ends with the discussions of the operational principle based on a modified string theory which has established the link between the frequency response of the LPG and the different parameters affecting it.
- Chapter 5 is focused on the discussions of the experimental results obtained when the acoustic signal varies in frequency and amplitude respectively, coupled with the change in the bending curvature of the sensor. The LPG-based sensor has shown a linear response to the variation of the acoustic pressure amplitude, ranging from 66.8dB to 86.3dB ref 20 $\mu$ Pa in air and 92.8dB to 112.3dB ref 1 $\mu$ Pa in water. The results obtained have confirmed that the LPG-based is sensitive to acoustic signals at a low frequency range from about 10Hz to 3 kHz. The lowest detectable acoustic pressure was found to be 37dB at 1.45 kHz. The sensor response to the curvature variation, however, has shown a very good agreement with the theoretical model derive from the modified string theory and the bending effect of the LPG. In order to validate the quality and consistency of the results, the experiments have been repeated several times, showing the consistency of the data sampling throughout the whole experimental process which is quantified by standard deviations.

## 6.2. Future work

Although the results obtained using these sensors have been very positive, the fact that they are configured in a transmission mode makes them difficult to be used in practical applications. It is important in the future to consider its practicality, for example, to convert the sensor layout to be in the reflective mode, allowing both for the easy access to the sensor system and for the sensor installation. One possible solution is to coat a silver mirror at one end surface of the fibre where a LPG is written in and in this case the light propagates twice through the LPG.

In this work, the LPG has been fixed between two pillars, with one being movable. Such a bulky layout can be difficult to be used in reality; therefore improvements on the clamping mechanism are required to enable both the miniaturisation of the sensor and the tunability of the LPG curvature. One possible solution is to encapsulate the LPG so that it can be easily integrated into an acoustic sensing unit.

In addition improvements on the signal to noise ratio of the signal obtained could be made by simulating the noise level using highly performant operational amplifiers and aiming at reducing it as much as possible on the detection stage.

## 6.3. List of publications

### Journal papers

J.-O. Gaudron, F. Surre, T. Sun, K.T.V. Grattan, Long Period Grating-based optical fibre sensor for the underwater detection of acoustic waves, *Sensors and Actuators A: Physical*, Volume 201, 15 October 2013, Pages 289-293

J.-O. Gaudron, F. Surre, T. Sun, K.T.V. Grattan, LPG-based optical fibre sensor for acoustic wave detection, *Sensors and Actuators A: Physical*, Volume 173, Issue 1, January 2012, Pages 97-101

### Conferences

J.-O. Gaudron; F. Surre; T. Sun; K.T.V. Grattan, "Optimized acoustic wave detector based on long period grating," *Sensors, 2011 IEEE*, vol., no., pp.2046,2049, 28-31 Oct. 2011

J.-O. Gaudron ; F. Surre ; T. Sun ; K. T. V. Grattan; Long period grating for acoustic wave detection. Proc. SPIE 7753, 21st International Conference on Optical Fiber Sensors, 77539N (May 17, 2011)

---

# References

1. Dietrich M. Theory of dielectric optical waveguides. Academic Press; 1974. 257 p.
2. Keiser G. Optical fiber communications [Internet]. 4th ed. McGraw-Hill Education; 2008. 624 p. Available from: <http://books.google.co.uk/books?id=5JeN4QhYo8kC>
3. Grattan KTV, Meggitt BT. Optical Fiber Sensor Technology. London: Chapman & Hall; 1998. 440 p.
4. Snyder AW, Love J. Optical Waveguide Theory. Springer Science & Business Media; 1983. 766 p.
5. Bhatia V. Properties and sensing applications of long-period gratings. [Virginia Polytechnic Institute and State University, Blacksburg, Virginia]; 1996.
6. Bhatia V, Vengsarkar AM. Optical fiber long-period grating sensors. Opt Lett. 1996 May 1;21(9):692–4.
7. Hill K, Fujii Y, Johnson D, Kawasaki B. Photosensitivity in optical fiber waveguides: Application to reflection filter fabrication. Appl Phys Lett. 1978 May 15;32(10):647–9.
8. Li Sheng, Jiang De-sheng. Structural large strain monitoring based on FBG sensor. Photonics and Optoelectronics, 2009 SOPO 2009 Symposium on. 2009. p. 1–4.
9. James SW, Dockney ML, Tatam RP. Simultaneous independent temperature and strain measurement using in-fibre Bragg grating sensors. Electron Lett. 1996;32(12):1133–4.
10. Betz D, Thursby G, Culshaw B, Staszewski WJ. Identification of structural damage using multifunctional Bragg grating sensors: I. Theory and implementation. Smart Mater Struct. 2006;15(5):1305.
11. Choi K-S, Geun-Jin Kim J-YS, Young J, Baik S-J, Im K, Kim J-M, et al. Enhancement of FBG multiplexing capability using a spectral tag method. Photonics Technol Lett IEEE. 2008;20(23):2013–5.

12. Vengsarkar AM, Lemaire PJ, Judkins JB, Bhatia V, Erdogan T, Sipe JE. Long-period fiber gratings as band-rejection filters. *Light Technol J Of.* 1996;14(1):58–65.
13. James SW, Tatam RP. Optical fibre long-period grating sensors: characteristics and application. *Meas Sci Technol.* 2003;14(5):49–61.
14. Hou R, Ghassemlooy Z, Hassan A, Lu C, Dowker KP. Modelling of long-period fibre grating response to refractive index higher than that of cladding. *Meas Sci Technol.* 2001;12(10):1709–13.
15. Bhatia V. Applications of long-period gratings to single and multi-parameter sensing. *Opt Express.* 1999 May 24;4(11):457–66.
16. Savin S, Digonnet MJF, Kino GS, Shaw HJ. Tunable mechanically induced long-period fiber gratings. *Opt Lett.* 2000 May 15;25(10):710–2.
17. Lin C-Y, Chern G-W, Wang LA. Periodical corrugated structure for forming sampled FBG and LPG with tunable coupling strength. *J Light Technol.* 2001;19(8):1212–20.
18. Davis DD, Gaylord TK, Glytsis EN, Kosinski SG, Mettler SC, Vengsarkar AM. Long-period fibre grating fabrication with focused CO<sub>2</sub> laser pulses. *Electron Lett.* 1998;34(3):302–3.
19. Poole CD, Presby HM, Meester JP. Two-mode fibre spatial-mode converter using periodic core deformation. *Electron Lett.* 1994;30(17):1437–8.
20. Palai P, Satyanarayan MN, Das M, Thyagarajan K, Pal BP. Characterization and simulation of long period gratings fabricated using electric discharge. *Opt Commun.* 2001 Jun 15;193(1-6):181–5.
21. Rego G, Okhotnikov O, Dianov E, Sulimov V. High-temperature stability of long-period fiber gratings produced using an electric arc. *Light Technol J Of.* 2001;19(10):1574–9.
22. Kondo Y, Nouchi K, Mitsuyu T, Watanabe M, Kazansky PG, Hirao K. Fabrication of long-period fiber gratings by focused irradiation of infrared femtosecond laser pulses. *Opt Lett.* 1999 May 15;24(10):646–8.

23. Hindle F, Fertein E, Przygodzki C, Durr F, Paccou L, Bocquet R, et al. Inscription of long-period gratings in pure silica and Germano-silicate fiber cores by femtosecond laser irradiation. *IEEE Photonics Technol Lett.* 2004 Aug;16(8):1861–3.
24. Changrui Liao, Ying Wang, Wang DN, Long Jin. Femtosecond laser inscribed long-period gratings in all-solid photonic bandgap fibers. *IEEE Photonics Technol Lett.* 2010 Mar;22(6):425–7.
25. Allsop T, Kalli K, Zhou K, Lai Y, Smith G, Dubov M, et al. Long period gratings written into a photonic crystal fibre by a femtosecond laser as directional bend sensors. *Opt Commun.* 2008 Oct 15;281(20):5092–6.
26. Ju J, Jin W. Long period gratings in photonic crystal fibers. *Photonic Sens* [Internet]. 2011 Jun 15 [cited 2011 Dec 17]; Available from: <http://www.springerlink.com/content/0847k16512442686/>
27. Fujimaki M, Ohki Y, Brebner JL, Roorda S. Fabrication of long-period optical fiber gratings by use of ion implantation. *Opt Lett.* 2000 Jan 15;25(2):88–9.
28. Meltz G, Morey WW, Glenn WH. Formation of Bragg gratings in optical fibers by a transverse holographic method. *Opt Lett.* 1989;14(15):823–5.
29. Hill KO, Malo B, Bilodeau F, Johnson DC. Photosensitivity in optical fibers. *Annu Rev Mater Sci.* 1993 Aug;23:125–57.
30. Hill KO, Malo B, Bilodeau F, Johnson DC, Albert J. Bragg gratings fabricated in monomode photosensitive optical fiber by UV exposure through a phase mask. *Appl Phys Lett.* 1993 Mar;62(10):1035–7.
31. Kohnke GE, Nightingale DW, Wigley PG, Pollock CR. Photosensitization of optical fiber by UV exposure of hydrogen loaded fiber. *Optical Fiber Communication Conference, 1999, and the International Conference on Integrated Optics and Optical Fiber Communication OFC/IOOC '99 Technical Digest.* IEEE; 1999. p. PD20/1–PD20/3 Suppl.

32. Chen KP, Herman PR, Tam R, Zhang J. Rapid long-period grating formation in hydrogen-loaded fibre with 157 nm F2-laser radiation. *Electron Lett.* 2000;36(24):2000–1.
33. Shu X, Allsop T, Gwandu B, Zhang L, Bennion I. High-temperature sensitivity of long-period gratings in B-Ge codoped fiber. *Photonics Technol Lett IEEE.* 2001;13(8):818–20.
34. Venugopalan T, Yeo TL, Sun T, Grattan KTV. High sensitivity long-period grating-based temperature monitoring using a wide wavelength range to 2.2 $\mu$ m. *Opt Commun.* 2006 Dec 1;268(1):42–5.
35. Pal S, Mandal J, Sun T, Grattan KTV, Fokine M, Carlsson F, et al. Characteristics of potential fibre Bragg grating sensor-based devices at elevated temperatures. *Meas Sci Technol.* 2003 Jul 1;14(7):1131–6.
36. Jang J-N, Kim SY, Kim S-W, Kim M-S. Novel temperature insensitive long-period grating by using the refractive index of the outer cladding. *Optical Fiber Communication Conference, 2000. IEEE; 2000.* p. 29–31.
37. Yan W, Xiaoping Z, Dan L, Xingliu H. Based on the spectrum of long-period fiber grating in liquid level measurement. *Mechatronic Science, Electric Engineering and Computer (MEC), 2011 International Conference on.* 2011. p. 653–6.
38. Keith J, Puckett S, Pacey GE. Investigation of the fundamental behavior of long-period grating sensors. *Talanta.* 2003;61(4):417–21.
39. Grice S, Zhang W, Sugden K, Bennion I. Liquid level sensor utilising a long period fiber grating. *Proceedings of SPIE [Internet].* 2009. p. 72120C. Available from: <http://dx.doi.org/10.1117/12.809104>
40. Bhatia V. Temperature-insensitive and strain-insensitive long-period grating sensors for smart structures. *Opt Eng.* 1997;36(7):1872.
41. Wang Y-P, Xiao L, Wang DN, Jin W. Highly sensitive long-period fiber-grating strain sensor with low temperature sensitivity. *Opt Lett.* 2006 Dec 1;31(23):3414–6.

42. Zhang L, Liu Y, Everall L, Williams JAR, Bennion I. Design and realization of long-period grating devices in conventional and high birefringence fibers and their novel applications as fiber-optic load sensors. *IEEE J Sel Top Quantum Electron*. 1999 Sep;5(5):1373–8.
43. Patrick HJ, Chang C, Vohra ST. Long period fibre gratings for structural bend sensing. *Electron Lett*. 1998;34(18):1773–5.
44. Liu Y, Zhang L, Williams JAR, Bennion I. Bend sensing by measuring the resonance splitting of long-period fiber gratings. *Opt Commun*. 2001 Jun 15;193(1-6):69–72.
45. Patrick HJ. Self-aligning bipolar bend transducer based on long period grating written in eccentric core fibre. *Electron Lett*. 2000 Oct 12;36(21):1763–4.
46. Allsop T, Gillooly A, Mezentsev V, Earthgrowl-Gould T, Neal R, Webb DJ, et al. Bending and orientational characteristics of long period gratings written in D-shaped optical fiber [directional bend sensors]. *Instrum Meas IEEE Trans On*. 2004;53(1):130–5.
47. Liu Y, Williams JA., Bennion I. Optical bend sensor based on measurement of resonance mode splitting of long-period fiber grating. *IEEE Photonics Technol Lett*. 2000 May;12(5):531–3.
48. Van Brakel A. Sensing Characteristics of an Optical Fibre Long-Period Grating Michelson Refractometer [PhD thesis]. [South Africa]: Rand Afrikaans University; 2004.
49. Shu X, Hu X, Wang Q, Jiang S, Shi W, Huang Z, et al. Dual resonant peaks of LP015 cladding mode in long-period gratings. *Electron Lett*. 1999 Apr 15;35(8):649–51.
50. Ye CC, James SW, Tatam RP. Simultaneous temperature and bend sensing with long-period fiber gratings. *Opt Lett*. 2000 Jul 15;25(14):1007–9.
51. Du W, Tam H, Liu M, Tao X. Long-period fiber grating bending sensors in laminated composite structures. *SPIE [Internet]*. San Diego, CA, USA: SPIE; 1998. p. 284–92. Available from: <http://dx.doi.org/doi/10.1117/12.316984>

52. Tanaka S, Wada A, Takahashi N. Highly sensitive operation of LPG vibration sensor using bending-induced spectral change. SPIE [Internet]. Ottawa, Canada: SPIE; 2011. p. 77539Q. Available from: <http://dx.doi.org/doi/10.1117/12.885055>
53. Bell AG. Selenium and the Photophone. *Nature*. 1880 Sep 23;22(569):500–3.
54. Pabst von Ohain HJ. Ein Interferenzlichtrelais für weißes Licht. *Ann Phys*. 1935;415(5):431–41.
55. Culshaw B, Davies DEN, Kingsley SA. Acoustic sensitivity of optical-fibre waveguides. *Electron Lett*. 1977;13(25):760–1.
56. Fulenwider JE, Gonsalves JPF. Transducer for converting acoustic energy directly into optical energy. Waltham, MA; 4071753, 1978. p. 753.
57. Spillman WB, McMahon DH. Schlieren multimode fiber optic hydrophone. *Appl Phys Lett*. 1980 Jul;37(2):145–7.
58. Morfey C. *The Dictionary of Acoustics*. 2000. 430 p.
59. Spillman WB, McMahon DH. Frustrated-total-internal-reflection multimode fiber-optic hydrophone. *Appl Opt*. 1980 Jan 1;19(1):113–7.
60. Giallorenzi T, Bucaro JA, Dandridge A, Sigel G, Cole J, Rashleigh S, et al. Optical fiber sensor technology. *Quantum Electron IEEE J Of*. 1982;18(4):626–65.
61. Sun A, Semenova Y, Farrell G. A novel highly sensitive optical fiber microphone based on single mode–multimode–single mode structure. *Microw Opt Technol Lett*. 2011 Feb 2;53(2):442–5.
62. Garthe D. A fiber-optic microphone. *Sens Actuators Phys*. 1991 Mar;26(1-3):341–5.
63. Garthe D. Fiber- and integrated-optical microphones based on intensity modulation by beam deflection at a moving membrane. *Sens Actuators Phys*. 1993 Jun;37-38(Proceedings of Eurosensors VI):484–8.
64. Hadjiloucas S, Walker GC, Bowen JW, Karatzas LS. Performance limitations of piezoelectric and force feedback electrostatic transducers in different applications. *J Phys Conf Ser*. 2009 Jul 1;178(1):012036.

65. Song J-H, Lee S-S. Photonic microphone based on a dual-core multimode fiber head combined with a micromirror diaphragm. *Microw Opt Technol Lett.* 2007 Jan 1;49(1):135–7.
66. Sun A, Semenova Y, Farrell G. Low cost disposable reflective optical fiber microphone. *Microw Opt Technol Lett.* 2010;52(7):1504–7.
67. Parker TR, Farhadiroushan M, Handerek VA, Rogers AJ. Temperature and strain dependence of the power level and frequency of spontaneous Brillouin scattering in optical fibers. *Opt Lett.* 1997 Jun 1;22(11):787–9.
68. Parker TR, Farhadiroushan M, Handerek VA, Rogers AJ. A fully distributed simultaneous strain and temperature sensor using spontaneous Brillouin backscatter. *Photonics Technol Lett IEEE.* 1997;9(7):979–81.
69. Fields JN, Cole JH. Fiber microbend acoustic sensor. *Appl Opt.* 1980 Oct;19(19):3265–7.
70. Tsutsui H, Kawamata A, Sanda T, Takeda N. Detection of impact damage of stiffened composite panels using embedded small-diameter optical fibers. *Smart Mater Struct.* 2004 Sep 27;13(6):1284–90.
71. Sheem SK, Cole JH. Acoustic sensitivity of single-mode optical power dividers. *Opt Lett.* 1979 Oct 1;4(10):322–4.
72. Chen R, Bradshaw T, Burns J, Fernando GF, Pedder D, Cole P, et al. Linear location of acoustic emission using a pair of novel fibre optic sensors. *Meas Sci Technol.* 2006;17(8):2313.
73. Irvine JJ, Hadjiloucas S, Keating DA, Usher MJ. An automatic optical fibre feedback potometer for transpiration studies. *Meas Sci Technol.* 1996 Nov 1;7(11):1611.
74. Culshaw B, Giles I. Frequency Modulated Heterodyne Optical Fiber Sagnac Interferometer. *IEEE Trans Microw Theory Tech.* 1982 Apr;30(4):536–9.
75. Dandridge A, Tveten AB, Giallorenzi TG. Homodyne demodulation scheme for fiber optic sensors using phase generated carrier. *IEEE J Quantum Electron.* 1982 Oct;18(10):1647–53.

76. Tayag TJ. Quantum-noise-limited sensitivity of an interferometer using a phase generated carrier demodulation scheme. *Opt Eng.* 2002;41(2):276–7.
77. Bucaro JA, Dardy HD, Carome EF. Optical fiber acoustic sensor. *Appl Opt.* 1977 Jul 1;16(7):1761–2.
78. Bucaro JA, Dardy H, Carome E. Fiber optic hydrophone. *J Acoust Soc Am.* 1977;62(5):1302–4.
79. Jarzynski J, Hughes R, Hickman TR, Bucaro JA. Frequency response of interferometric fiber optic coil hydrophones. *J Acoust Soc Am.* 1981;69(6):1799–808.
80. Cole J, Johnson R, Bhuta P. Fiber optic detection of sound. *J Acoust Soc Am.* 1977 Nov;62(5):1136–8.
81. Zeng N, Shi C, Wang D, Zhang M, Liao Y. Diaphragm type fiber-optic interferometric acoustic sensor. *Opt Eng.* 2003;42(9):2558–662.
82. Wild G, Hinckley S. Acousto-Ultrasonic Optical Fiber Sensors: Overview and State-of-the-Art. *Sens J IEEE.* 2008 Jul;8(7):1184–93.
83. Cranch G, Crickmore R, Kirkendall C, Bautista A, Daley K, Motley S, et al. Acoustic performance of a large-aperture, seabed, fiber-optic hydrophone array. *J Acoust Soc Am.* 2004;115(6):2848–58.
84. Alcoz JJ, Lee CE, Taylor HF. Embedded fiber-optic Fabry-Perot ultrasound sensor. *IEEE Trans Ultrason Ferroelectr Freq Control.* 1990;37(4):302–6.
85. Lima SE, Frazao O, Arujo FM, Ferreira LA, Miranda V, Santos JL. Extrinsic and intrinsic fiber optic interferometric sensors for acoustic detection in high-voltage environments. *Opt Eng.* 2009;48(2):024401.
86. Imai M, Ohashi T, Ohtsuka Y. Fiber-optic Michelson interferometer using an optical power divider. *Opt Lett.* 1980 Oct 1;5(10):418–20.
87. Garrett S, Brown D, Beaton B, Wetterskog K, Serocki J. General purpose fiber optic hydrophone made of castable epoxy. *SPIE [Internet]. SPIE; 1991. p. 13. Available from: <http://dx.doi.org/doi/10.1117/12.24725>*

88. Hill D, Nash P. Fiber-optic hydrophone array for acoustic surveillance in the littoral. SPIE [Internet]. Orlando, FL, USA: SPIE; 2005. p. 1–10. Available from: <http://dx.doi.org/doi/10.1117/12.607550>
89. Ho K-P, Kahn JM. Methods for crosstalk measurement and reduction in dense WDM systems. *J Light Technol.* 1996 Jun;14(6):1127–35.
90. Singh SP, Sharma AK, Singh N. Crosstalk reduction in WDM systems using hybrid amplification technique. *Opt Commun.* 2012 Sep 1;285(19):3931–4.
91. Kersey AD, Dandridge A, Tveten AB. Time-division multiplexing of interferometric fiber sensors using passive phase-generated carrier interrogation. *Opt Lett.* 1987 Oct 1;12(10):775–7.
92. Vakoc BJ, Digonnet MJF, Kino GS. A novel fiber-optic sensor array based on the Sagnac interferometer. *Light Technol J Of.* 1999;17(11):2316–26.
93. Blin S, Bishop M, Parameswaran K, Digonnet MJF, Kino GS. Pickup suppression in sagnac-based fiber-optic acoustic sensor array. *Light Technol J Of.* 2006;24(7):2889–97.
94. Webb D, Surowiec J, Sweeney M, Jackson D, Gavrilov L, Hand J, et al. Miniature fiber optic ultrasonic probe. SPIE [Internet]. Denver, CO, USA: SPIE; 1996. p. 76–80. Available from: <http://dx.doi.org/doi/10.1117/12.255383>
95. Fomitchov P, Krishnaswamy S. Response of a fiber Bragg grating ultrasonic sensor. *Opt Eng.* 2003;42(4):956–63.
96. Takahashi N, Hirose A, Takahashi S. Underwater Acoustic Sensor with Fiber Bragg Grating. *Opt Rev.* 1997 Nov 1;4(6):691–4.
97. Coppola G, Minardo A, Cusano A, Breglio G, Zeni L, Cutolo A, et al. Analysis of feasibility on the use of fiber Bragg grating sensors as ultrasound detectors. SPIE [Internet]. Newport Beach, CA, USA: SPIE; 2001. p. 224–32. Available from: <http://dx.doi.org/doi/10.1117/12.435523>

98. Tanaka S, Yokosuka H, Takahashi N. Temperature-independent fiber Bragg grating underwater acoustic sensor array using incoherent light. *Acoust Sci Technol*. 2006;27(1):50–2.
99. Perez I, Cui H, Udd E. Acoustic emission detection using fiber Bragg gratings. SPIE [Internet]. Newport Beach, CA, USA: SPIE; 2001. p. 209–15. Available from: <http://dx.doi.org/doi/10.1117/12.435542>
100. Cusano A, D’Addio S, Cutolo A, Giordano M, Campopiano S, Balbi M, et al. Plastic Coated Fiber Bragg Gratings As High Sensitivity Hydrophones. *Sensors*, 2006 5th IEEE Conference on. Daegu: IEEE; 2006. p. 166–9.
101. Moccia M, Consales M, Iadicicco A, Pisco M, Giordano M, Cutolo A, et al. Resonant hydrophones based on coated fiber Bragg gratings. Part II: experimental analysis. SPIE [Internet]. Ottawa, Canada: SPIE; 2011. p. 775383. Available from: <http://dx.doi.org/doi/10.1117/12.886064>
102. Moccia M, Pisco M, Cutolo A, Galdi V, Cusano A. Resonant hydrophones based on coated fiber Bragg gratings. Part I: numerical analysis. SPIE [Internet]. Ottawa, Canada: SPIE; 2011. p. 775384. Available from: <http://dx.doi.org/doi/10.1117/12.886011>
103. Iida T, Nakamura K, Ueha S. A microphone array using fiber Bragg gratings. *Optical Fiber Sensors Conference Technical Digest, 2002 OFS 2002, 15th*. Portland, Oregon, USA; 2002. p. 239–42.
104. Mohanty L, Koh LM, Tjin SC. Fiber Bragg grating microphone system. *Appl Phys Lett*. 2006;89(16):161109–161109 – 3.
105. Rashleigh SC. Acoustic sensing with a single coiled monomode fiber. *Opt Lett*. 1980 Sep;5(9):392–4.
106. Chan HLW, Chiang KS, Gardner JL. Polarimetric optical fiber sensor for ultrasonic power measurement. *Ultrasonics Symposium, 1988 Proceedings, IEEE 1988*. Chicago, IL , USA; 1988. p. 599–602.

107. Thursby G, Culshaw B. Ultrasonic modal detection in carbon fibre plates using fibre optic sensors. SPIE [Internet]. Porto, Portugal: SPIE; 2010. p. 765338. Available from: <http://dx.doi.org/doi/10.1117/12.866437>
108. Takahashi N, Tetsumura K, Imamura K, Takahashi S. Fiber Bragg grating WDM underwater acoustic sensor with directivity. Boston, MA, USA: SPIE; 1999. p. 18–26. Available from: <http://dx.doi.org/doi/10.1117/12.339083>
109. Fomitchov PA, Krishnaswamy S. Fiber Bragg grating ultrasound sensor for process monitoring and NDE applications. Thompson DO, Chimenti DE, Poore L, Nessa C, Kallsen S, editors. AIP Conf Proc. 2002 May 25;615(1):937–44.
110. Betz D, Staszewski WJ, Thursby G, Culshaw B. Acousto-ultrasonic sensing using fiber Bragg gratings. Smart Mater Struct. 2003;12(1):122.
111. Betz D, Staszewski WJ, Thursby G, Culshaw B. Structural damage identification using multifunctional Bragg grating sensors: II. Damage detection results and analysis. Smart Mater Struct. 2006;15(5):1313.
112. Nakamura K, Fujisue T, Ueha S. An FBG microphone array system with signal demodulator using AWG. In: Udd E, editor. Fiber Optic Sensors and Applications V [Internet]. Boston, MA, USA: SPIE; 2007. p. 677006–8. Available from: <http://link.aip.org/link/?PSI/6770/677006/1>
113. Johannessen K, Drakeley BK, Farhadiroushan M. Distributed Acoustic Sensing - A New Way of Listening to Your Well/Reservoir. Society of Petroleum Engineers; 2012 [cited 2015 Jan 6]. Available from: <https://www.onepetro.org/conference-paper/SPE-149602-MS>
114. Owen A, Duckworth G, Worsley J. OptaSense: Fibre Optic Distributed Acoustic Sensing for Border Monitoring. Intelligence and Security Informatics Conference (EISIC), 2012 European. 2012. p. 362–4.
115. Dakin J. The distributed fibre optic sensing handbook. IFS Publications; 1990. 230 p.

116. Thévenaz L. Next generation of optical fibre sensors: new concepts and perspectives. 2014 [cited 2014 Dec 30]. p. 9157AN – 9157AN – 4. Available from: <http://dx.doi.org/10.1117/12.2064896>
117. Wild G, Hinckley S. Electro-acoustic and acousto-optic communications for robotic agents in smart structures. SPIE [Internet]. Adelaide, Australia: SPIE; 2006. p. 64140Q. Available from: <http://dx.doi.org/doi/10.1117/12.695750>
118. Campopiano S, Cutolo A, Cusano A, Giordano M, Parente G, Lanza G, et al. Underwater Acoustic Sensors Based on Fiber Bragg Gratings. *Sensors*. 2009;9(6):4446–54.
119. Venugopalan T, Yeo TL, Tong Sun, Grattan K. LPG-Based PVA Coated Sensor for Relative Humidity Measurement. *IEEE Sens J*. 2008 Jul;8(7):1093–8.
120. Costa RZV, Possetti GRC, de Arruda R. L. V., Muller M, Fabris JL. Curvature vector smart sensing with a long-period fibre grating probed by artificial intelligence. *Meas Sci Technol*. 2010;21(9):094027.
121. Klaf A. *Calculus Refresher*. Courier. Dover; 1956. p. 151–68.
122. Young HD, Freedman RA. *Mechanical Waves*. University physics. 12th ed. San Francisco: Pearson Addison-Wesley; 2008. p. 498–513.
123. Kersey AD, Berkoff TA, Morey WW. High-resolution fibre-grating based strain sensor with interferometric wavelength-shift detection. *Electron Lett*. 1992 Jan 30;28(3):236–8.
124. Block UL, Dangui V, Digonnet MJF, Fejer MM. Origin of apparent resonance mode splitting in bent long-period fiber gratings. *Light Technol J Of*. 2006;24(2):1027–34.
125. Lin C, Liu S, Liou W, Chang C. Improving the high frequency response of a loudspeaker using hydrogen-free diamond-like carbon film coating at low temperature. *Sci China Phys Mech Astron*. 2012 Mar 1;55(3):385–91.
126. Frost GL. Inventing Schemes and Strategies: The Making and Selling of the Fessenden Oscillator. *Technol Cult*. 2001 Jul;42(3):462–88.

127. Crocker M. Handbook of Acoustics. John Wiley & Sons; 1998. 1461 p.